N 62 51050

# NATIONAL ADVISORY COMMITTEE FOR AERONAUTICS

---

REPORT 1050

# FORMULAS FOR THE SUPERSONIC LOADING, LIFT AND DRAG OF FLAT SWEPT-BACK WINGS WITH LEADING EDGES BEHIND THE MACH LINES

By DORIS COHEN

1951

For sale by the Superintendent of Documents, U. S. Government Printing Office, Washington 25, D. C. Yearly subscription $10; foreign $11.25; single copy price varies according to size ---------- Price 35 cents

ERRATA NO. 1

NACA REPORT NO. 1050

FORMULAS FOR THE SUPERSONIC LOADING, LIFT AND DRAG OF FLAT SWEPT-BACK WINGS WITH LEADING EDGES BEHIND THE MACH LINES

By Doris Cohen

1951

Page 27.- The argument of the inverse cosine in equation (81) should read

$$\frac{(1 - a)(t_a - m_t) - (m_t - a)(1 - t_a)}{(1 - m_t)(t_a - a)}$$

Page 40.- In equation (C8), change $K$ to $K_o$.

NACA - Langley Field, Va.

# REPORT 1050

## FORMULAS FOR THE SUPERSONIC LOADING, LIFT AND DRAG OF FLAT SWEPT-BACK WINGS WITH LEADING EDGES BEHIND THE MACH LINES

By DORIS COHEN

Ames Aeronautical Laboratory
Moffett Field, Calif.

# National Advisory Committee for Aeronautics

*Headquarters, 1724 F Street NW., Washington 25, D. C.*

Created by act of Congress approved March 3, 1915, for the supervision and direction of the scientific study of the problems of flight (U. S. Code, title 50, sec. 151). Its membership was increased from 12 to 15 by act approved March 2, 1929, and to 17 by act approved May 25, 1948. The members are appointed by the President, and serve as such without compensation.


JEROME C. HUNSAKER, Sc. D., Massachusetts Institute of Technology, *Chairman*

ALEXANDER WETMORE, Sc. D., Secretary, Smithsonian Institution, *Vice Chairman*

DETLEV W. BRONK, PH. D., President, Johns Hopkins University.

JOHN H. CASSADY, Vice Admiral, United States Navy, Deputy Chief of Naval Operations.

EDWARD U. CONDON, PH. D., Director, National Bureau of Standards.

HON. THOMAS W. S. DAVIS, Assistant Secretary of Commerce.

JAMES H. DOOLITTLE, Sc. D., Vice President, Shell Oil Co.

R. M. HAZEN, B. S., Director of Engineering, Allison Division, General Motors Corp.

WILLIAM LITTLEWOOD, M. E., Vice President, Engineering, American Airlines, Inc.

THEODORE C. LONNQUEST, Rear Admiral, United States Navy, Deputy and Assistant Chief of the Bureau of Aeronautics.

HON. DONALD W. NYROP, Chairman, Civil Aeronautics Board.

DONALD L. PUTT, Major General, United States Air Force Acting Deputy Chief of Staff (Development).

ARTHUR E. RAYMOND, Sc. D., Vice President, Engineering, Douglas Aircraft Co., Inc.

FRANCIS W. REICHELDERFER, Sc. D., Chief, United States Weather Bureau.

GORDON P. SAVILLE, Major General, United States Air Force, Deputy Chief of Staff (Development).

HON. WALTER G. WHITMAN, Chairman, Research and Development Board, Department of Defense.

THEODORE P. WRIGHT, Sc. D., Vice President for Research, Cornell University.

---

HUGH L. DRYDEN, PH. D., *Director*

JOHN F. VICTORY, LL. D., *Executive Secretary*

JOHN W. CROWLEY, JR., B. S., *Associate Director for Research*

E. H. CHAMBERLIN, *Executive Officer*

---

HENRY J. E. REID, D. Eng., Director, Langley Aeronautical Laboratory, Langley Field, Va.

SMITH J. DEFRANCE, B. S., Director Ames Aeronautical Laboratory, Moffett Field, Calif.

EDWARD R. SHARP, Sc. D., Director, Lewis Flight Propulsion Laboratory, Cleveland Airport, Cleveland, Ohio

---

## TECHNICAL COMMITTEES

AERODYNAMICS
POWER PLANTS FOR AIRCRAFT
AIRCRAFT CONSTRUCTION
OPERATING PROBLEMS
INDUSTRY CONSULTING

*Coordination of Research Needs of Military and Civil Aviation*
*Preparation of Research Programs*
*Allocation of Problems*
*Prevention of Duplication*
*Consideration of Inventions*

---

LANGLEY AERONAUTICAL LABORATORY, Langley Field, Va.

AMES AERONAUTICAL LABORATORY, Moffett Field, Calif.

LEWIS FLIGHT PROPULSION LABORATORY, Cleveland Airport, Cleveland, Ohio

*Conduct, under unified control, for all agencies, of scientific research on the fundamental problems of flight*

---

OFFICE OF AERONAUTICAL INTELLIGENCE, Washington, D. C.

*Collection, classification, compilation, and dissemination of scientific and technical information on aeronautics*

# CONTENTS


| | Page |
|---|---|
| SUMMARY | 1 |
| INTRODUCTION | 1 |
| I—METHOD OF THE SUPERPOSITION OF CONICAL FLOWS | 2 |
| System of Notation for Conical Flows | 2 |
| Boundary Conditions for Cancellation of Lift | 3 |
| Cancellation of Nonuniform Lift | 3 |
| II—LOADING ON WING WITH SUBSONIC LEADING EDGE | 4 |
| Load Distribution Over Triangular Wing | 4 |
| Swept-Back Wing With Supersonic Trailing Edge (Tip Correction) | 4 |
| Elementary Solution for a Streamwise Tip | 4 |
| Tip-Induced Correction to the Loading | 5 |
| Value at the side edge | 5 |
| Drop in lift across tip Mach line | 5 |
| Swept-Back Wing With Subsonic Trailing Edge | 7 |
| Primary Trailing-Edge Corrections | 7 |
| Procedure for canceling lift in the wake region | 7 |
| Symmetrical solution | 8 |
| Oblique solutions for the wake region | 8 |
| Correction of loading near the trailing edge | 9 |
| Secondary Corrections | 9 |
| Secondary corrections at the trailing edge | 9 |
| Secondary correction at the tip | 10 |
| Numerical Example | 10 |
| Swept-Back Wings With Interacting Trailing and Leading Edges | 12 |
| Leading-Edge Corrections | 12 |
| Elementary solution for the region ahead of the leading edge | 12 |
| Leading-edge correction to the loading | 13 |
| Further Corrections | 15 |
| Numerical Results (Without Tip Effect) | 16 |
| Application of Two-Dimensional Formulas to Calculation of Load Distribution | 17 |
| Correlation of two-dimensional and swept-back-wing loadings | 17 |
| Numerical results | 19 |
| Discussion of the $\sigma$ function | 21 |
| Calculation of tip effect | 23 |
| Numerical examples, tip effect | 25 |
| III—LIFT | |
| General Procedure for Conical Flows | 26 |
| General Formula for the Lift Induced by a Single Tip Element | 26 |
| General Formula for the Lift Induced by an Oblique Trailing-Edge Element | 27 |
| Wing With Subsonic Leading Edge | 27 |
| Uncorrected Lift | 27 |
| Wing With Supersonic Trailing Edge (Tip Correction) | 28 |
| Wing With Subsonic Trailing Edge | 28 |
| Tip correction with subsonic trailing edge | 28 |
| Trailing-edge corrections | 29 |
| Wing With Interacting Leading and Trailing Edges | 30 |
| Lift on Inboard Portion of Wing | 30 |
| Lift on Outer Portions of Wing | 31 |
| Tip-Induced Correction to the Lift | 31 |
| Application of Lift Formulas | 33 |
| Cases Computed | 33 |
| Summary of Computations | 34 |
| Discussion of Results | 34 |
| IV—DRAG DUE TO LIFT | 34 |
| V—SUMMARY OF FORMULAS | 35 |
| APPENDIX A: SYMBOLS | 37 |
| APPENDIX B: EVALUATION OF THE INTEGRAL IN EQUATION (26) | 38 |
| APPENDIX C: INTEGRATION FOR LOSS OF LIFT AT THE TIP OF WING WITH SUBSONIC LEADING EDGE | 39 |
| REFERENCES | 40 |

# REPORT 1050

## FORMULAS FOR THE SUPERSONIC LOADING, LIFT, AND DRAG OF FLAT SWEPT-BACK WINGS WITH LEADING EDGES BEHIND THE MACH LINES

By Doris Cohen


### SUMMARY

*The method of superposition of linearized conical flows has been applied to the calculation of the aerodynamic properties, in supersonic flight, of thin flat, swept-back wings at an angle of attack. The wings are assumed to have rectilinear plan forms, with tips parallel to the stream, and to taper in the conventional sense. The investigation covers the moderately supersonic speed range where the Mach lines from the leading-edge apex lie ahead of the wing. The trailing edge may lie ahead of or behind the Mach lines from its apex. The case in which the Mach cone from one tip intersects the other tip is not treated.*

*Formulas are obtained for the load distribution, the total lift, and the drag due to lift. For the cases in which the trailing edge is outside the Mach cone from its apex (supersonic trailing edge), the formulas are complete. For the wing with both leading and trailing edges behind their respective Mach lines, a degree of approximation is necessary. It has been found possible to give practical formulas which permit the total lift and drag to be calculated to within 2 or 3 percent of the accurate linearized-theory value. The local lift can be determined accurately over most of the wing, but the trailing-edge-tip region is treated only approximately.*

*Charts of some of the functions derived are included to facilitate computing, and several examples are worked out in outline.*


### INTRODUCTION

It is customary, in supersonic wing theory, to describe any straight segment of the boundary of a wing plan form as supersonic or subsonic accordingly as the segment lies outside or is contained within its foremost Mach cone; that is, as the component of the flight velocity normal to the edge is greater than or less than the speed of sound. These two circumstances result in fundamentally different types of flow over the surface. It is apparent that the real reference is not to a property of the wing plan form, but to a combination of plan-form geometry and the velocity of the wing relative to the speed of sound. Thus (see fig. 1) every swept-back wing, on entering the supersonic regime, has subsonic leading and, in most cases, subsonic trailing edges. At a higher Mach number, the same plan form may have subsonic leading edges and supersonic trailing edges. Finally, if the Mach number is increased sufficiently, both leading and trailing edges will become supersonic.

Interference effects also depend on the flight Mach number, since the extent of the various disturbance fields is determined by the angle between the Mach lines. Thus, no single concise formula or method of treatment has as yet been developed to predict, even approximately, the aerodynamic characteristics of an arbitrary wing plan form through the supersonic speed range.

The present report is concerned with the loading, lift, and drag, according to linearized theory, of thin, flat, swept-back wings with rectilinear boundaries and conventional taper. Various methods are available for the calculation of these properties when the leading edge is supersonic. Of these, the method of reference 1 is perhaps the most convenient. Formulas obtained by this method for the loading and lift-curve slope of wings with supersonic leading and trailing edges are presented in reference 2. In the following, therefore, the emphasis will be on the solution of the problems arising from the interaction of the flow fields in the presence of subsonic leading edges (figs. 1 (b), (c),

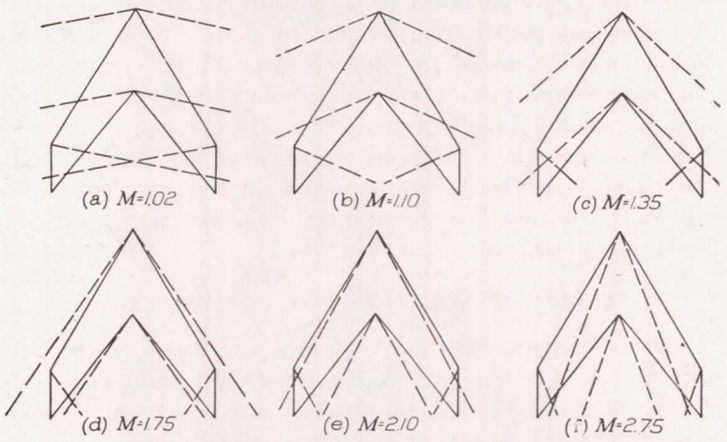


FIGURE 1.—A typical tapered swept-back wing at six supersonic Mach numbers, showing the Mach lines from the leading- and trailing-edge apexes and from the tips.

and (d)). The case (fig. 1 (a)) in which the Mach number and aspect ratio are so low that interaction takes place between the tip flow fields will not be treated. An approximate solution to this problem may be found in reference 3.

When a wing with a subsonic leading edge is to be studied, considerable simplification of the problem may be achieved by making use of the solutions, available in reference 4

and other sources, for the infinite triangular wing.[1] From these solutions the aerodynamic characteristics of a variety of swept-back plan forms can be calculated by the use of the superposition principle of linearized theory to cancel any lift beyond the specified wing boundaries. Two methods of cancellation have been developed: one, presented in reference 5, uses supersonic doublets and is general enough to apply to curved boundaries; the other, originally due to Busemann (reference 6), cancels by means of the superposition of conical flow fields. In the present report the conical-flow method is used, since it appears to offer some advantages for the straight-sided plan forms under consideration, particularly in determining the integrated lift.

The material presented in this report is largely drawn from references 7, 8, and 9, with some simplifications suggested by practical experience. In particular, the formulas for the total lift have been reworked to substitute, with no increase in computational labor, a combined "primary" and "secondary" correction for each of the "primary" corrections in reference 7. Also, the formulas containing elliptic integrals have been rewritten to take full advantage of available tables. As in the preceding papers, the final formulas will be derived for unyawed wings with tips parallel to the stream, but the application of the general method and the basic solutions to other plan forms and problems will be apparent. Some numerical examples will be included in order to show the magnitude of the effects discussed and to summarize the method. A table summarizing the formulas is also included.

## I—METHOD OF THE SUPERPOSITION OF CONICAL FLOWS

A conical flow field is one in which the velocity components $u$, $v$, and $w$ in the stream, cross-stream and vertical directions, respectively, are constant in magnitude along any ray from the foremost point, or apex, of the field. Such flows are found as solutions of the linearized potential equation for supersonic flow. A detailed discussion of their derivation and use is contained in reference 4. In the cancellation-of-lift procedure, only solutions of the so-called "mixed" type described in section V of reference 4 are required, except for the basic solution (for the infinite triangular wing) which is itself of conical form.

### SYSTEM OF NOTATION FOR CONICAL FLOWS

The Cartesian coordinate system is placed so that the origin coincides with the projection of the leading-edge apex on the horizontal plane, the positive $x$ axis extending downstream from the origin and the $y$ axis extending perpendicular to the $x$ axis in the horizontal plane. (See fig. 2.) For the conical flow fields, it is further convenient to define a variable to designate a particular ray in the $xy$ plane, since the flow velocities are constant along such a ray. If the apex of the field is specified, then the ray is most readily described by its slope, measured from the downstream direction. The conical solutions of the supersonic flow equation are, however, functions of the ratio of the slope of the ray to the slope $\frac{1}{\beta}$ of the Mach lines, where $\beta$ is $\sqrt{M^2-1}$ and $M$ is the free-stream Mach number. For the triangular-wing flow with its origin at the apex of the wing, therefore, the conical variable will be chosen as

$$a=\beta\frac{y}{x} \tag{1}$$

At the Mach lines from the leading-edge apex, $a$ equals $\pm 1$. The ray from 0, the wing apex, making the angle $\tan^{-1}\frac{a}{\beta}$ with the stream will hereinafter be referred to as the ray $a$, and the subscript $a$ will indicate association with a constant-load sector (to be introduced later) of which such a ray is one of the boundaries.

For each of the conical fields to be superposed at the edges of the wing plan form, a new coordinate system is set up with its origin at the apex of the field. In conformity with the notation of reference 4, the conical variable relative to the displaced origin is called $t$, with subscripts to denote the location of the origin. Thus, if $x_a,y_a$ is the point of intersection of the ray $a$ with the plan-form boundary and is to serve as the apex of a canceling conical field,

$$t_a=\beta\frac{y-y_a}{x-x_a} \tag{2}$$

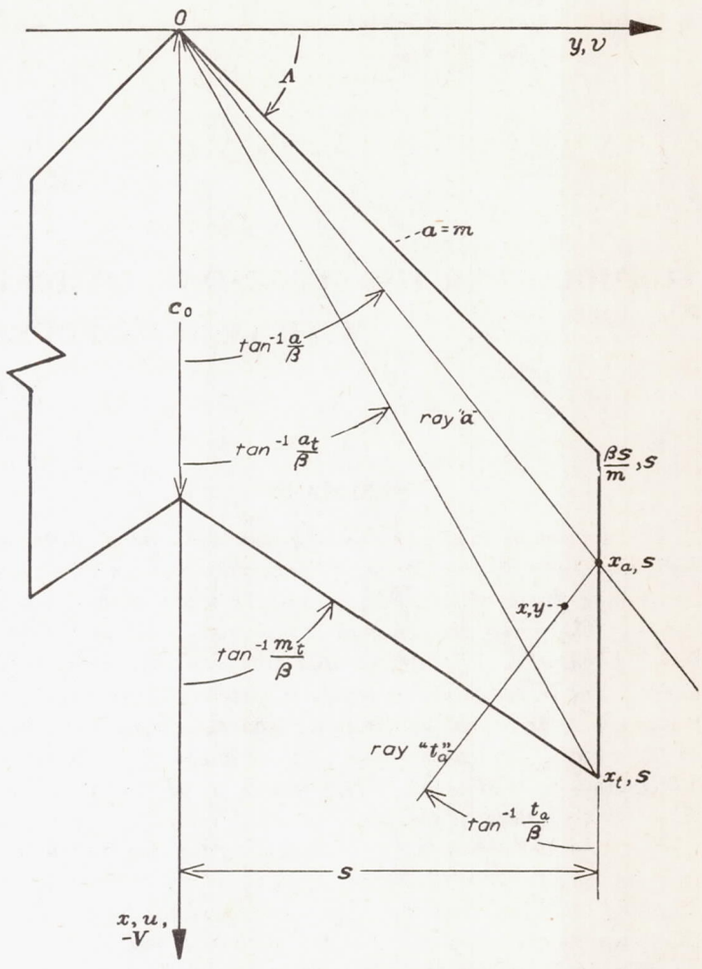


FIGURE 2.—Coordinate system, conical variables, and other symbols.

[1] The present report covers in detail only unyawed wings. However, yawed wings may be treated similarly, starting with the yawed triangular-wing solutions. This problem is the subject of a paper, NACA TN 2262, 1950, by Lampert, prepared concurrently with the present report.

is the ratio of the slope of the ray $t_a$ of that field to the slope of the Mach lines.

If the ratio of the slope of the leading edge to the slope of the Mach lines is

$$m=\beta \cot \Lambda \tag{3}$$

where $\Lambda$ is the angle of sweepback, then at the leading edge $a=m$, and a ray from the leading-edge tip is designated by $t_m$. If $s$ is the wing semispan, the leading-edge tip has the coordinates $\frac{\beta s}{m}$, $s$ and any point $x,y$ has the conical coordinate

$$t_m=\beta\frac{y-s}{x-\frac{\beta s}{m}} \tag{4}$$

in the field with apex at $\frac{\beta s}{m}$, $s$.

Other symbols referring to angular locations will be defined in the same way as needed. A summary of the symbols will be found in appendix A.

## BOUNDARY CONDITIONS FOR CANCELLATION OF LIFT

The general problem of deriving the flow over a wing of finite dimensions from the known flow over an infinite wing is the problem of determining the induction effects due to the edges. These effects may be thought of as associated with the cancellation of the lifting pressure at the boundaries of the finite wing. In the linearized lifting-surface theory, they may be evaluated by the superposition of flow fields with negative lifting pressure over the portion of the infinite wing outside the boundaries of the finite plan form, provided the other boundary conditions are not disturbed. In the case of a flat wing at an angle of attack, the latter provision means that the canceling field must (1) induce no downwash within the boundaries of the finite wing and (2) introduce no new lifting pressure outside those boundaries.

In accordance with thin-airfoil theory, the boundary conditions will be satisfied in the horizontal plane rather than on the surface of the wing. Also, by thin-airfoil theory, the conditions on the lifting pressure are converted to conditions on the velocity field through the relation

$$\frac{\Delta p}{q}=4\left(\frac{u}{V}\right)_{z=+0} \tag{5}$$

In the simplest case, the lift to be canceled will be distributed uniformly over a semi-infinite region bounded by two straight lines. The boundary conditions of the problem may then be said to be conical with respect to the intersection of the two lines, which become "rays" of the canceling conical field. The boundary conditions on the canceling velocity field in this case may be summarized as follows:

(1) The streamwise velocity $u$ must approach values equal in magnitude and opposite in direction on the upper and lower surfaces of the horizontal plane.

(2) In the horizontal plane, $u$ must be constant over the infinite sector in which lift is to be canceled.

(3) The vertical velocity $w$ must be zero in the portion of the $z=0$ plane occupied by the projection of the finite wing.

(4) From equation (5), $u$ must equal zero in the portion of the horizontal plane not covered by conditions (2) or (3).

(5) In supersonic flow there exists the additional condition that all the velocities must go to zero on the Mach cone from the apex of the field.

## CANCELLATION OF NONUNIFORM LIFT

The foregoing are the general conditions for a uniformly loaded canceling flow field. Under the proper conditions, a nonuniform distribution of lift may be canceled by the superposition of a number of such fields. This procedure is best explained by a concrete example.

Consider the problem of a swept-back wing flying at a high Mach number such that, as in figure 1 (e), the Mach lines from the leading-edge apex intersect the tips of the wing. The method of deriving the swept-back wing from an infinite triangular wing in that case is indicated in figure 3. It may be noted at the start that, according to linear theory, the lift behind the supersonic trailing edge may be canceled in any way without affecting the velocities on the wing. Thus it remains only to consider the effect of canceling the lift outboard of the tips.

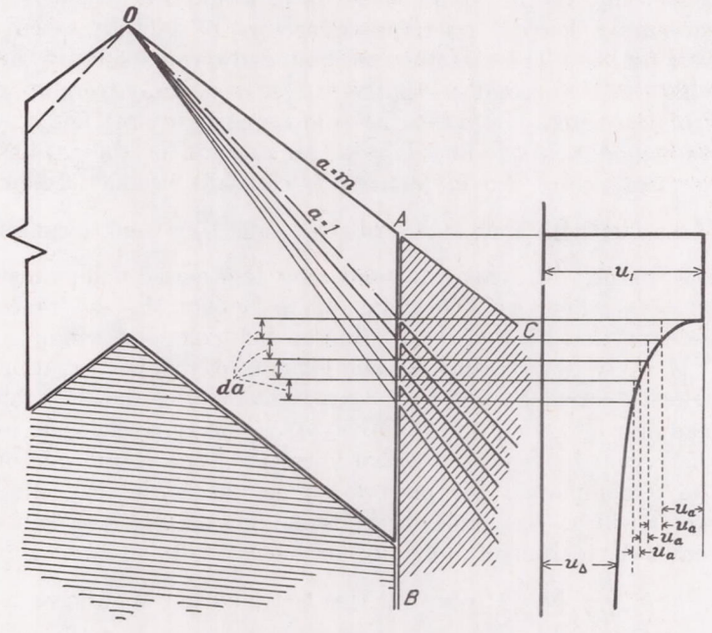


FIGURE 3.—Method of cancellation of lift beyond the tip when the leading-edge Mach line intersects the side edge of the wing.

An infinite triangular wing with supersonic leading edges has a load distribution which is constant over the portions of the wing between the leading edge and the Mach lines from the leading-edge apex (see fig. 4). This constant load may be canceled outboard of each of the tips of the swept-back wing by a single negatively loaded triangle of infinite extent, one side coinciding with the side edge of the wing and a second side coinciding with the extension of the leading edge. However, the area to be removed (region BAC, fig. 3) includes also a region over which the pressure varies, and is conical with respect to 0. Since the boundaries of the region are conical with respect to A, no one conical solution can satisfy the requirements of the problem. The problem is brought within the limitations of the conical solutions by

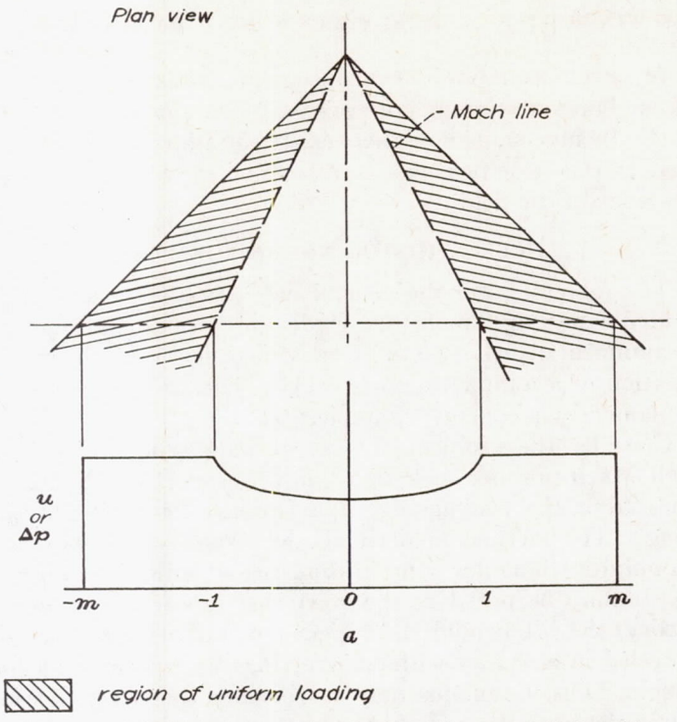


FIGURE 4.—Lift distribution on a triangular wing with supersonic leading edges.

considering the lift to be made up of an infinite number of constantly loaded, overlapping sectors of infihite extent. (See fig. 3.) These sectors are bounded on one side by the wing tip; the second side is the extension of a ray from apex 0 of the wing. Between the leading edge ($a=m$) and the leading-edge Mach line ($a=1$), no division of the field is necessary since the lift density is constant in that region. If a sector with apex at A and angle $\tan^{-1}\frac{m}{\beta}$ is used to cancel this uniform lift, then the remaining superposed fields must be used where $a<1$ (see fig. 4) to restore the difference between that lift and the loading on the triangular wing.

If $u_1$ is the streamwise component of the perturbation velocity corresponding to the constant loading ahead of the leading-edge Mach lines, and $u_\Delta(a)$ is the same velocity in the region between the Mach lines, then the magnitude of the $u$ component of the velocity in the initial canceling sector will be $-u_1$, and on the remaining sectors (see fig. 3) minus the increment in $u_1-u_\Delta$ corresponding to an increment in $a$, or $\frac{du_\Delta}{da}da$. (Note that this last quantity is positive, as required). To determine the total effect of canceling the loading outboard of the tip, the velocities induced by the latter infinitesimally loaded elements are integrated and added to the negative effect of the initial constant-load sector.

## II—LOADING ON WING WITH SUBSONIC LEADING EDGE

### LOAD DISTRIBUTION OVER TRIANGULAR WING

In the notation of this paper, the velocity distribution over a flat lifting triangle with leading edge behind the Mach lines may be written

$$u_\Delta=\frac{mu_0}{\sqrt{m^2-a^2}} \tag{6}$$

where

$$u_0=\frac{mV\alpha}{\beta E'(m)} \tag{7}$$

is the (constant) velocity along te cen ter lin e $a=0$. In the expression for $u_0$, $E'(m)$ is the complete elliptic integral of the second kind, of modulus $\sqrt{1-m^2}$. The load distribution is obtained from the velocity distribution by equation (5).

### SWEPT-BACK WING WITH SUPERSONIC TRAILING EDGE (TIP CORRECTION) [2]

If the problem is now to find the loading on a swept-back wing with subsonic leading edges, but supersonic trailing edges, only the tip effects will modify the triangular-wing distribution. The calculation of the tip effect on a wing with subsonic leading edge ($m<1$) is somewhat complicated by the fact that the pressure becomes infinite at the leading edge, but otherwise follows the procedure outlined in the preceding section.

It will first be necessary to present the expression for the previously described conical field with uniformly loaded sector to be used as the element in canceling the lift outboard of the tip.

#### ELEMENTARY SOLUTION FOR A STREAMWISE TIP

If $s$ is the semispan of the wing, the apex of any element $a$ (see the section on Notation) is at

$$x_a=\frac{\beta s}{a},\ y_a=s \tag{8}$$

and, from equation (2),

$$t_a=\beta\frac{y-s}{x-\frac{\beta s}{a}} \tag{9}$$

Then, if $u_a$ is the constant perturbation-velocity component to be canceled over the region between the tip and the extension of the ray $a$, the previously listed boundary conditions for each of the required canceling fields may be written as follows (see fig. 5):

(1) and (2) When $0\leq t_a\leq a$, $u=\pm u_a$ (constant for the field)
(3) When $t_a<0$, $w=0$
(4) When $t_a>a$, $u=0$
(5) When $|t_a|\geqq 1$, $u=v=w=0$.

The solution of the supersonic flow equation satisfying the above boundary conditions has been derived in reference 4.[3] In the $xy$ plane, the streamwise component of the velocity is

$$u=\pm r.p.\ \frac{u_a}{\pi}\cos^{-1}\frac{a+t_a+2at_a}{t_a-a} \tag{10}$$

The signs refer to the upper and lower surfaces, respectively.

In figure 5, the essential features of the solution are shown. At the top is a detail view of the wing side edge and shows the boundary conditions. In the center is a typical plot of the argument of the inverse cosine in equation (10), against $t_a$. Where this quantity is less than $-1$ (i. e., $0\leq t_a\leq a$), the real part of the inverse cosine is $\pi$. Where the argument is greater than $+1$ ($t_a>a$ and $t_a<-1$), the

[2] Approximate formulas, valid when $m$ is close to 1, have been presented for this case in reference 10.

[3] The corresponding solutions for raked-in or raked-out tips may also be found in reference 4, or deduced from later sections in the present report.

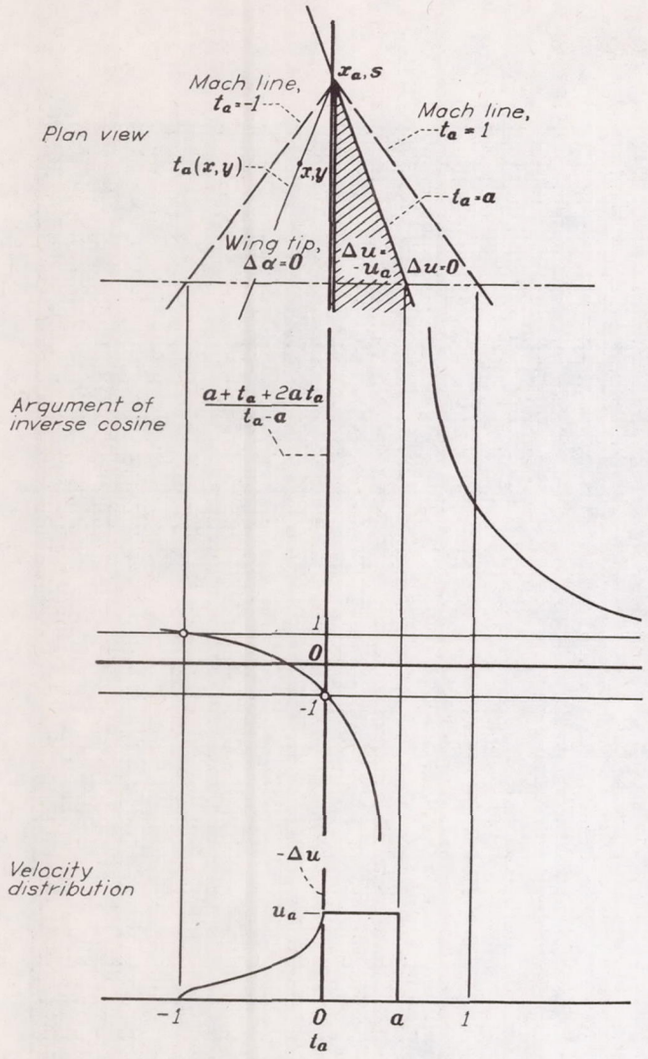


FIGURE 5.—Elementary solution for canceling lift at the tip.

real part of the inverse cosine is zero. On the wing $(-1\leq t_a<0)$, the argument goes from $+1$ to $-1$ and the inverse cosine is real. Thus in canceling, or subtracting, the velocity $u_a$ between $t_a=0$ and $t_a=a$, the increment in velocity

$$u(x,y,a)=-\frac{u_a}{\pi}\cos^{-1}\frac{a+t_a+2at_a}{t_a-a} \tag{11}$$

is induced on the wing upper surface.

### TIP-INDUCED CORRECTION TO THE LOADING

Following the procedure outlined in Part I, we proceed to determine the effect of canceling the lift outboard of the wing tip. Since the value of $u_a$ for the initial canceling field $-u_\Delta(m)$ and the value for the first incremental field $\frac{du_\Delta}{da}da$ are both infinite when the leading edge is subsonic, it is first necessary to write the induced velocity at a point $x,y$ as

$$(\Delta u)_{tip}=\lim_{a\to m}\left[\frac{-u_\Delta(a)}{\pi}\cos^{-1}\frac{a+t_a+2at_a}{t_a-a}+\frac{1}{\pi}\int_{a_0}^{a}\frac{du_\Delta}{da}\cos^{-1}\frac{a+t_a+2at_a}{t_a-a}\,da\right] \tag{12}$$

where the limit $a_0$ is the value of $a$ corresponding to the rearmost sector including the point $x,y$ in its Mach cone. The value of $a_0$ is found by setting $t_a$ (equation (9)) equal to $-1$. Thus, for the tip correction,

$$a_0=\frac{\beta s}{x+\beta(y-s)} \tag{13}$$

This parameter will be additionally useful as the value of $a$ at which the velocity correction given by equation (11) goes to zero and its derivative has a singularity.

Before performing the integration of equation (12), $t_a$ must be replaced by its expression in terms of $x$, $y$, and $a$. Then integration of the second term by parts results in a term which, at the upper limit, exactly cancels the first term, and at the other limit is zero, leaving, after substitution for $u_\Delta$,

$$(\Delta u)_{tip}=\frac{-m(x+\beta y)u_0}{\pi\sqrt{s}}\int_{a_0}^{m}\frac{\sqrt{a_0(s-y)}\,da}{(ax-\beta y)\sqrt{(m^2-a^2)(1+a)(a-a_0)}} \tag{14}$$

This integral is finite and can be evaluated in terms of elliptic integrals as follows:

$$(\Delta u)_{tip}=u_0\left[\sqrt{\frac{m\beta(s-y)}{2(x+\beta y)}}\,K_0-\frac{mx}{\sqrt{m^2x^2-\beta^2y^2}}\Lambda_0(k,\psi)\right] \tag{15}$$

where

$$\Lambda_0=K_0E(\psi,k')-(K_0-E_0)F(\psi,k') \tag{16}$$

and $K_0$ and $E_0$ are $2/\pi$ times the complete elliptic integrals $K$ and $E$ of modulus

$$k=\sqrt{\frac{(m-a_0)(1-m)}{2m(a_0+1)}}$$

In equation (16), $F(\psi,k')$ and $E(\psi,k')$ are the incomplete integrals with the complementary modulus $k'=\sqrt{1-k^2}$ and argument

$$\psi=\sin^{-1}\sqrt{\frac{a_0(mx+\beta y)}{\beta s(a_0+m)}}$$

The functions $K_0$, $E_0$ and $\Lambda_0$ are tabulated in reference 11[4] or may be computed from the tables of reference 12. A plot of $\Lambda_0$ is given in figure 6.

**Value at the side edge.**—At the tip, $y$ is equal to $s$ and the first term in equation (15) vanishes. In the second term, $\psi$ becomes $\pi/2$ and $E(\psi,k')$ and $F(\psi,k')$ reduce to the complete integrals $E'=E(k')$ and $K'=K(k')$, respectively. Then, since, by Legendre's relation,

$$K'E-K'K+KE'=\pi/2$$

$\Lambda_0$ reduces to 1. The induced velocity correction is seen to be exactly equal to $-u_\Delta$, bringing the lift to zero at the wing tip.

**Drop in lift across tip Mach line.**—An interesting effect shows itself at the other limit of the tip region, that is, at the Mach line from the tip of the leading edge. Along this line only the influence of the leading-edge pressure is felt, so that

[4] The quantity $K_0$ is called $F_0$ in reference 11.

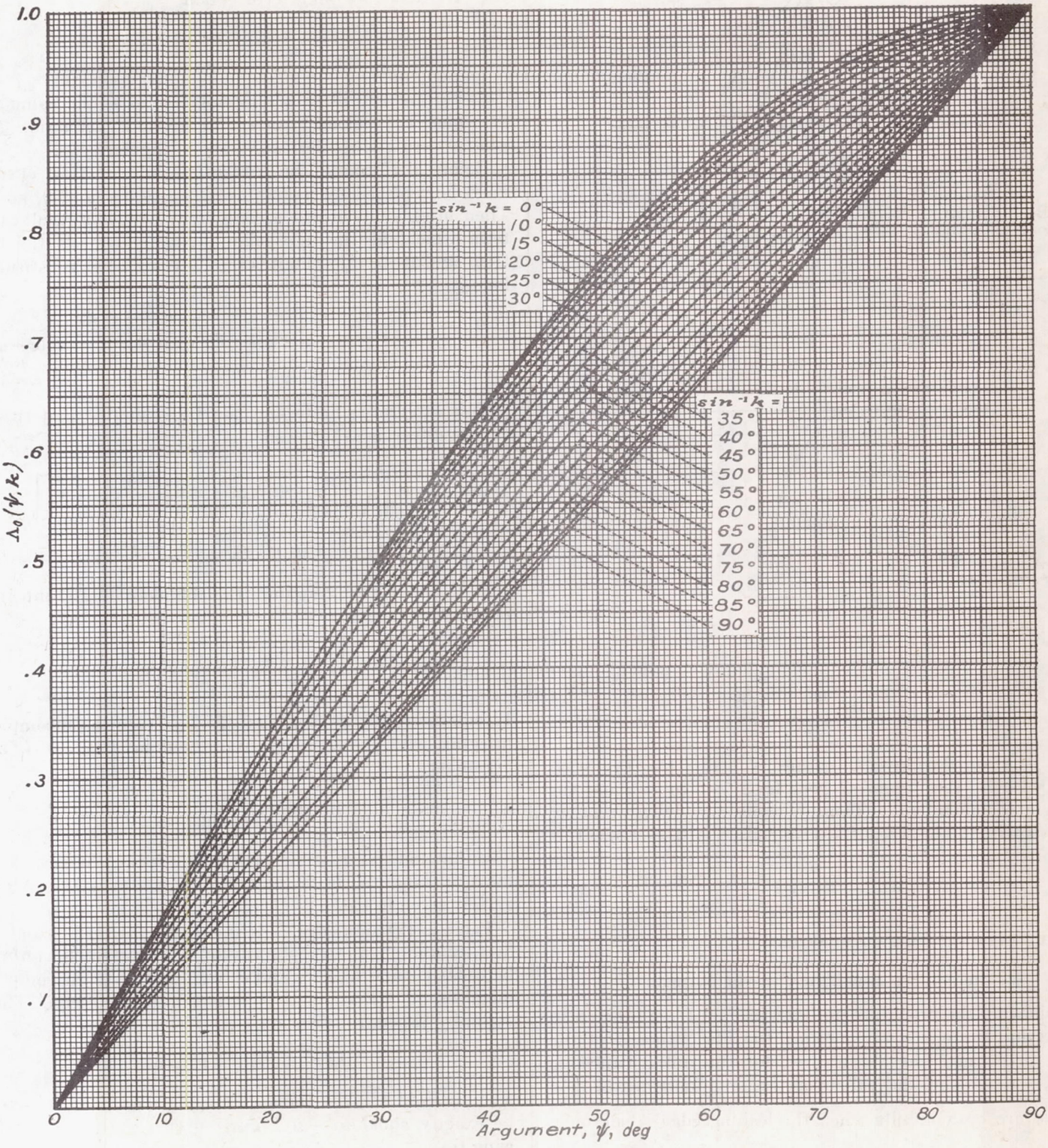


FIGURE 6.—The elliptic function $\Lambda_0(\psi,k)=K_0E(\psi,k')-(K_0-E_0)F(\psi,k')$.

$a_0=m$. Then $k=0$, $k'=1$, $K=\pi/2$, $E(\psi,k')$ reduces to $\sin\psi=\sqrt{\frac{mx+\beta y}{2\beta s}}$, and finally

$$(\Delta u)_{tip}(t_m=-1)\equiv\Delta u^*=\frac{-u_0\beta s}{\sqrt{2(x+\beta y)(mx-\beta s)}} \tag{17a}$$

or, since along the tip Mach line $\beta(s-y)=x-\frac{\beta s}{m}$,

$$\Delta u^*=\frac{-u_0\sqrt{m\beta s}}{\sqrt{2(1+m)(mx-\beta s)}} \tag{17b}$$

This result indicates a finite drop in pressure across the Mach line from the tip, an effect which is associated with the cancellation of infinite pressure at the leading edge and consequently does not appear as long as the leading edge is ahead of the Mach lines. The ratio of the drop in lift across the tip Mach line to the uncorrected lift can be written

$$\frac{\Delta u^*}{u_\Delta}=-\sqrt{\frac{(1+a)(m+a)}{2m(1+m)}} \tag{18}$$

This ratio is plotted against $a/m$ in figure 7 and shows the percentage loss of lift at the tip to be very large. In fact, for any but the lowest-aspect-ratio wings, the lift remaining in that region is almost negligible. This effect, which should be of considerable practical interest, was first indicated in the results of reference 13 for the limiting case of $m=0$.

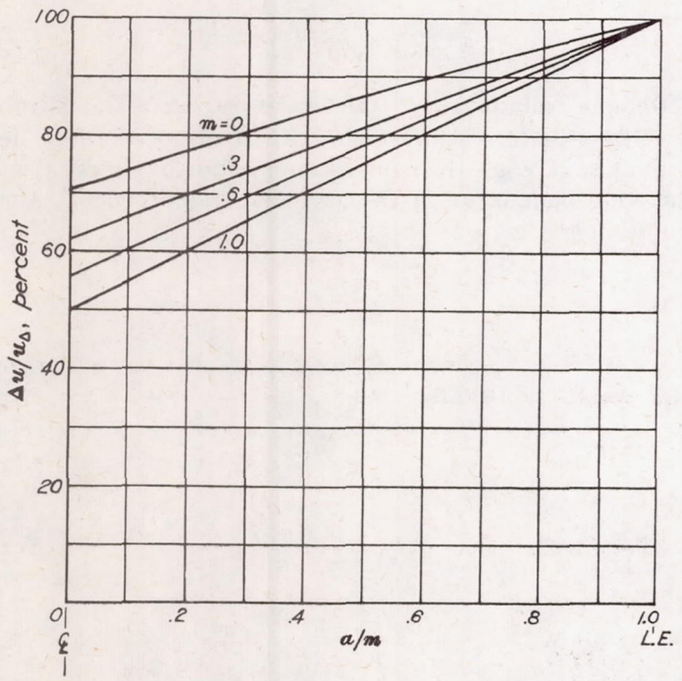


FIGURE 7.—Percent drop in lift across Mach line from tip.

## SWEPT-BACK WING WITH SUBSONIC TRAILING EDGE

The tip-effect correction just derived applies equally to wings with supersonic or subsonic trailing edges. The effect of a subsonic trailing edge is calculated separately, and is primarily due to canceling the triangular-wing loading in the wake region. If, however, the triangular-wing loading has been modified by the introduction of side edges, then this modification must also be taken into account when canceling the lift behind the trailing edge. In the conical-flow method, the various component flow fields must be canceled individually. The sections immediately following will discuss the cancellation of the triangular-wing loading; cancellation of the tip-induced components of velocity will be considered under the heading "Secondary Corrections."

### PRIMARY TRAILING-EDGE CORRECTIONS

**Procedure for canceling lift in the wake region.**—The basic procedure is again to consider the load to be canceled to be built up by the superposition of uniformly loaded sectors, bounded on one side (see fig. 8) by the rays $a$, and on the other by the trailing edge of the wing. It is convenient at this point to introduce the parameter

$m_t=\beta\times\cot$ (angle of sweep of trailing edge)

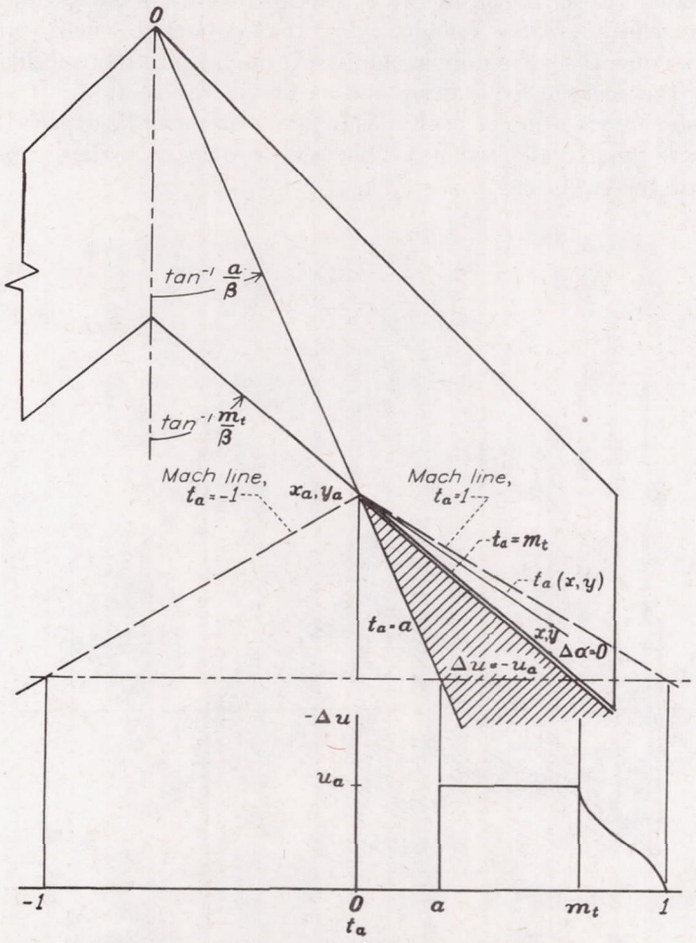


FIGURE 8.—Oblique constant-lift element (shaded) for cancellation of lift at subsonic trailing edge, and induced velocity distribution.

The boundary conditions to be satisfied by the $u$ component of the elementary canceling velocity field are indicated for the right span in figure 8; each field must have constant velocity $u_a$ when $a\leq t_a\leq m_t$ and zero streamwise velocity over the wake region, $-1\leq t_a<a$. The concomitant vertical velocity must be zero on the wing surface. However, when $a$ is small, the region $-1\leq t_a<a$ will include a portion of the left-hand wing panel. Since in this region the $u$ component of velocity has already been specified, the vertical velocity

will not, in general, be zero. Nor is it possible to modify the field to satisfy the boundary condition on the far wing, since the area involved is not conical with respect to the apex of the field.

The error involved in the foregoing procedure is minimized by the use of a symmetrical flow field to cancel the initial load $u_0$ at $a=0$, where a single conical field can be made to satisfy the boundary conditions exactly on both wing panels. This flow field (see fig. 9) would have its origin at the apex $c_0,0$ of the trailing edge, and the constant-load region would extend over the entire wake region. Between the trailing edge of the wing and the Mach lines from $c_0,0$ the induced downwash would be zero in the plane of the wing, while the pressure would vary as required to satisfy the fundamental flow equations.

In figure 9, a typical curve of $u_\Delta$ is shown, from which it can be seen that the load to be canceled is very nearly constant over a considerable fraction of the wake region. Cancellation of the velocity $u_0$ by the symmetrical field will consequently leave only a small variation in $u$ to be canceled by the oblique fields described earlier in the section. The resulting violation of the flat-plate condition may be expected to be small,[5] and will take place only over a small region near the tip of the trailing edge.

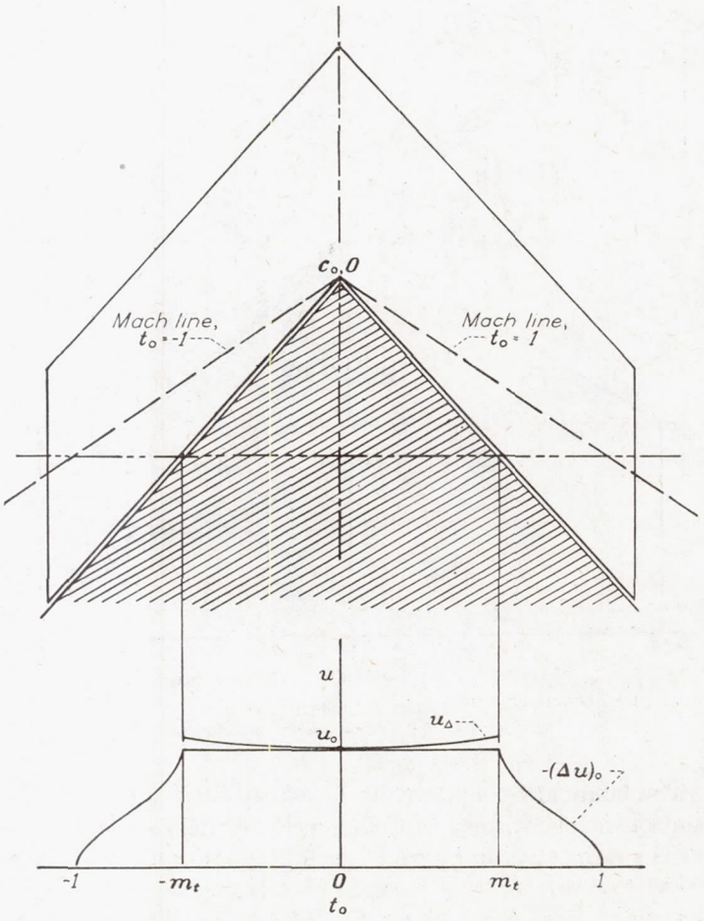


FIGURE 9.—Symmetrical field for cancellation of $u_0$ at subsonic trailing edge.

[5] Calculations made to check this statement have shown the induced downwash angles to be less than 0.5 percent of the angle of attack, even in the most unfavorable circumstances.

**Symmetrical solution.**—For the symmetrical solution we define the conical variable

$$t_0=\frac{\beta y}{x-c_0} \tag{19}$$

which is zero along the center line of the wing and equals $\pm m_t$ at either trailing edge. Then the boundary conditions to be satisfied in the $xy$ plane may be summarized as follows:

$$-m_t \leq t_0 \leq +m_t \qquad u=\pm u_0$$

$$m_t < |t_0| \leq 1 \qquad w=0$$

The required solution is given in reference 14. The $u$ component in the $xy$ plane is

$$r.\,p.\ \frac{\pm u_0}{K'(m_t)}\,F(\phi,\sqrt{1-m_t^2})$$

where $K'(m_t)$ is the complete elliptic integral of the first kind of modulus $\sqrt{1-m_t^2}$ and $F(\phi,\sqrt{1-m_t^2})$ is the corresponding incomplete integral of argument

$$\phi=\sin^{-1}\sqrt{\frac{1-t_0^2}{1-m_t^2}}$$

The form of the induced velocity on the wing (see fig. 9) is very similar to the inverse cosine curves of the tip solutions.

On the wing, $\phi$ is real and the symbols $r.\,p.$ may be omitted. The velocity induced on the upper surface by cancellation of $u_0$ behind the trailing edge is therefore

$$(\Delta u)_0=-\frac{u_0}{K'(m_t)}\,F(\phi,\sqrt{1-m_t^2}) \tag{20}$$

**Oblique solutions for the wake region.**—The symbol $t_a$ will be used as before to indicate a ray of the flow field with apex at $x_a,y_a$, the point of intersection of the ray $a$ with the wing boundary—in this case the trailing edge. Along the trailing edge,

$$y_a=\frac{m_t}{\beta}(x_a-c_0)$$

Since $a=\beta\ (y_a/x_a)$, we may solve for $x_a$ and $y_a$ as functions of $a$ and the constants $m_t$ and $c_0$:

$$x_a=\frac{m_t c_0}{m_t-a} \tag{21}$$

$$\beta y_a=\frac{m_t c_0 a}{m_t-a} \tag{22}$$

Then

$$t_a=\frac{\beta y(m_t-a)-m_t c_0 a}{x(m_t-a)-m_t c_0} \tag{23}$$

The boundary conditions to be satisfied by the elementary solution are (for $a>0$)

$$a \leq t_a \leq m_t \qquad u=\pm u_a$$

$$m_t < t_a \leq +1 \qquad w=0$$

$$-1 \leq t_a < a \qquad u=0$$

The solution satisfying these conditions may be obtained from the tip solutions by an oblique transformation. (See reference 4.) In the $xy$ plane, the resulting expression for the $u$ component is

$$r.\,p.\pm\frac{u_a}{\pi}\cos^{-1}\frac{(1-a)(t_a-m_t)-(m_t-a)(1-t_a)}{(1-m_t)(t_a-a)}$$

Then the velocity induced at any point $x,y$ on the upper surface of the wing by the cancellation of the infinitesimal increment of perturbation velocity $u_a$ over the sector bounded by the ray $a$ and the trailing edge is

$$\frac{d\Delta u}{da}\,da=(\Delta u)_a=\frac{-u_a}{\pi}\cos^{-1}\frac{(1-a)\,(t_a-m_t)-(m_t-a)\,(1-t_a)}{(1-m_t)\,(t_a-a)} \tag{24}$$

**Correction of loading near the trailing edge.**—To determine the lift at any point $x,y$ near the trailing edge of the wing, it is first necessary to determine the most rearward canceling sector $a_0$ that will influence that point. Setting $t_a$ (equation (23)) equal to 1, we solve for

$$a_0=m_t\frac{x-\beta y-c_0}{x-\beta y-m_t c_0} \tag{25}$$

Then the total correction to the triangular-wing velocity $u_\Delta$ obtained as a result of canceling that velocity behind the trailing edge is

$$(\Delta u)_{T.E.}\,(x,y)=(\Delta u)_0+\int_0^{a_0}\frac{d\Delta u}{da}\,da \tag{26a}$$

The integral in the foregoing expression has been evaluated in terms of an incomplete elliptic integral of the third kind, which may be computed with the aid of the tables of references 11 and 15. Because it will be necessary to define several new functions it was thought better to present the results in an appendix (appendix B). For practical use, graphical or numerical integration may be preferred, in which case a convenient form is obtained by rewriting $u_a$ as $(du_\Delta/da)\,da$, or $du_\Delta$, in equation (24). Thus equation (26a) becomes

$$(\Delta u)_{T.E.}\,(x,y)=(\Delta u)_0-$$

$$\frac{1}{\pi}\int_{v_0}^{u_\Delta(a_0)}\cos^{-1}\frac{(1-a)\,(t_a-m_t)-(m_t-a)\,(1-t_a)}{(1-m_t)\,(t_a-a)}\,du_\Delta \tag{26b}$$

where $t_a$ and $u_\Delta$ must be evaluated for selected values of $a$ between zero and $a_0$. The integrand, of course, goes to zero at $u_\Delta(a_0)$. At points along the leading edge (in cases in which the leading edge extends into the zone of influence of the trailing edge), the integral takes on a somewhat simpler form, with the result that the entire trailing-edge correction at such points can be written

$$(\Delta u)_{T.E.}\left(x,\frac{mx}{\beta}\right)=-u_0\left\{\frac{F\,(\phi,\sqrt{1-m_t^2})}{K\,(\sqrt{1-m_t^2})}-\right.$$

$$\frac{1}{\pi}\cos^{-1}\frac{(t_0-m_t)-m_t(1-t_0)}{(1-m_t)\,t_0}+$$

$$\left.\frac{1}{\pi}\sqrt{\frac{2\,(t_0-m_t)}{(1-m)\,(1-m_t)\,t_0}}\left[F\,(\psi,k)-\frac{1-a_0}{m-a_0}E\,(\psi,k)\right]\right\} \tag{26c}$$

where the first term inside the braces is $\frac{(\Delta u)_0}{u_0}$ and, in the last term,

$$\psi=\sin^{-1}\sqrt{\frac{2a_0}{m+a_0}}$$

and

$$k=\sqrt{\frac{(1-m)\,(m+a_0)}{2m\,(1-a_0)}}$$

### SECONDARY CORRECTIONS

The term "secondary corrections" is used here to designate the effect of canceling the lift introduced outside the boundaries of the wing in the process of canceling the original triangular-wing loading beyond the tips and behind the trailing edge. As previously mentioned, cancellation of lift at the tip introduces new (negative) components of lift to be canceled at the trailing edge. The original cancellation of lift behind the trailing edge, on the other hand, will introduce negative incremental pressures outboard of the tip and, under certain circumstances (see figs. 1 (a) and (b)), ahead of the leading edge. The distribution of lift to be canceled in each case is no longer part of a single conical field, but is composed of an infinite number of superposed conical fields originating at various points along the trailing edge or tip. In order to cancel these pressures accurately, it would be necessary to set up, for each of the original canceling elements, an infinity of positively loaded elements at the opposite boundary. Thus, each secondary correction would require a double integration for each point, and would obviously be quite tedious. The procedure is described in detail in references 7 and 8. The more recent work of Mirels (reference 5) offers an alternative method which, while no less tedious at the computational state, is somewhat easier to set up for computing. Nevertheless, the exact calculation of the secondary corrections, and of the succeeding corrections arising as the secondary corrections are in turn canceled at the opposite edges, appears feasible only with the aid of high-speed computing machinery.

These corrections may be thought of as a converging series, since in each case (except in the neighborhood of the leading edge) the induced effect is smaller than the canceled lift. Over most of the wing, the secondary correction is of the same order of magnitude as the tolerable error. Formulas for obtaining a major part of the secondary corrections can be given rather simply and should suffice to give results of practical accuracy in problems (fig. 1(c)) not involving leading-edge corrections. Problems of the type shown in figure 1(b) will be discussed in a later section.

**Secondary corrections at the trailing edge.**—The pressure differences induced by the tip are in the main due to cancellation of the infinite pressure at the leading edge. It should therefore be permissible, for the secondary corrections, to approximate the tip-correction field by a single conical field from the leading-edge tip. The lift associated with this field may then be canceled behind the wing (see fig. 10) by a single infinity of superposed fields, as was the original triangular-wing loading. If the values of $(\Delta u)_{tip}$ calculated for points $x_b,y_b$ along the trailing edge are assumed to apply all along the corresponding rays $t_m(x_b,y_b)$ from the tip, then the

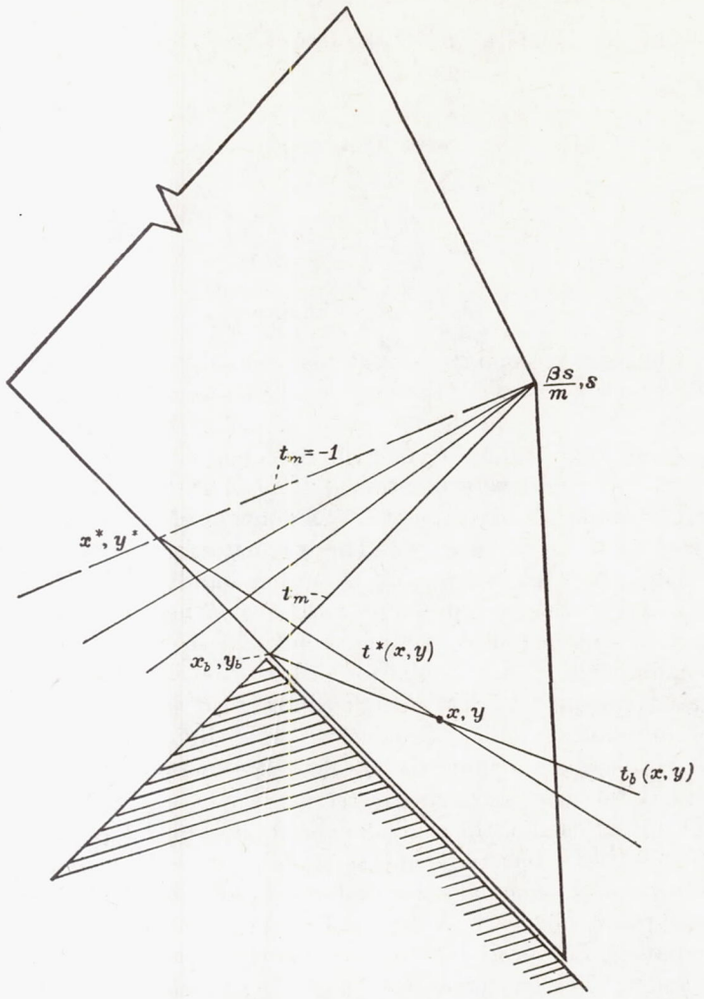


FIGURE 10.—Sketch for approximate cancellation of extraneous lift introduced behind the leading edge by the tip correction.

lifting pressure will be exactly canceled along the trailing edge and the remaining variation of pressure in the wake will have very little effect on the flow over the wing.

The cancellation fields are of the previously used oblique type, with $a$ replaced by

$$t_m=\frac{\beta(y_b-s)}{x_b-\frac{\beta_s}{m}} \tag{27}$$

Let the particular point at which the line $t_m=-1$ intersects the trailing edge be designated by $x^*,y^*$ and other symbols referring to that point be similarly starred. Then the velocity induced at any point $x,y$ on the wing by removal of $(\Delta u)_{tip}$ along the trailing edge will be (from equation (24))

$$\frac{-\Delta u^*}{\pi}\cos^{-1}\frac{2(t^*-m_t)-(m_t+1)(1-t^*)}{(1-m_t)(t^*+1)}-$$
$$\frac{1}{\pi}\int_{-1}^{t_m(x_0,y_0)}\frac{d(\Delta u)_{tip}}{dt_m}\cos^{-1}\frac{(1-t_m)(t_b-m_t)-(m_t-t_m)(1-t_b)}{(1-m_t)(t_b-t_m)}\,dt_m \tag{28}$$

where $\Delta u^*$ is given by equation (17), $t^*$ and $t_b$ are calculated by

$$t^*=\frac{\beta(y-y^*)}{x-x^*} \tag{29}$$

and

$$t_b=\frac{\beta(y-y_b)}{x-x_b} \tag{30}$$

respectively, and $x_0, y_0$ is the point of intersection of the Mach forecone from $x$, $y$ with the trailing edge.

The derivative $\frac{d}{dt_m}(\Delta u)_{tip}$ would have to be determined numerically or graphically from a plot of the calculated values of $(\Delta u)_{tip}$ against $t_m$. In order to avoid this procedure, it is preferable to rewrite expression (28) as

$$\frac{-\Delta u^*}{\pi}\cos^{-1}\frac{2(t^*-m_t)-(m_t+1)(1-t^*)}{(1-m_t)(t^*+1)}-$$
$$\frac{1}{\pi}\int_{\Delta u^*}^{(\Delta u)_{tip}(x_0,y_0)}\cos^{-1}\frac{(1-t_m)(t_b-m_t)-(m_t-t_m)(1-t_b)}{(1-m_t)(t_b-t_m)}\,d(\Delta u)_{tip} \tag{31}$$

and integrate by plotting the inverse cosine function against $(\Delta u)_{tip}$.

As long as the aspect ratio of the wing is greater than $1/\beta$ (a condition already imposed by the exclusion of the problem shown in fig. 1 (a)), $\Delta u^*$ will be more than half $(\Delta u)_{tip}$ at any other point on the trailing edge. Since, moreover, the integral term in equation (31) has zero slope at the Mach cone ($t^*=1$), while the first term starts with infinite slope, it is apparent that the secondary correction may be simplified still further by omitting the calculation of the integral. For points near the trailing edge, the loading can usually be faired to zero with sufficient accuracy.

**Secondary correction at the tip.**—A similar method of approximating the secondary correction at the tip cannot be formulated with equal confidence. Since, however, over most of the wing the symmetrical correction $(\Delta u)_0$ contributes the larger part of the total subsonic-trailing-edge effect, it will again be assumed that the entire effect constitutes a single conical field, with its apex at $c_0$, 0. The $u$ velocity along each ray $t_0$ will have the value $(\Delta u)_{T.E.}(x_b, s)$ of the trailing-edge correction at the intersection $x_b$, $s$ of the ray with the tip. The canceling fields will have the same form as those (equation (10)) used in deriving the primary tip correction, and the total approximate correction to the $u$ velocity will be

$$-\frac{1}{\pi}\int_{t_0=1}^{(\Delta u)_{T.E.}(x_0,s)}\cos^{-1}\frac{t_0+t_b+2t_0t_b}{t_b-t_0}\,d(\Delta u)_{T.E.} \tag{32}$$

in which

$$t_b=\frac{\beta(y-s)}{x-x_b} \tag{33}$$

$x_0$ is the value of $x_b$ which makes $t_b=-1$, and $(\Delta u)_{T.E.}$ is calculated for $x=x_b$, $y=s$ by equation (26b).

## NUMERICAL EXAMPLE

Before proceeding to consider the problem of interaction between the leading and trailing edges, which introduces some radically different effects, the results so far obtained will be illustrated by a numerical example. The loading over an untapered wing, with $\beta$ cot $\Lambda=0.6$ and reduced aspect ratio $\beta A=1.92$, has been calculated at four spanwise stations: 25-, 50-, 75-, and 95-percent semispan. The wing plan form and section lift distributions are shown in figure 11.

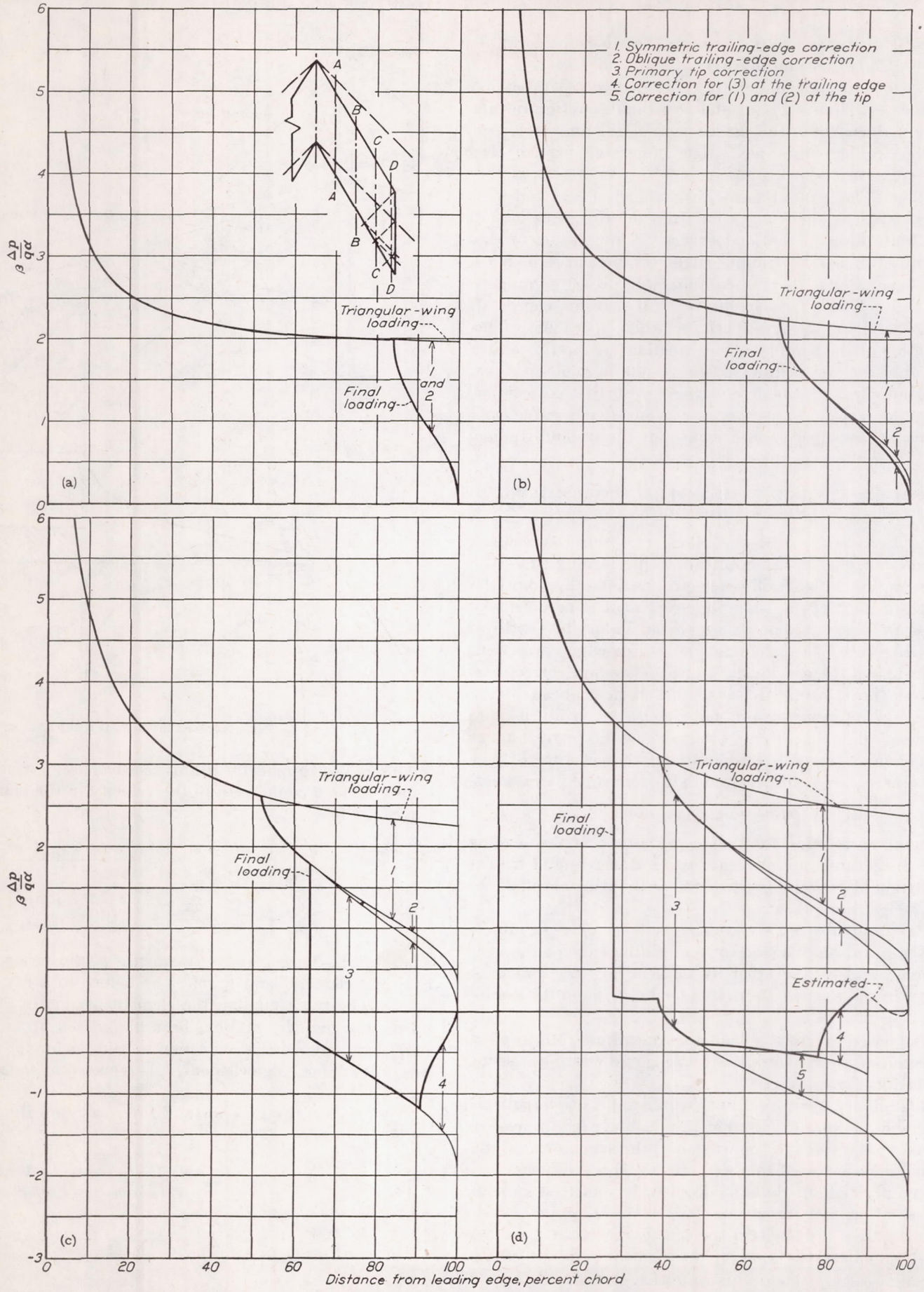


(a) Section A–A $y/s=0.25$ (b) Section B–B $y/s=0.50$ (c) Section C–C $y/s=0.75$ (d) Section D–D $y/s=0.95$

FIGURE 11.—Load distributions calculated for four streamwise sections of an untapered wing; $m=0.6$; $\beta A=1.92$.

The results of the calculations are presented in the form of values of $\beta(\Delta p/q\alpha)$ (equation (5)).

The various components of lift are presented separately as calculated. In figures 11 (a) and (b), the discontinuities in slope show the effect of the cancellation of the finite velocity $u_0$ at the trailing-edge apex. The integrated part of the trailing-edge correction (component 2) has zero slope at the Mach line. The two outboard sections (figs. 11 (c) and (d)) are intersected by the Mach cone from the tip, as indicated by the finite drop in the load curves. Cancellation of the finite tip effect at the trailing edge (component 4 in both figures) results in a sharp discontinuity in pressure gradient along the reflected Mach line, at 91-percent chord at $y/s=0.75$ and at 78-percent chord when $y/s=0.95$. The cancellation of the trailing-edge corrections at the tip, which affects only the last section shown, results in another break in the load curve at 49-percent chord. Further corrections enter at the rear of the section as a result of successive cancellations of the superposed pressures at the tip and trailing edge. Their effect has been only estimated.

## SWEPT-BACK WINGS WITH INTERACTING TRAILING AND LEADING EDGES

When, as in figure 1 (b), the Mach cone from the trailing-edge apex includes a region ahead of the leading edge, the previously calculated trailing-edge corrections to $u$ must be canceled in that region, since they represent a discontinuity in pressure which cannot be supported in the free stream. Thus there must be calculated a leading-edge correction, which is one of the previously defined secondary corrections. However, the location of the disturbed field ahead of the wing causes its influence on the wing to be so much more widespread than that of the other secondary corrections as to require more careful consideration. A new type of flow field is also required, as discussed in the following paragraphs.

### LEADING-EDGE CORRECTIONS

**Elementary solution for the region ahead of the leading edge.**—In general, the elementary solution required for the cancellation of pressure in the plane of the wing ahead of the leading edge is one that:

1. Provides constant streamwise velocity over an infinite sector bounded on one side by the leading edge of the wing (extended) and on the other by an arbitrary ray extending outward into the stream from some point $x_b$, $y_b$ on the leading edge. (See fig. 12.)
2. Induces no vertical velocity, or downwash, on the wing.
3. Induces no lift except on the wing and within the sector described in condition 1.

At first glance these conditions would appear to be satisfied by the oblique solutions used at the trailing edge, if properly oriented with respect to the wing, and the same form of solution might be expected to apply. In reference 4, however, it has been pointed out that the downwash connected with the latter solution remains constant over the wing only if the wing area does not include the line $y$=constant extending downstream from the apex of the element. In the case of the leading-edge element this condition is violated (fig. 12) and an additional term is needed to bring the downwash to zero throughout the area of the wing affected by the element.

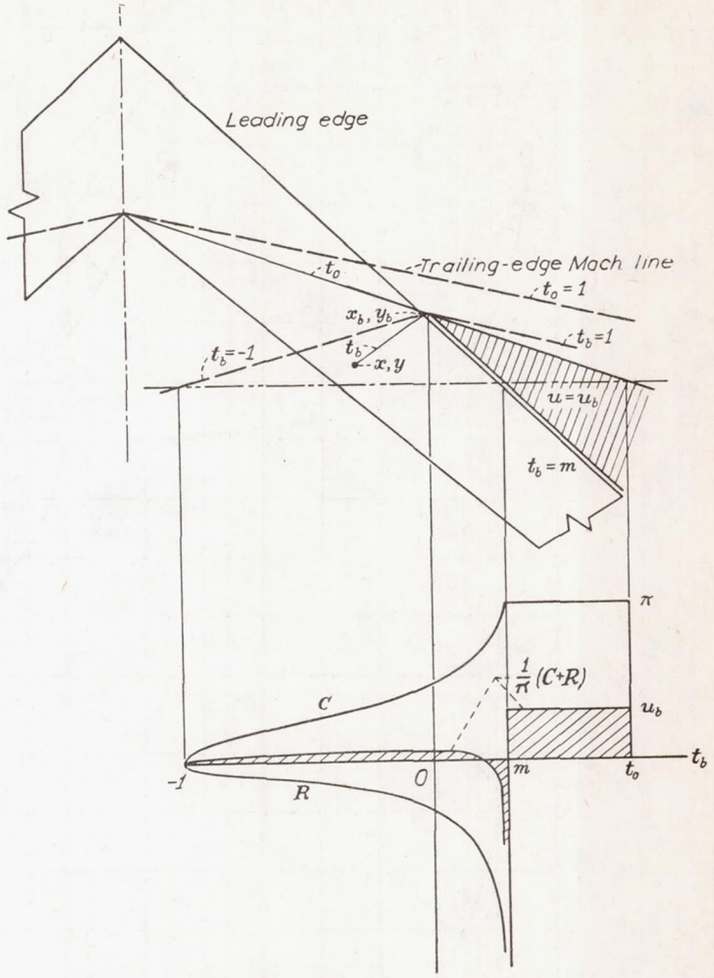


FIGURE 12—Leading-edge element and induced-velocity function.

The solution applicable to this case has been given in reference 4. The $u$ component of the velocity in the plane of the wing is as follows:

$$u=r.\,p.\,\frac{u_b}{\pi}\left[\cos^{-1}\frac{(t_a-m)(1+t_b)-(m-t_b)(1+t_a)}{(1+m)(t_b-t_a)}-\frac{2m}{(1+m)t_a}\sqrt{(t_a-m)(1+t_a)}\sqrt{\frac{1+t_b}{m-t_b}}\right] \tag{34}$$

where $u_b$ is the constant streamwise perturbation velocity over the element, and $t_b$ refers as before to a ray from its apex. The ray bounding the element originates at a point on the trailing edge and has been designated, from equation (24), as $t_a$. When the correction is being made for the symmetrical trailing-edge element, $t_a$ is replaced in equation (34) by $t_0$.

For brevity, the two parts of the correction function will be referred to as

$$C(t_a)=r.\,p.\,\cos^{-1}\frac{(t_a-m)(1+t_b)-(m-t_b)(1+t_a)}{(1+m)(t_b-t_a)} \tag{35}$$

and

$$R(t_a)=r.\,p.\,\frac{-2m}{(1+m)t_a}\sqrt{(t_a-m)(1+t_a)}\sqrt{\frac{1+t_b}{m-t_b}} \tag{36}$$

The variation with $t_b$ of these functions and the induced velocity (equation (34)) are illustrated in figure 12.

**Leading-edge correction to the loading.**—The single conical field of $(\Delta u)_0$ will be considered first. (See fig. 13.) The velocity field to be superposed ahead of the leading edge to cancel the velocity $(\Delta u)_0$ induced in the plane of the wing by the symmetrical solution (equation (20)) can be built up, as shown in figure 13, of overlapping constant-velocity sec-

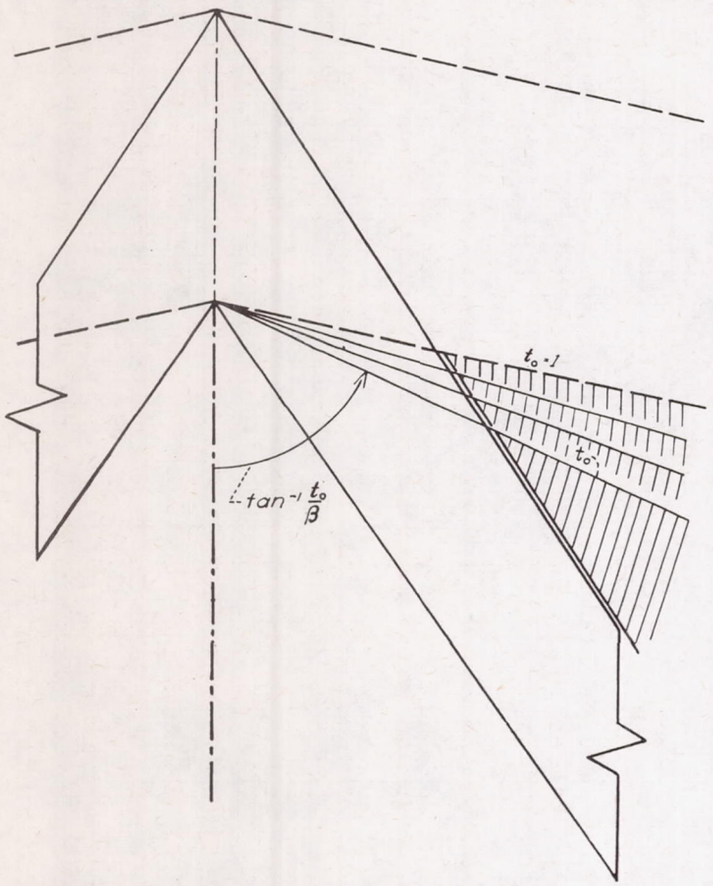


FIGURE 13—Cancellation of the pressure field introduced ahead of the leading edge in the course of canceling $u_0$ behind the trailing edge.

tors having one edge along the leading edge of the wing and one along the extended ray $t_0$ from the apex of the trailing edge. The magnitude of the constant velocity on each element is $\frac{d(\Delta u)_0}{dt_0}dt_0$ or, from equation (20),

$$\frac{u_0\,dt_0}{K'(m_t)\sqrt{(1-t_0^2)\,(t_0^2-m_t^2)}} \tag{37}$$

Applying equation (34) to the cancellation of the symmetrical-correction velocities $(\Delta u)_0$ ahead of the wing results in the following induced velocity increment at any point $(x, y)$ on the wing:

$$(\Delta_2 u)_0=\frac{1}{\pi}\int_{\tau_0}^{1}\frac{d(\Delta u)_0}{dt_0}\,[C(t_0)+R(t_0)]\,dt_0 \tag{38}$$

where $\tau_0$ is that value of $t_0$ for which $t_b=-1$, and designates the most rearward leading-edge element containing the point $x$, $y$ within its Mach cone. In terms of $x$ and $y$,

$$\tau_0=\frac{m(x+\beta y)}{(x+\beta y)-(1+m)c_0} \tag{39}$$

976745—52——3

Integration of $\frac{d(\Delta u)_0}{dt_0}C(t_0)\,dt_0$ is not feasible by elementary means. For graphical integration it is advisable to rewrite $\frac{d(\Delta u)_0}{dt_0}dt_0$ as $d(\Delta u)_0$ to avoid the infinite value of the derivative at $t_0=1$.

The second term of the product in equation (38) can be integrated in closed form as follows:

$$\int_{\tau_0}^{1}\frac{d(\Delta u)_0}{dt_0}R(t_0)dt_0=\frac{-4m^{3/2}u_0K(k)}{m_t(1+m)K'(m_t)}\sqrt{\frac{x+\beta y}{mx-\beta y}}\,Z(\psi,k) \tag{40}$$

where

$$k=\sqrt{\frac{2m_t(1-\tau_0)}{(1-m_t)(\tau_0+m_t)}}$$

and

$$Z(\psi,k)=E(\psi,k)-\frac{E(k)}{K(k)}F(\psi,k) \tag{41}$$

with

$$\psi=\sin^{-1}\sqrt{\frac{\tau_0+m_t}{2\tau_0}}$$

The function $Z(\psi, k)$ is tabulated in reference 16; a plot of $\frac{Z(\psi,k)}{k\sin\psi}$ against $\psi$ is given in figure 14.

Similarly, for each oblique trailing-edge element $a$ (see fig. 15), a canceling field can be built up ahead of the leading edge by the superposition of sectors bounded by the leading edge and by rays $t_a$ from the apex $x_a$, $y_a$ of the element $a$, and having a constant velocity of the magnitude

$$\frac{\partial(\Delta u)_a}{\partial t_a}dt_a=-\frac{1}{\pi}u_a\frac{\partial}{\partial t_a}\cos^{-1}\frac{(1-a)(t_a-m_t)-(m_t-a)(1-t_a)}{(1-m_t)(t_a-a)}\,dt_a \tag{42}$$

(from equation (24)). If the symbol $\Delta u_{L.E.}$ is used to designate the total leading-edge correction to the $u$ component of velocity at any point, then the part due to canceling the field of a single oblique trailing-edge element $a$ is

$$\frac{d\Delta u_{L.E.}}{da}da=\frac{1}{\pi}\int_{\tau_a}^{1}\frac{\partial(\Delta u)_a}{\partial t_a}\,[C(t_a)+R(t_a)]\,dt_a \tag{43}$$

where

$$\tau_a=\frac{m(m_t-a)(x+\beta y)-m_tc_0(1+m)a}{(m_t-a)(x+\beta y)-m_tc_0(1+m)} \tag{44}$$

is the value of $t_a$ for which $t_b=-1$ and the leading-edge correction function vanishes.

When the expression (equation (42)) for $\frac{\partial(\Delta u)_a}{\partial t_a}$ is substituted in equation (43), it is again impractical to attempt to write a closed expression for the integral of the first term $\frac{\partial(\Delta u)_a}{\partial t_a}C(t_a)$ of the product. The integral of the second term is

$$\int_{\tau_a}^{1}\frac{\partial(\Delta u)_a}{\partial t_a}R(t_a)dt_a=$$

$$\frac{-4m}{\pi(1+m)}\frac{u_a}{a}\sqrt{\frac{(m_t-a)(1-m)(x+\beta y)-m_tc_0(1+m)(1-a)}{(1-m_t)(mx-\beta y)}}\times$$

$$K(k_a)\left[\sqrt{1+a}\,\frac{Z(\psi_a,k_a)}{k_a\sin\psi_a}-\sqrt{1-a}\,\frac{Z(\psi_0,k_a)}{k_a\sin\psi_0}\right] \tag{45}$$

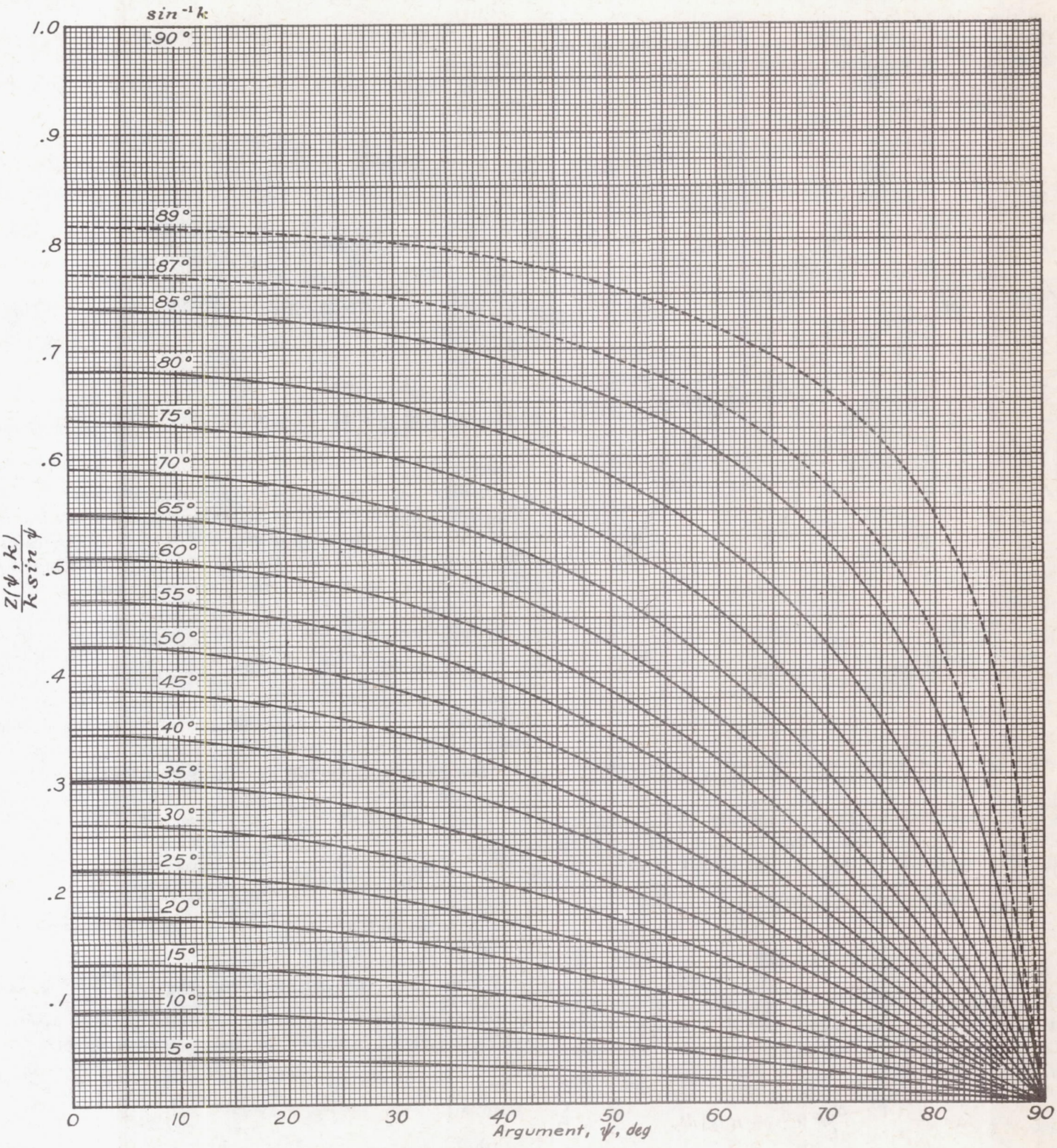


FIGURE 14.—The elliptic function $\frac{Z(\psi,k)}{k \sin \psi}$

where

$$k_a=\sqrt{\frac{(1+m_t)(1-\tau_a)}{(1-m_t)(1+\tau_a)}}$$

$$\psi_a=\sin^{-1}\sqrt{\frac{(m_t-a)(1+\tau_a)}{(\tau_a-a)(1+m_t)}}$$

$$\psi_0=\sin^{-1}\sqrt{\frac{m_t(1+\tau_a)}{\tau_a(1+m_t)}}$$

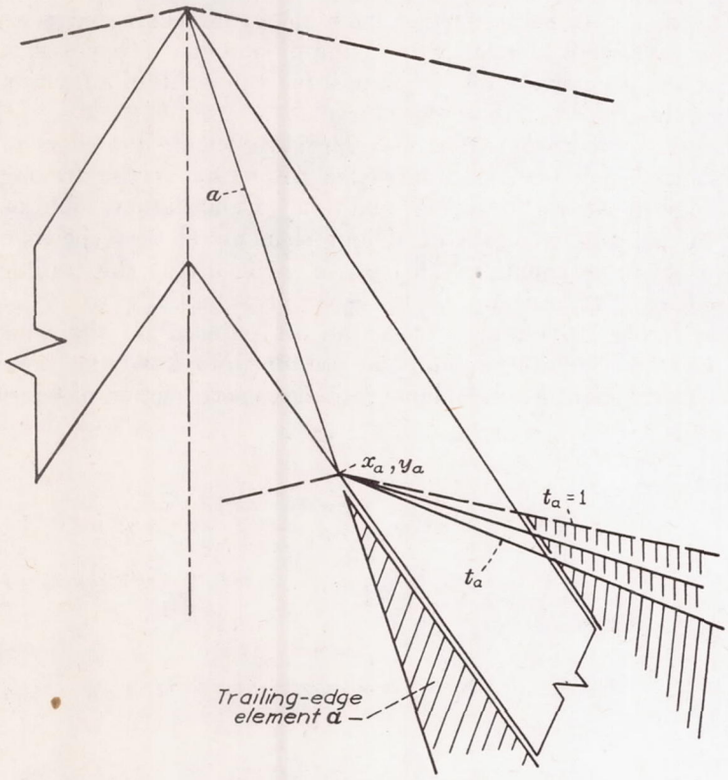


FIGURE 15—Cancellation of the pressure field introduced ahead of the leading edge by a single oblique trailing-edge element.

Then the total leading-edge correction to the velocity $u$ at any point $x$, $y$ is

$$(\Delta u)_{L.E.}=(\Delta_2 u)_0+\int_0^{a_0'}\frac{d(\Delta u)_{L.E.}}{da}\,da \qquad (46)$$

where $(\Delta_2 u)_0$ is obtained from equations (38) and (40), $\frac{d(\Delta u)_{L.E.}}{da}$ from equations (43) and (45), and

$$a_0'=\frac{(1+m)c_0-(1-m)(x+\beta y)}{(1+m)m_t c_0-(1-m)(x+\beta y)}m_t \qquad (47)$$

is the value of $a$ at which $\tau_a(x, y, a)$ (equation (44)) is equal to 1.

The last term in equation (46) will seldom be found to contribute any significant amount to the loading, but will be needed in calculating the leading-edge thrust.

### FURTHER CORRECTIONS

Omitting for the moment any specification of tip location, it is in any case necessary, as seen in figure 12, to consider the effect of a further cancellation necessitated by the excess lift introduced behind the trailing edge by the leading-edge cancellation field. To compute this effect by the conical-flow method would be feasible only with the aid of high-speed computing machinery. The previously mentioned cancellation method of reference 5, being more direct, would be somewhat easier to use in this connection, but the calculations would still be very lengthy. It will be shown by numerical example that the effect of the first cancellation at the trailing edge of the leading-edge correction, which is initially quite small, may be estimated with adequate accuracy when the section loading is considered as a whole, provided the fraction of the chord affected is not too large.

If the product $\beta$ cot $\Lambda$ is low or the aspect ratio high, still further cancellations will be required (see fig. 16) at both leading and trailing edges. It is clear that calculation of the effect of these further cancellations by the conical-flow method is all but impossible. The doublet-distribution method of reference 5 does not appear to offer any considerable advantage in this application since, in canceling lift ahead of a subsonic leading edge, it is necessary to find not only the pressure distribution to be canceled, but the associated sidewash distribution as well.

It is apparent that an alternative method must be sought for describing the flow in the outboard regions of a high-aspect-ratio wing or a wing the sweep of which is large compared to the sweep of the Mach line. If the wing could be

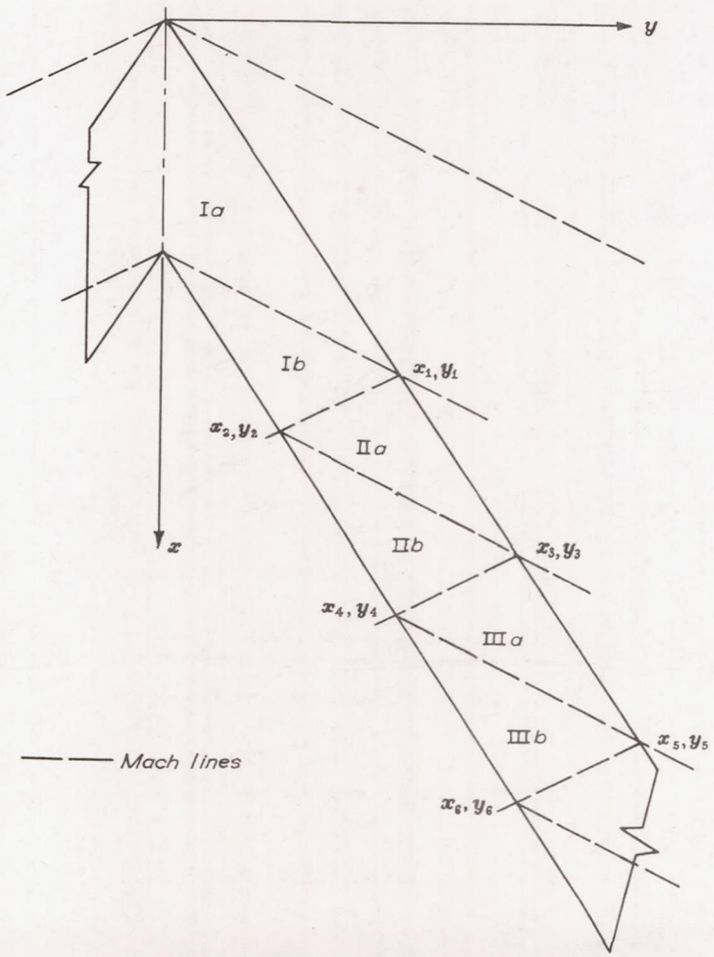


FIGURE 16.—Plan view of central portion of high-aspect-ratio wing, showing pattern of Mach lines arising at leading and trailing edges.

extended indefinitely, it is known that the flow must eventually approach the two-dimensional subsonic flow, in accordance with simple sweep theory. The question then arises, can the flow at a distance of the order of a semispan from the apex of the swept-back wing be related to the two-dimensional asymptotic flow? While the flow field appears to be too complex to obtain an answer to this question on analytical grounds, numerical values, presented in the following paragraph, suggest a practical approach.

### NUMERICAL RESULTS (WITHOUT TIP EFFECT)

Load distributions have been calculated by the conical-flow method for three combinations of taper, sweep, and Mach number as follows:

| | Untapered | | Tapered |
|---|---|---|---|
| $m=$ | 0.2 | 0.4 | 0.4 |
| $m_t=$ | 0.2 | 0.4 | 0.6 |

These values of $m$ and $m_t$ represent, by virtue of the Prandtl-Glauert transformation, a variety of sweep angles at Mach numbers between 1 and 2; as for example, 0.2 would be the value of $m$ for a wing with 63° sweep of the leading edge at a Mach number of 1.075, or 75° sweep at a Mach number of 1.25. Similarly, $m=0.4$ would correspond to 45° of sweep at $M=1.08$, 60° at $M=1.22$, or 75° at $M=1.80$. The trailing-edge sweep angles at these latter Mach numbers, if $m_t=0.6$, are 34°13′, 49°, and 68°, respectively.

Figure 17 presents the lift distributions at two stations of the tapered wing. Each component is plotted independently in order to show the magnitudes at the leading edge. Section A–A contains the intersection of the trailing-edge Mach line with the leading edge, so that the value of the leading-edge correction is zero at the leading edge of this section. At points farther back along the leading edge, as at $\beta y/c_0=0.8$, the correction is minus infinity. However, it is seen to increase to a small positive value within a fraction of the chord length at this station.

At both stations it is necessary to estimate the effect of cancellation of the leading-edge correction at the trailing edge to satisfy the Kutta condition. Cancellation would be carried out by means of oblique elements of the type used previously (equation (24)) in canceling lift at the trailing edge. The pressure to be canceled is initially (i. e., at $x_2,y_2$ (fig. 16)) zero. Then the lift induced on the wing by this cancellation may be presumed to have the same general shape as the oblique trailing-edge correction of figure

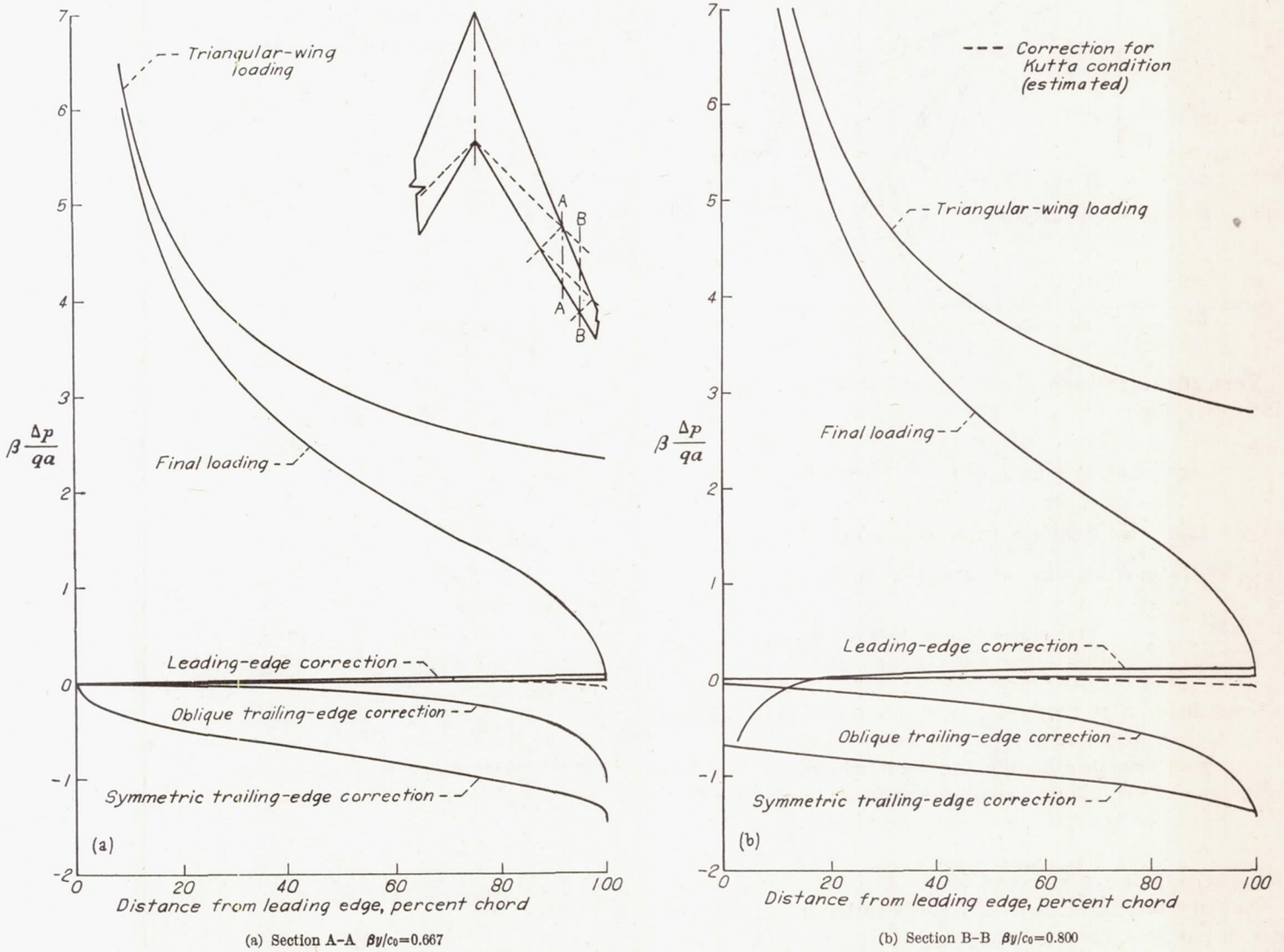


(a) Section A–A $\beta y/c_0=0.667$

(b) Section B–B $\beta y/c_0=0.800$

FIGURE 17.—Load distributions calculated by the conical-flows method for two streamwise sections of a tapered swept-back wing; $m=0.4$; $m_t=0.6$.

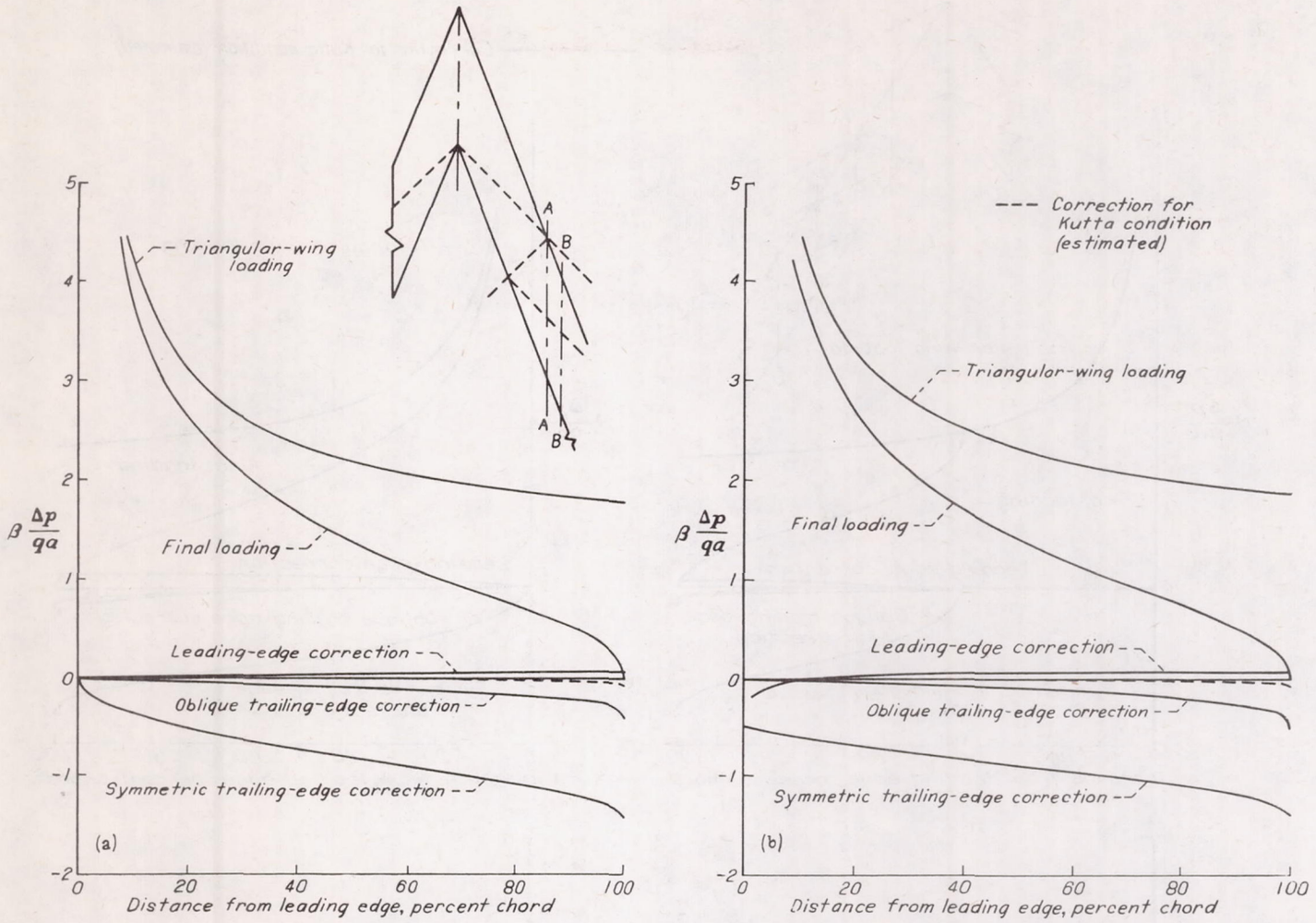


(a) Section A-A $\beta y/c_0=0.667$ (b) Section B-B $\beta y/c_0=0.800$

FIGURE 18.—Load distributions calculated by the conical-flows method for two streamwise sections of an untapered wing; $m=0.4$.

11, falling along a modified inverse cosine curve from the value of the error at the trailing edge to zero, with zero slope, at the boundary of the region affected. With this boundary (the Mach line from the point $x_2,y_2$), it is possible to draw a satisfactory estimate (dotted curve) of the correction needed to bring the pressure once more to zero at the trailing edge.

The untapered wing with the same sweep ($m=0.4$) relative to the Mach lines is shown in figure 18, with the load distributions calculated at the same stations.

Four section lift distributions are presented (fig. 19) for $m=0.2$. At $\frac{\beta y}{c_0}=0.15$ only the rear 60 percent is influenced by the subsonic trailing edge. The reflection of this influence at the leading edge alters the pressure over the rear 40 percent of the section. At section B–B, the leading- and trailing-edge interaction affects the entire section. A further reflection of this effect at the trailing edge must be estimated.

At section C–C the influence of cancellation of the leading-edge correction at the trailing edge extends over the whole of the chord and any estimate of its magnitude would be necessarily arbitrary. Also, a second pair of reflections must be taken into account. The final pressure distribution has therefore been drawn as a band within which the true curve may be shown to lie. Its height is the error introduced at the trailing edge by the first leading-edge correction, except very near the leading edge, where an infinite negative correction is known to be introduced by the second leading-edge correction. The calculations were also carried out for $\beta y/c_0=0.45$. The margin of uncertainty was found not to have increased by any appreciable amount. (See fig. 19 (d).)

## APPLICATION OF TWO-DIMENSIONAL FORMULAS TO CALCULATION OF LOAD DISTRIBUTION

**Correlation of two-dimensional and swept-back-wing loadings.**—It is apparent from the calculated results that, whenever the plan form and the Mach number are such that the trailing-edge Mach line intersects the leading edge, the load distribution behind the Mach lines from the point of intersection resembles in shape the theoretical load distribution over an infinitely long flat plate in incompressible flow. However, as the results have been plotted, the quantitative agreement is not good, particularly in the case of the tapered wing. On the other hand, if the load distributions in cross sections normal to the stream are examined, a near proportionality of the curves is observed. In order to determine the factor of proportionality, it is only necessary to find the ratio of the strengths of the singularities at the

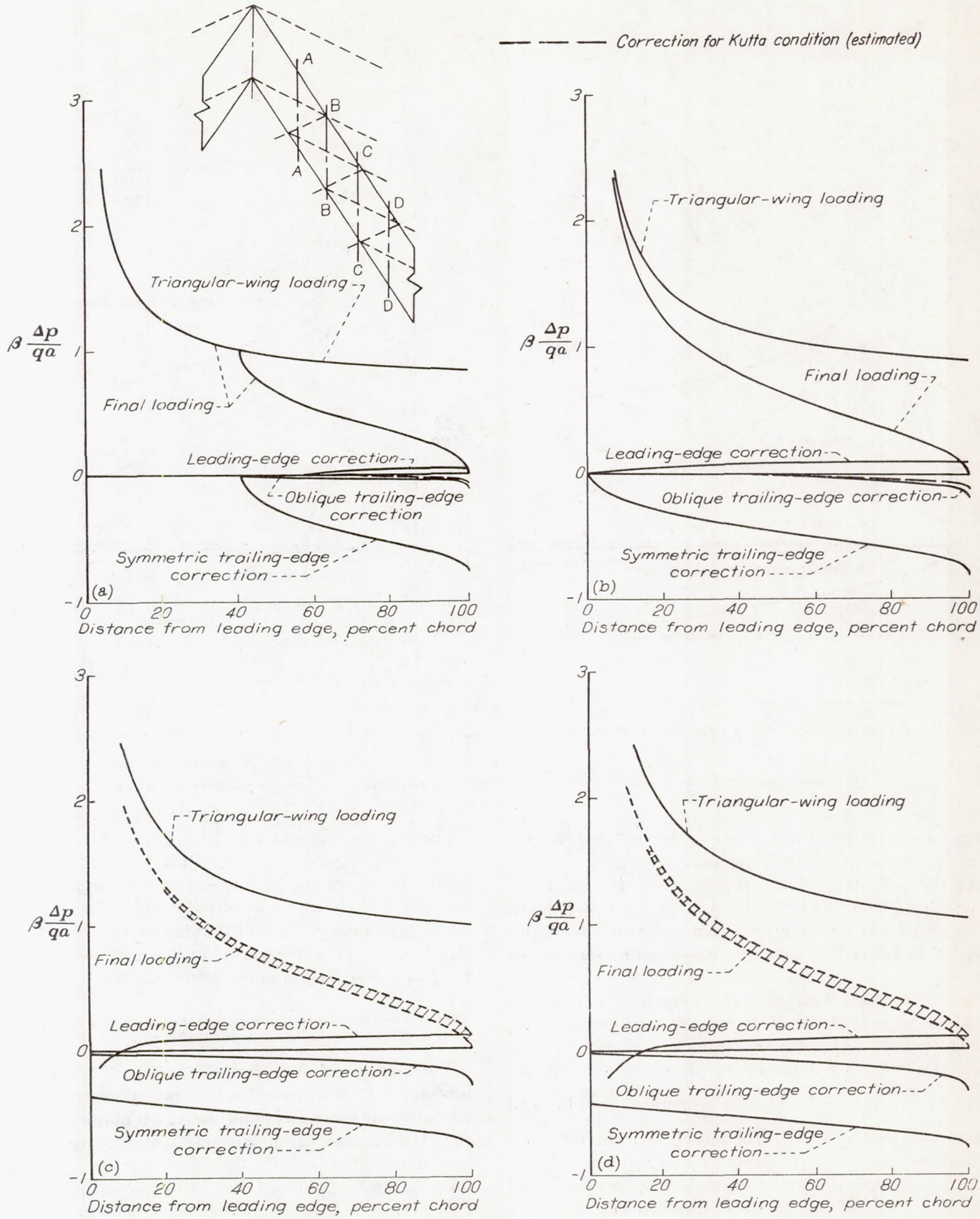


(a) Section A–A $\beta y/c_0=0.15$
(b) Section B–B $\beta y/c_0=0.25$
(c) Section C–C $\beta y/c_0=0.35$
(d) Section D–D $\beta y/c_0=0.45$

FIGURE 19.—Load distributions calculated by the conical-flows method for four streamwise sections of an untapered wing; $m=0.2$.

leading edge. Then an approximate expression for the loading on the outer portions of a high-aspect-ratio wing can be obtained by adjusting the two-dimensional loading by that factor.

Both the swept-back-wing and the subsonic two-dimensional loadings approach infinity as the reciprocal of the square root of the distance to the leading edge. In sections normal to the stream, the distance from any point $x,y$ to the leading edge may be written $\frac{1}{\beta}(mx-\beta y)$. The value at the leading edge of the coefficient of $(mx-\beta y)^{-1/2}$ will be referred to as the strength of the leading-edge singularity.

The subsonic two-dimensional perturbation velocity has the form

$$u=B\sqrt{\frac{1-\eta}{\eta}} \tag{48}$$

where $\eta$ is the distance to the leading edge, expressed as a fraction of the chord, and $B$ is a constant. If the section of the swept-back wing is taken perpendicular to the stream ($x$ constant), the chord length is

$$\frac{1}{\beta}[mx-m_t(x-c_0)] \tag{49}$$

and

$$\eta=\frac{mx-\beta y}{mx-m_t(x-c_0)} \tag{50}$$

Substitution for $\eta$ in equation (48) gives

$$u=B\sqrt{\frac{\beta y-m_t(x-c_0)}{mx-\beta y}}. \tag{51}$$

Then the strength of the leading-edge singularity in $u$ is

$$B\sqrt{mx-m_t(x-c_0)} \tag{52}$$

The leading-edge singularity in the loading on the swept-back wing is initially (region I, fig. 16) that in the triangular-wing loading. Introduction of the leading-edge corrections to the load, in region II, reduces the strength of the singularity there through the terms $R(t_0)$ and $R(t_a)$. (The inverse-cosine function is always finite.) The coefficient of $(mx-\beta y)^{-1/2}$ in $u_\Delta$ is, from equation (6),

$$\frac{mxu_0}{\sqrt{mx+\beta y}}$$

reducing to

$$C_\Delta=u_0\sqrt{\frac{mx}{2}} \tag{53}$$

at the leading edge.

From equations (40) and (45), decrements to this coefficient may be derived for the portion of the leading edge just behind the intersection $x_1,y_1$ with the trailing-edge Mach line, as follows:

$$(\Delta C)_0=\frac{-4mu_0K(k)}{\pi m_tK'(m_t)}\sqrt{\frac{mx}{1+m}}\,Z(\psi,k) \tag{54}$$

and, for each value of $a$ from 0 to that value $a_0'$ which makes $\tau_a$ equal to one,

$$\frac{d\Delta C}{da}\,da=\frac{-4m}{\pi^2\sqrt{1+m}}\frac{u_a}{a}\sqrt{\frac{(m_t-a)x-(1-a)m_tc_0}{1-m_t}}\,K(k_a)\times\left[\sqrt{1+a}\,\frac{Z(\psi_a,k_a)}{k_a\sin\psi_a}-\sqrt{1-a}\,\frac{Z(\psi_0,k_a)}{k_a\sin\psi_0}\right] \tag{55}$$

where $\tau_0$ (equation (39)) and $\tau_a$ (equation (44)) reduce to

$$\tau_0=\frac{mx}{x-c_0}$$

and

$$\tau_a=\frac{(m_t-a)mx-m_tc_0a}{(m_t-a)x-m_tc_0}$$

and the arguments and moduli of the elliptic integrals follow as for equations (40) and (45).

The coefficient of $(mx-\beta y)^{-1/2}$ at the leading edge is, therefore, in region II, figure 16,

$$C_\Delta+(\Delta C)_0+\int_0^{a_0'}\frac{d\Delta C}{da}\,da \tag{56}$$

with $a_0'$ reducing to

$$a_0'\left(x,\frac{m}{\beta}x\right)=m_t\,\frac{c_0-(1-m)x}{m_tc_0-(1-m)x} \tag{57}$$

Equating the two coefficients, expressions (56) and (52), gives for any one section

$$B=\frac{1}{\sqrt{mx-m_t(x-c_0)}}\left[C_\Delta+(\Delta C)_0+\int_0^{a_0'}\frac{d\Delta C}{da}\,da\right] \tag{58}$$

For convenience, a nondimensional cofficient

$$\sigma(x)=\frac{1}{V\alpha\sqrt{c_0}}\left[C_\Delta+(\Delta C)_0+\int_0^{a_0'}\frac{d\Delta C}{da}\,da\right] \tag{59}$$

is defined, so that

$$B=V\alpha\,\frac{\sigma(x)\sqrt{c_0}}{\sqrt{mx-m_t(x-c_0)}}$$

By substituting for $B$ in equation (51), the loading on the outer portions of a swept-back wing is obtained as

$$\frac{u}{V\alpha}=\sigma(x)\sqrt{\frac{c_0[\beta y-m_t(x-c_0)]}{[mx-m_t(x-c_0)](mx-\beta y)}} \tag{60}$$

**Numerical results.**—The closeness with which the foregoing procedure predicts the theoretical loading over swept-back wings is indicated by figures 20, 21, and 22, where the previously calculated load distributions are compared with those calculated by equation (60). Even in the case of the highly tapered wing, the agreement is seen to be good. At the most inboard section of the $m=0.2$ wing (fig. 19 (a)) there is, of course, no agreement over that portion, forward of the 60-percent-chord point, where the flow is essentially conical. At station B–B, however, the agreement is very good. At sections C–C and D–D, where the exact theoretical

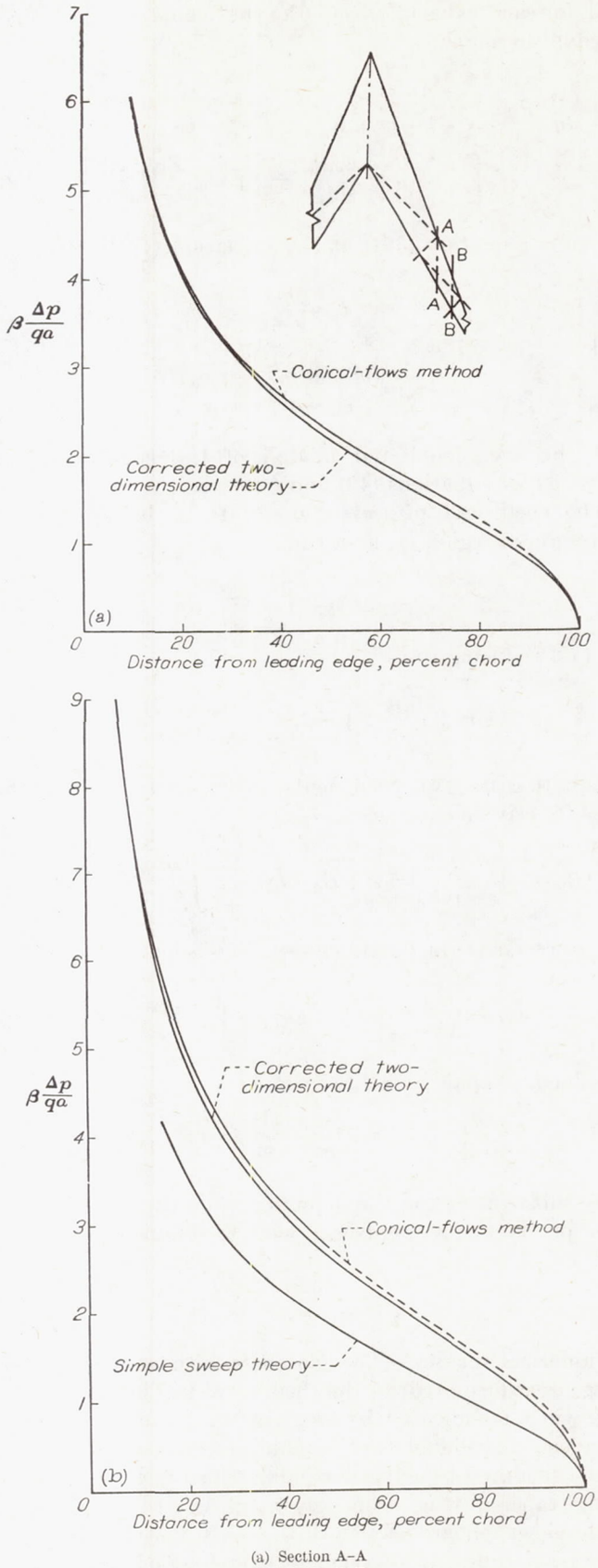


(a) Section A–A
(b) Section B–B

FIGURE 20—Load distributions on the tapered wing as calculated by the conical-flows method, compared with the two-dimensional approximation.

loading had not been determined, the two-dimensional-type loading lies within the band prescribed by the conical-flow calculations. Since the discrepancy between the corrected two-dimensional loading and the exact theoretical distribution is already, at section B–B (fig. 22 (b)), less than the width of the bands in figures 22 (c) and (d) and must diminish to zero at infinity, it may be supposed that the corrected two-dimensional curve is at least as satisfactory an approximation to the correct curves at sections C–C and outboard as at section B–B. It is probably more satisfactory than can be obtained by a limited application of the conical-flow method.

The load distributions derived by simple sweep theory are included in the last part of each figure to show the magnitude of the plan-form effect and also, in the case of the untapered wings, the curves that the load distributions must

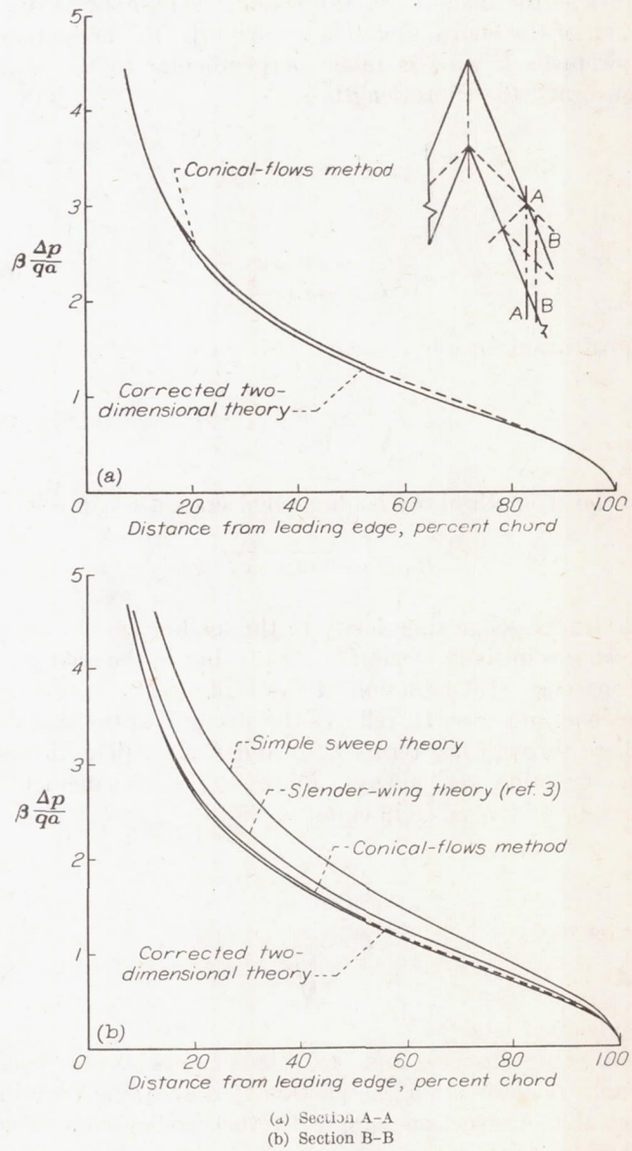


(a) Section A–A
(b) Section B–B

FIGURE 21.—Load distributions on the untapered wing, $m=0.4$, as calculated by the conical-flows method, compared with the two-dimensional approximation.

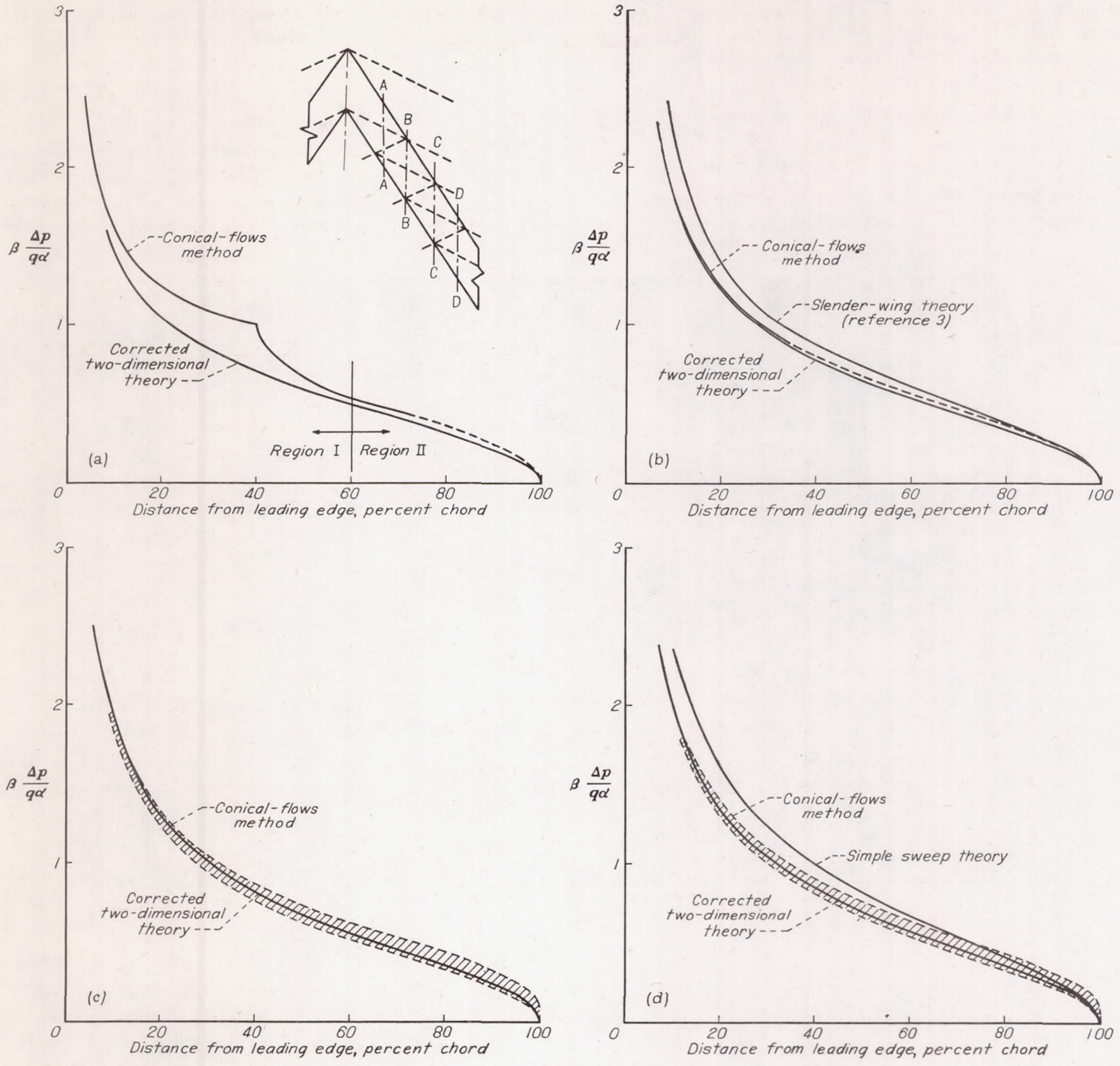


(a) Section A-A
(b) Section B-B
(c) Section C-C
(d) Section D-D

FIGURE 22.—Load distributions on the untapered wing, $m=0.2$, as calculated by the conical-flows method, compared with the two-dimensional approximation.

approach as the distance from the plane of symmetry is increased. In figures 21 (b) and 22 (b), comparison is also made with results of the slender-wing theory of reference 3.

**Discussion of the $\sigma$ function.**—In the calculation of the pressure coefficient at points toward the rear of most of the sections considered in figures 20, 21, and 22, it was necessary to find $\sigma(x)$ for values of $x$ greater than $x_3$ (fig. 16). In deriving $\sigma(x)$, it was mentioned that expression (56) applied to region II. In region III, the strength of the leading-edge singularity is affected by further modifications of the flow taking place in region IIb, so that additional terms in $\sigma(x)$ should be considered when $x$ is greater than $x_3$. Evaluation of these terms by presently known methods would require, as suggested earlier, the aid of high-speed computing machinery. However, the successive terms are all initially zero and enter with zero slope at $x_3$, zero slope and curvature at $x_5$, and so on, so that the three-term expression for $\sigma$ given by equation (59) may be used with satisfactory accuracy

for some distance beyond the last value of $x$ for which it is strictly valid. In practice, the third term in equation (58) may also be neglected for values of $x$ only slightly greater than $x_1$.

Charts have been prepared (fig. 23) giving $\left(\frac{\beta}{m}\sqrt{\frac{1-m}{m}}\right)\sigma$ as a function of $\frac{x-x_1}{c_0}$ for several values of the ratio $m/m_t$. This last parameter is the ratio of the tangents of the semi-apex angles of the leading and trailing edges and is constant through the Mach number range for any one wing. The value of $x_1$ is readily determined:

$$x_1=\frac{c_0}{1-m} \tag{61}$$

The curves were computed using equation (59) and are therefore exact only up to $x=x_3$ (shown by a vertical mark on each curve). Cross marks are drawn at the points $x=x_5$ to indicate a more practical limit to which use of the curves

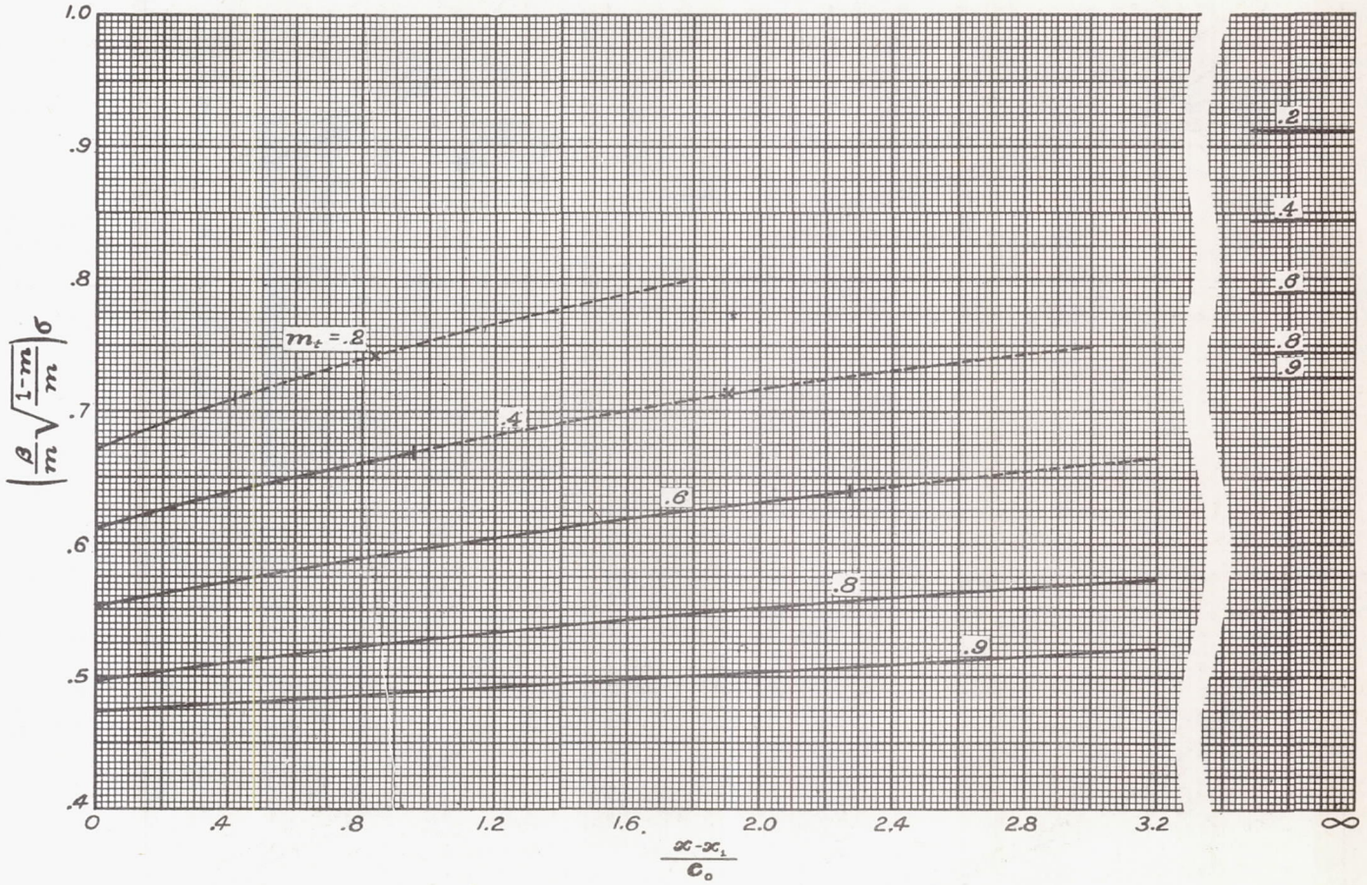


(a) $m/m_t=1.0$

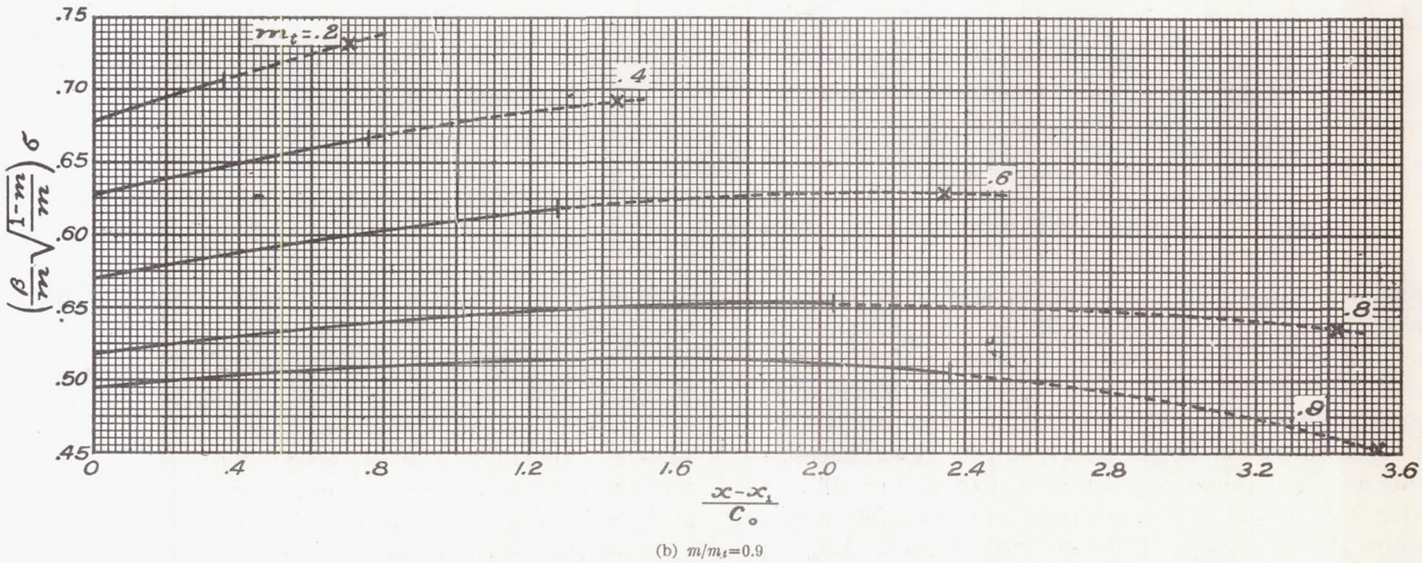


(b) $m/m_t=0.9$

FIGURE 23.—Charts for determining $\sigma$, the strength of the leading-edge singularity.

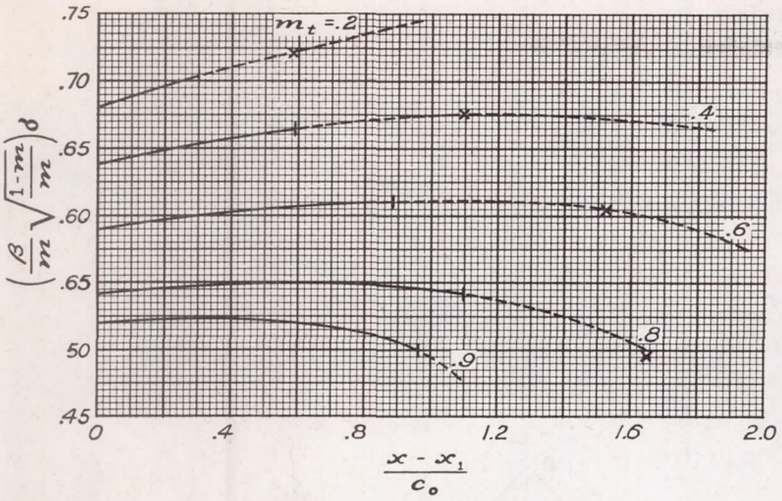


(c) $m/m_t=0.8$

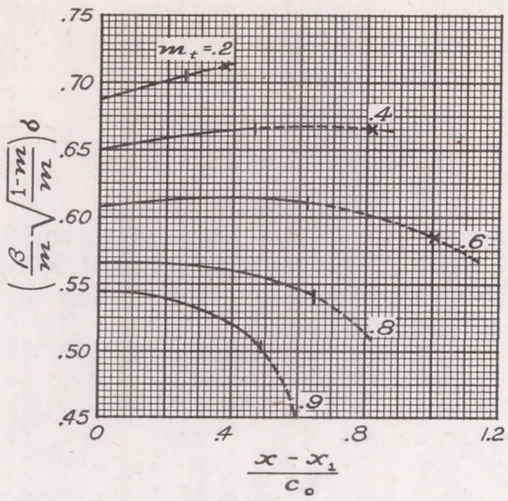


(d) $m/m_t=0.7$

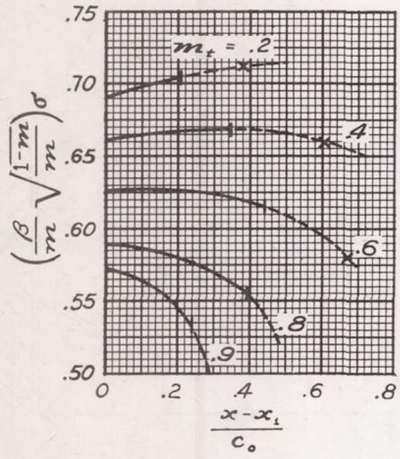


(e) $m/m_t=0.6$

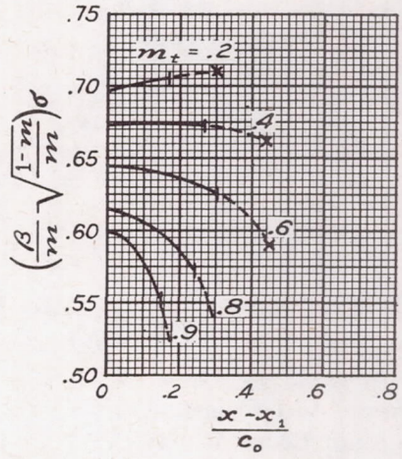


(f) $m/m_t=0.5$

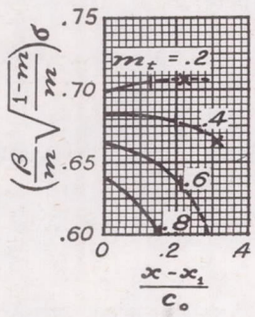


(g) $m/m_t=0.4$

FIGURE 23—Continued.

may be extended. (These points are off the scale for $m_t=0.8$ and 0.9 in figure 23 (a).) When the wings are untapered ($m/m_t=1.0$), asymptotes

$$\frac{\beta\sigma(\infty)}{m}\sqrt{\frac{1-m}{m}}=\frac{1}{\sqrt{1+m}}$$

derived from simple sweep theory, may be drawn.

The curves, for the most part, are regular enough to permit interpolation within intervals of 0.2 in $m_t$. However, at $m_t=1.0$ the lines diminish to a point on the vertical axis; a curve for $m_t=0.9$ was therefore inserted in the charts for values of $m/m_t$ equal to or greater than 0.5. When $m/m_t$ is less than 0.5, $m=0.9$ represents, if the leading edge extends beyond $x_1,y_1$, such extreme taper that the successive reflection of the Mach lines (at $x_3$, $x_5$, . . .) take place within a very small fraction of a chord length and no useful curve can be drawn. No curves are drawn for values of $m_t$ smaller than 0.2 because of the tip-interference limitation mentioned in the introduction.

**Calculation of tip effect.**—The foregoing assumption of two-dimensional flow can be extended to give fairly simple approximate formulas for the tip effect on a high-aspect-ratio wing. It is assumed that the velocity distribution to be canceled in the stream outboard of the tip is cylindrical; that is, is an extension of the velocity distribution calculated for the tip section along lines parallel to the leading edge. For this purpose the approximate load distribution given by equation (60) is used, still further simplified by assuming $\sigma$ to remain constant at its value at the leading edge of the tip section. (Where the wing is tapering to a point and $\sigma$ is changing very rapidly, the tip region is so small that the entire calculation of tip effects could probably be omitted.)

The assumption of constant $\sigma$ results in a failure to cancel exactly the lift along the tip. The assumption of cylindrical flow, while reasonable for the untapered wing (compare fig. 21 (a) with fig. 21 (b), for example) would appear to be too drastic for the tapered wing, where neither the chord nor the loading remains constant. However, as has been mentioned earlier, the major part of the tip effect results from the cancellation of the infinite pressure along the leading edge, and this part will be accurately calculated. The effect of the residual lift on the rearward portion of the tip section and in the stream should be small.

The distribution of perturbation velocity at the tip station $y=s$, with the simplification of constant $\sigma$, is, from equation (60), approximately

$$u(x_c, s)=\sigma_s V\alpha\sqrt{\frac{[\beta s-m_t(x_c-c_0)]\,c_0}{[mx_c-m_t(x_c-c_0)]\,(mx_c-\beta s)}} \tag{62}$$

where $x_c,s$ are the coordinates of a point on the tip and $\sigma_s$ is the value of $\sigma$ at the leading edge of the tip section.

This expression may be more conveniently written in terms of the parameter

$$\mu=1-\frac{m}{m_t} \tag{63}$$

and the variable

$$\xi_c=\frac{x_c-\frac{\beta s}{m}}{c_t} \tag{64}$$

which is the distance of $x_c,s$ from the leading edge (see fig. 24) expressed as a fraction of the tip chord $c_t$. Since

$$c_t=\left(c_0+\frac{\beta s}{m_t}\right)-\frac{\beta s}{m}$$

equation (62) may be written

$$u(\xi_c, s)=\frac{\sigma_s V\alpha}{\sqrt{m\lambda}}\sqrt{\frac{1-\xi_c}{(1-\mu\xi_c)\,\xi_c}} \tag{65}$$

where $\lambda$ is the taper ratio $c_t/c_0$.

If the velocity distribution $u$ is assumed to be constant beyond $y=s$ along lines parallel to the leading edge, it may be canceled by the superposition of conical flow fields of which the constant-velocity regions have one edge along the tip and the other parallel to the leading edge, with apexes displaced along the tip by increments in $\xi_c$. The velocity induced at a point $x,y$ by each such element would be (equation (11))

$$\frac{u_c}{\pi}\cos^{-1}\frac{m+t_c+2mt_c}{t_c-m} \tag{66}$$

where

$$t_c=\frac{\beta(y-s)}{x-x_c} \tag{67}$$

and $u_c$ is the velocity on each sector.

Following the procedure used in deriving equation (14), the corresponding equation may be written for the pressures induced by canceling the cylindrical flow

$$\left(\frac{\Delta u}{V\alpha}\right)_{tip}=\frac{-\sqrt{m(1+m)\,(x-x_0)}}{\pi V\alpha}\int_{\frac{\beta s}{m}}^{x_0}\frac{u(x_c, s)\,dx_c}{[(1+m)x-x_0-mx_c]\sqrt{x_0-x_c}} \tag{68}$$

where $x_0,s$ is the intersection of the Mach forecone from $x,y$ with the tip.

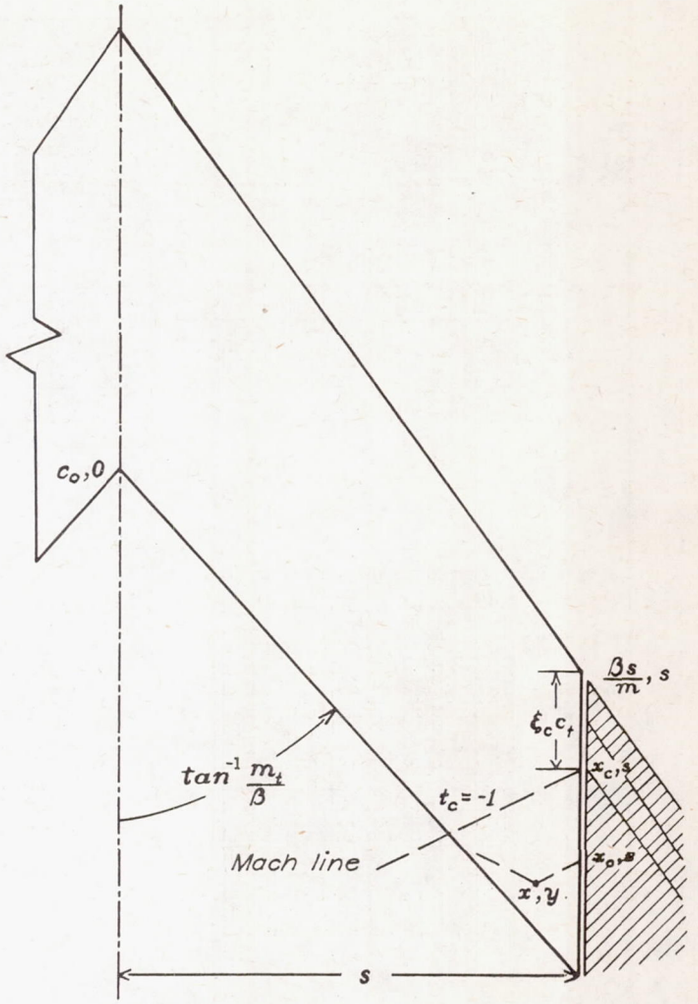


FIGURE 24.—Sketch for derivation of approximate tip correction to loading at $x,y$.

If the distances of $x,y$ and $x_0,s$ back of the leading edge, measured as fractions of the tip chord, are

$$\xi=\frac{1}{c_t}\left(x-\frac{\beta y}{m}\right) \tag{69}$$

and

$$\xi_0=\frac{1}{c_t}\left(x_0-\frac{\beta s}{m}\right) \tag{70}$$

it can be shown that

$$(1+m)\,(x-x_0)=mc_t(\xi-\xi_0) \tag{71}$$

from which equation (68) can be written (with the substitution for $u(x_c,s)$ from equation (65))

$$\left(\frac{\Delta u}{V\alpha}\right)_{tip}=-\frac{\sigma_s\sqrt{\xi-\xi_0}}{\pi\sqrt{m\lambda}}\int_0^{\xi_0}\frac{d\xi_c}{\xi-\xi_c}\sqrt{\frac{1-\xi_c}{(\xi_0-\xi_c)(1-\mu\xi_c)\xi_c}} \tag{72}$$

In integrating equation (72), three cases must be distinguished: (1) $\xi<1$ (always true for the untapered wing), (2) $1<\xi<\frac{1}{\mu}$ (when the point $x,y$ lies more than a tip-chord length behind the leading edge), and (3) $\xi>\frac{1}{\mu}$

(a possible condition for some points near the trailing edge of a highly swept or tapered wing).

In the first case ($\xi<1$)

$$\left(\frac{\Delta u}{V\alpha}\right)_{tip}=\frac{-\sigma_s}{\sqrt{m\lambda}}\left[\frac{m}{m_t(1-\mu\xi)}\sqrt{\frac{\xi-\xi_0}{1-\mu\xi_0}}K_0+\sqrt{\frac{1-\xi}{\xi(1-\mu\xi)}}\Lambda_0(\psi_1,k)\right] \tag{73a}$$

where

$$k=\sqrt{\frac{m\xi_0}{m_t(1-\mu\xi_0)}}$$

$$\psi_1=\sin^{-1}\sqrt{\frac{(1-\xi)(1-\mu\xi_0)}{(1-\xi_0)(1-\mu\xi)}}$$

and $\Lambda_0$ is the function (equation (16)) plotted in figure 6.

In the second case $\left(1<\xi<\frac{1}{\mu}\right)$

$$\left(\frac{\Delta u}{V\alpha}\right)_{tip}=-\frac{\sigma_s}{\sqrt{m\lambda}}\frac{K_0}{\xi\sqrt{1-\mu\xi_0}}\left[\sqrt{\xi-\xi_0}-\sqrt{(\xi-1)\xi_0}\frac{Z(\psi_2,k)}{k\sin\psi_2}\right] \tag{73b}$$

where

$$\psi_2=\sin^{-1}\sqrt{\frac{m_t(1-\mu\xi)}{m\xi}}$$

and $Z$ is the function (equation (41)) plotted in figure 14.

In the third case $\left(\xi>\frac{1}{\mu}\right)$,

$$\left(\frac{\Delta u}{V\alpha}\right)_{tip}=\frac{-\sigma_s}{\sqrt{m\lambda\xi}}\frac{\Lambda_0(\psi_3,k)}{\sin\psi_3} \tag{73c}$$

where

$$\psi_3=\sin^{-1}\sqrt{\frac{\mu\xi-1}{\xi-1}}$$

Along the Mach line from the leading-edge tip all three equations reduce to the value

$$\frac{\Delta u^*}{V\alpha}=\frac{-\sigma_s}{\sqrt{m\lambda\xi}} \tag{74}$$

By the procedure just described, approximate cancellation of all pressure differences outboard of the tip has been effected, but the pressures induced by such cancellation now violate the condition of zero lift in the wake. Approximate cancellation of the induced pressure differences in the wake region can be accomplished, as before, by making use of the known value of the tip-induced velocity at the trailing edge of the wing, but assuming the entire error to originate at the leading edge of the tip. Equation (31) is directly applicable, with $\Delta u^*$ given by equation (74) and $(\Delta u)_{tip}$ by equation (73). On the trailing edge of an untapered wing, $\xi=1$ and

$$\left(\frac{\Delta u}{V\alpha}\right)_{\xi=1}=\frac{-\sigma_s}{\sqrt{m}}k'K_0 \tag{75}$$

There is no corresponding simplification for the tapered wing.

**Numerical examples, tip effect.**—Equations (73) and (31) have been used to calculate the tip effect in two cases, namely: $m=m_t=0.4$, $\beta s=0.94c_o$; and $m=0.4$, $m_t=0.6$, $\beta s=0.86c_o$. The tip effect has been calculated for each wing at $\beta y=0.8c_o$, where the loading was previously calculated (figs. (17b) and (18b)) assuming the wing to extend indefinitely. The tip locations were selected so that in each case only one reflection of the primary tip effect affected the section at $\beta y=0.8c_o$.

Figure 25 shows the results of the calculations. The heavy solid curve in each case was calculated entirely by the corrected two-dimensional theory—that is, by equations (60), (73), and (31). As a check on the accuracy of the cylindrical-flow approximation for the flow outboard of the tip location, the accurate theoretical loading was calculated

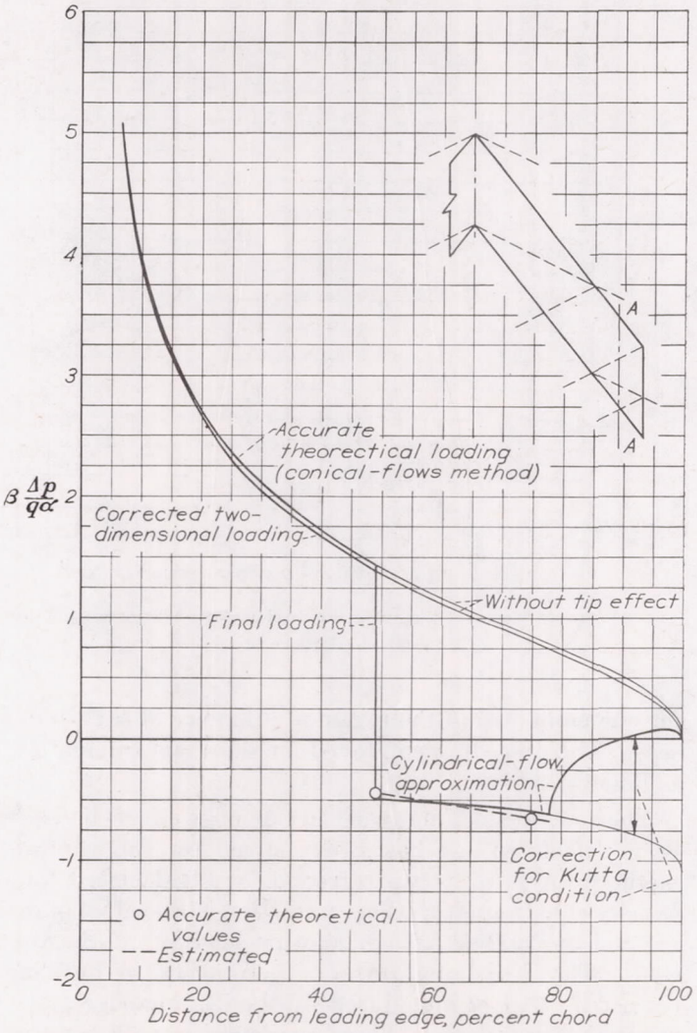


(a) Untapered wing; $m=0.4$; $\beta A=1.88$. Section at $\beta y=0.8c_0$, or 85 percent semispan

FIGURE 25.—Load distribution over streamwise section near tip as calculated by two-dimensional formulas, compared with more accurate theoretical values.

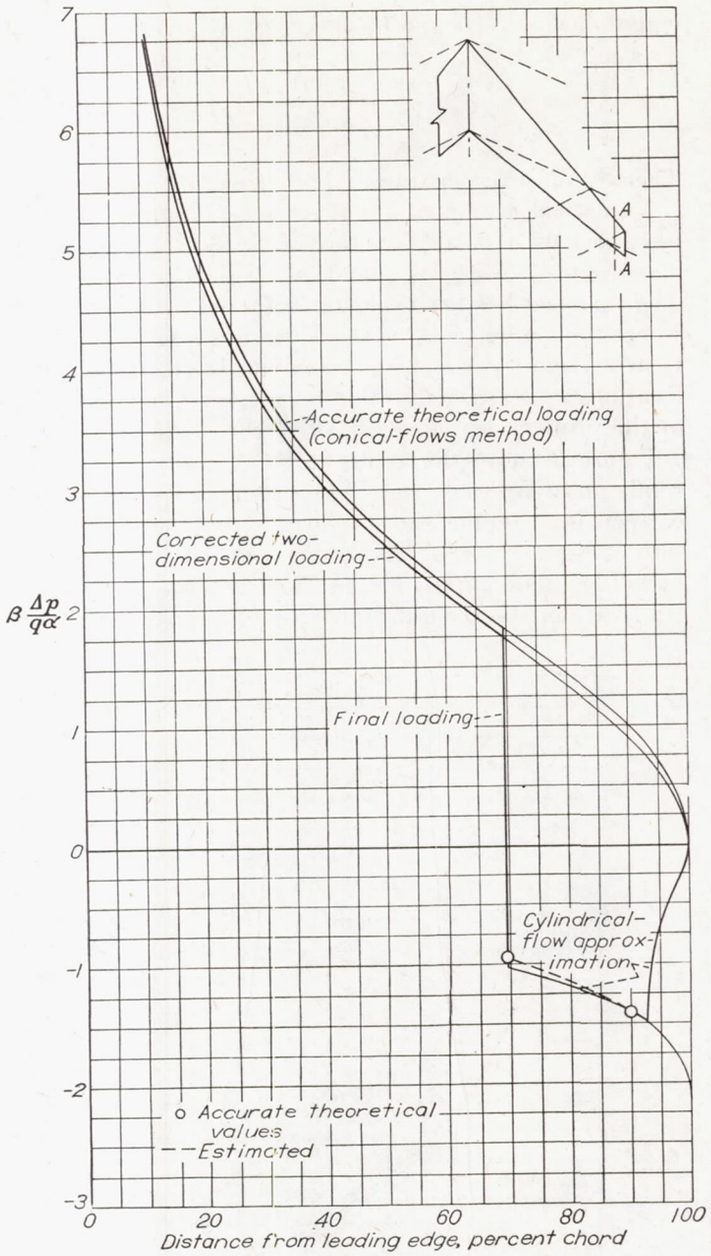


(b) Tapered wing; $m=0.4$; $m_t=0.6$. Section at $\beta y=0.8c_0$, or 93 percent semispan

FIGURE 25—Continued

for one point within the region of influence of the tip in each case. The procedure employed for the exact calculation was as follows:

The accurate loadings with no side-edge effects had already been calculated, as has been noted, by the conical-flow method. A primary tip correction was calculated for each case by equation (15). This correction is the effect of canceling the unmodified triangular-wing loading off the tip station. The remaining pressure differences to be canceled consisted of those introduced by the leading-edge and trailing-edge corrections. These pressures were computed by means of equations (26) and (46) of the present report and canceled by the method of reference 5.

The results are designated by the circled points on each figure. At the point at which the section enters the tip Mach cone in each case, a second circled point indicates the accurate theoretical loading. The value differs from that calculated by the approximate formulas only as the two loadings without tip effects differ.

It may be pointed out in concluding this section on load calculations that, while the formulas have been developed for plan forms with streamwise tips, the procedure may be adapted by obvious means to raked tips as well. However, in every case the deviation in the tip regions of the physical flow from the assumed potential flow must be borne in mind.

## III—LIFT [6]

### GENERAL PROCEDURE FOR CONICAL FLOWS

The total lift for any wing is, of course, the integral of the loading over the wing area. In general, however, it is difficult to obtain an analytic expression for the lift by a direct integration of the lift distribution. In the conical-flow method, advantage may be taken of the simplicity of the component fields by integrating the lift associated with each one and then combining the results in the same way as the pressure fields.

Conical elements of area are employed for the integrations. These are infinitesimal triangles bounded by two adjacent rays of the conical field and the intercepted boundary of the wing plan form. Over each of the infinitesimal triangles the velocity $u$ of the conical field will be constant. Thus it remains only to perform a single integration, with respect to the conical variable of the field, to obtain the total lift associated with that field.

#### GENERAL FORMULA FOR THE LIFT INDUCED BY A SINGLE TIP ELEMENT

The lift $(\Delta L)_a$ induced on the wing by a single canceling tip element is obtained first. Although the notation of the solution (equation (11)) used to cancel the triangular-wing loading is employed, the derivation will hold generally for any canceling element bounded on one side by the tip of a swept-back wing, since no use is made of the fact that the other boundary of the element passes through the origin of the $x,y$ axes. We write

$$(\Delta L)_a=2\rho V\int_{-1}^{0}(\Delta u)_a\frac{dS}{dt_a}\,dt_a \tag{76}$$

where $(\Delta u)_a$ (equation (11)) is the streamwise increment of velocity induced by the canceling field and $\frac{dS}{dt_a}\,dt_a$ (fig. 26) is the element of wing area $S$ for integration. For simplicity it will be specified that the Mach cone from the apex of the element does not include the apex of the trailing edge nor any part of the opposite tip. Then (see fig. 26)

$$\frac{dS}{dt_a}=\frac{m_t^2}{2\beta}\left(\frac{x_t-x_a}{m_t-t_a}\right)^2 \tag{77}$$

[6] It may be noted that, as a result of the reversibility property (reference 17), the formulas for the lift given herein for swept-back wings are equally applicable to the swept-forward wings having the same plan forms but reversed in heading.

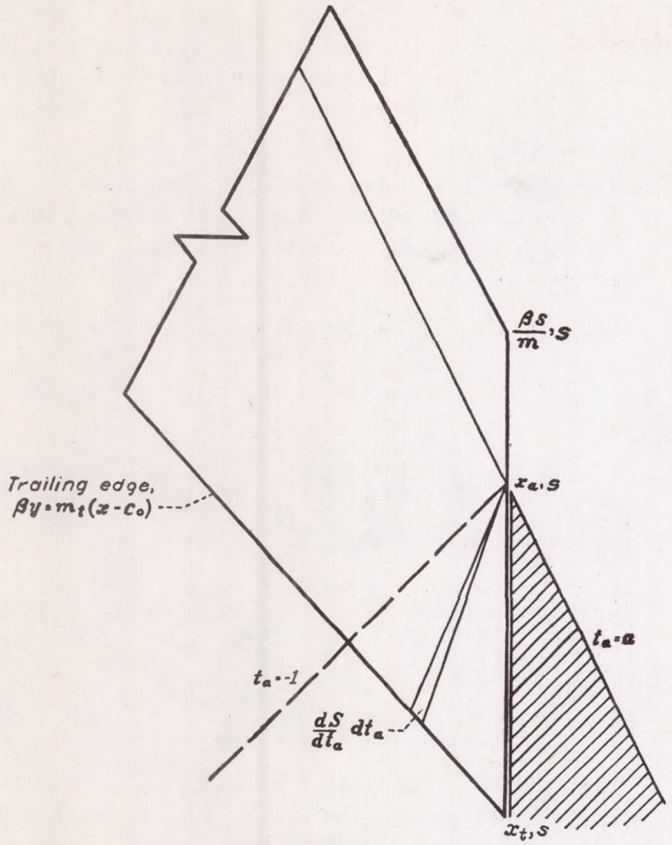


FIGURE 26.—Sketch for the determination of lift induced by a single tip element.

Substituting from equations (11) and (77) and integrating by parts, we obtain

$$(\Delta L)_a = \frac{\rho V m_t^2}{\beta} u_a (x_t - x_a)^2 g(a) \tag{78}$$

where

$$g(a) = \frac{1}{m_t - a}\left[\sqrt{\frac{a(1+a)}{m_t(1+m_t)}} - \frac{a}{m_t}\right] \tag{79}$$

and $x_t - x_a$ is the distance of the apex of the element from the trailing-edge tip.

#### GENERAL FORMULA FOR LIFT INDUCED BY OBLIQUE TRAILING-EDGE ELEMENT

With the notation of equation (24) for the velocity field of an oblique trailing-edge element, and on the assumption that the Mach lines from the apex of the element do not cross the leading edge, the formula for the elementary area of integration with apex on the trailing edge (fig. 27) is written

$$dS = \frac{\beta(s - y_a)^2}{2t_a^2} dt_a \tag{80}$$

where $s - y_a$ is the spanwise distance from the apex of the element to the wing tip. Then the lift associated with the element is

$$(\Delta L)_a = 2\rho V \frac{u_a}{\pi} \int_{m_t}^{1} \cos^{-1} \frac{(1-a)(t_a - m_t) - (mt - a)(1 - t_a)}{(1 - m_t)(t_a - a)} \frac{dS}{dt_a} dt_a \tag{81}$$

Integration of equation (81) gives

$$(\Delta L)_a = \rho V (s - y_a)^2 \beta \frac{u_a}{a}\left[\sqrt{\frac{(m_t - a)(1-a)}{m_t}} - \frac{m_t - a}{m_t}\right] \tag{82}$$

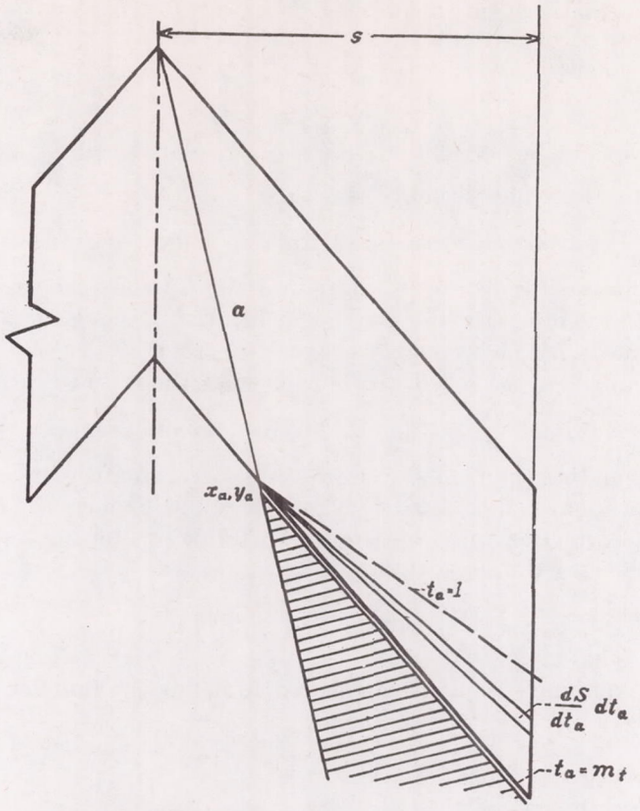


FIGURE 27.—Sketch for the determination of lift induced by a trailing-edge element.

### WING WITH SUBSONIC LEADING EDGE

#### UNCORRECTED LIFT

First, the uncorrected triangular-wing loading (equation (6)) is integrated over the wing plan form. The element of area is a triangle formed by two rays from the leading-edge apex $a$ and $a + da$ and either (1) the trailing edge of the wing or (2) the wing tip, accordingly as $a$ is less than or greater than $a_t$, the value of $a$ corresponding to the ray through the tip of the trailing edge. (See fig. 2.) In the first case the differential of area is

$$\frac{m_t^2 c_0^2}{2\beta(m_t - a)^2} da$$

and in the second

$$\frac{\beta s^2}{2a^2} da$$

so that the total uncorrected lift is

$$L_0 = \frac{4\rho V}{\beta}\left[\int_0^{a_t} \frac{m_t^2 c_0^2}{2(m_t - a)^2} u_\Delta \, da + \int_{a_t}^{m} \frac{\beta^2 s^2}{2a^2} u_\Delta \, da\right] \tag{83}$$

From the geometry of the wing, the relation

$$m_t c_0 = \frac{\beta s}{a_t}(m_t - a_t) \tag{84}$$

may be deduced. With this substitution, and the substitution for $u_\Delta$ from equation (6), equation (83) may be integrated to obtain

$$\frac{L_0}{q\alpha} = \frac{4s^2}{ma_t^2} \frac{\beta u_0}{V\alpha}\left\{\frac{m^2(m_t - a_t)^2}{m_t^2 - m^2}\left[\frac{m_t}{\sqrt{m_t^2 - m^2}}\left(\cos^{-1}\frac{m^2 - m_t a_t}{m(m_t - a_t)} - \cos^{-1}\frac{m}{m_t}\right) + \frac{m}{m_t}\right] - \frac{m_t(m^2 - m_t a_t)}{m_t^2 - m^2}\sqrt{m^2 - a_t^2}\right\} \tag{85a}$$

When $m_t=m$, this reduces to

$$\frac{L_0}{q\alpha}=\frac{8s^2}{3ma_t^2}\frac{\beta u_0}{V\alpha}\left[(m+a_t)\sqrt{m^2-a_t^2}-(m-a_t)^2\right] \quad (85b)$$

It should be noted that, for a given plan form, $\frac{L_0}{q\alpha}$ varies with Mach number only as $u_0$.

#### WING WITH SUPERSONIC TRAILING EDGE (TIP CORRECTION)

Proceeding to the calculation of the tip correction to the lift, we integrate the change in lift $(\Delta L)_a$ (equation (78)) induced by each element $a$ over the range $a_t\leq a\leq m$. The quantity $u_\Delta(m)$ is substituted for $u_a$ of the initial canceling element and $\frac{du_\Delta}{da}\,da$ for $u_a$ for the remaining ones. As in calculating the tip-induced pressure correction, the difficulty is encountered that $u_\Delta(m)$ is infinite, and therefore the total lift correction must be written in terms of limiting values. Following the substitution

$$x_t-x_a=\beta s\left(\frac{1}{a_t}-\frac{1}{a}\right) \quad (86)$$

in equation (78), it is convenient to define the function

$$G(a)=\frac{(a-a_t)^2}{a_t^2a^2}\,g(a)$$

Then the total induced lift may be written

$$\Delta L=2\rho V m_t^2\,\beta s^2\lim_{a\to m}\left[-u_\Delta(a)G(a)+\int_{a_t}^{a}\frac{du_\Delta}{da}\,G(a)da\right] \quad (87)$$

Integrating by parts results in cancellation of the first term inside the brackets. Since $G(a_t)$ is zero, equation (87) reduces to

$$\left(\frac{\Delta L}{q\alpha}\right)_{tip}=-4m_t^2\beta s^2\int_{a_t}^{m}\frac{u_\Delta(a)}{V\alpha}\,G'(a)da \quad (88a)$$

where

$$G'(a)=\frac{a-a_t}{a_t^2a^2}\left[\left(\frac{a_t}{a}+\frac{m_t-a_t}{m_t-a}\right)g(a)-\frac{a-a_t}{2(m_t-a)\sqrt{(m_t+m_t^2)(a+a^2)}}\right]$$

is the derivative of $G(a)$.

Equation (88a) has been integrated (appendix C) in terms of an incomplete elliptic integral of the third kind. If the necessary tables are not available, it may be preferable to integrate numerically.[7] In that case it is noted that

$$\frac{1}{\sqrt{m^2-a^2}}=\frac{d}{da}\sin^{-1}\frac{a}{m}$$

and $u_\Delta\,da$ is rewritten as

$$mu_0d\left(\sin^{-1}\frac{a}{m}\right)$$

Equation (88a) then becomes

$$\left(\frac{\Delta L}{q\alpha}\right)_{tip}=-4m_t^2m\beta s^2\frac{u_0}{V\alpha}\int_{\sin^{-1}\frac{a_t}{m}}^{\frac{\pi}{2}}G'(a)d\left(\sin^{-1}\frac{a}{m}\right) \quad (88b)$$

In this way infinite values in the integrand are avoided.

#### WING WITH SUBSONIC TRAILING EDGE

The expressions (equations (85)) for the uncorrected lift apply regardless of whether the trailing edge is subsonic or supersonic. The formulas for the tip correction may serve as a first approximation when the trailing edge is subsonic if the accuracy of a second correction is not required. For that purpose the special value for the untapered wing will be of interest:

If the wing is untapered the elliptic integrals in equation (88a) (see appendix C) reduce to the first and second kind and the primary induced lift may be written in the following closed form:

$$\left(\frac{\Delta L}{q\alpha}\right)_{tip}=-\frac{4s^2}{3ma_t^2}\frac{\beta u_0}{V\alpha}\left(2(m+a_t)\sqrt{m^2-a_t^2}+\sqrt{\frac{ma_t(m^2-a_t^2)}{(1+m)(1+a_t)}}\left\{\frac{3}{m}(m-a_t)-2m+\frac{(m-a_t)^2}{m(1+m)^2}\left[\frac{2}{a_t}-\frac{(1-m)^3}{2(m+a_t)}\right]-\right.\right.$$
$$\left.\left.\frac{2m^2(1+a_t)^3}{a_t(1+m)^2(m+a_t)}-\frac{m+a_t}{2}\right\}+\sqrt{\frac{2}{1+m}}\left\{\frac{(m-a_t)(m+2a_t)}{ma_t}F(\psi,k)-\left[\frac{2(m+a_t)}{a_t}-\frac{a_t}{m}-\frac{(m-a_t)^2}{2ma_t(1+m)}\right]E(\psi,k)\right\}\right) \quad (88c)$$

where

$$\psi=\sin^{-1}\sqrt{\frac{m-a_t}{m(1+a_t)}}\text{ and }k=\sqrt{\frac{1-m}{2}}$$

The primary tip correction, however, is usually quite large. It may therefore be desirable to take into account the secondary correction resulting from its cancellation at the subsonic trailing edge. Rather than compute a single secondary correction to the lift, as an additional item, it is again found advantageous to treat each superposed field individually, that is, to cancel each conical tip field at the trailing edge and find the net effect on the lift, then integrate over all the tip elements for a combined primary and secondary tip correction.

**Tip correction with subsonic trailing edge.**—For the cancellation at the trailing edge of a pressure field originating at a point $x_a$, $s$ on the wing tip, equation (82) is applied, with the parameter $a$, which defines one boundary of the oblique canceling field, replaced by $t_a$, referring to a ray from $x_a$,$s$. The velocity $u_a$ is the gradient

$$\frac{d\Delta u}{dt_a}\,dt_a$$

of the field (equation (11)) to be canceled. The distance from the apex of the canceling field to the wing tip is expressible as

$$-\frac{x_t-x_a}{\beta}\frac{m_t t_a}{m_t-t_a}$$

[7] Or see reference 10 for an approximate formula valid when $m$ is close to one.

Then the effect on the lift of canceling the single field from $x_a,s$ is

$$(\Delta_2 L)_a=\frac{-\rho V m_t^2 (x_t-x_a)^2}{\beta}\int_{-1}^{0}\frac{t_a}{(m_t-a)^2}\frac{d\Delta u}{dt_a}\times \left[\sqrt{\frac{(m_t-t_a)(1-t_a)}{m_t}}-\frac{m_t-t_a}{m_t}\right]dt_a \tag{89}$$

which may be integrated, after substitution for $\frac{d\Delta u}{dt_a}$, to give

$$(\Delta_2 L)_a=-\rho V m_t^2 u_a \frac{(x_t-x_a)^2}{\beta(m_t-a)}\left\{\sqrt{\frac{a(1+a)}{m_t(1+m_t)}}\,[1-E_0(k)]-\frac{a}{m_t}\left[1-\frac{\Lambda_0(\psi,k)}{\sin\psi}\right]\right\} \tag{90}$$

in which

$$k=\sqrt{\frac{1-m_t}{1+m_t}}$$

and

$$\psi=\sin^{-1}\sqrt{\frac{m_t-a}{m_t(1-a)}}$$

If the foregoing result is added to the lift associated with the original tip element, given by equations (78) and (79), it is found that the latter lift is exactly canceled by the algebraic terms in the reflected lift, leaving

$$(\Delta L)_a=\rho V m_t^2 u_a \frac{(x_t-x_a)^2}{\beta(m_t-a)}\left[\sqrt{\frac{a(1+a)}{m_t(1+m_t)}}E_0-\frac{a}{m_t}\frac{\Lambda_0(\psi,k)}{\sin\psi}\right] \tag{91}$$

for the lift induced by one tip element and its cancellation at the trailing edge. It will generally be found that further steps in the cancellation process are unnecessary for engineering accuracy.

For the total tip-induced correction to the lift, it is necessary to write as before

$$(\Delta L)_{tip}=2\rho V m_t^2 \beta s^2 \lim_{a\to m}\left[-u_\Delta(a)J(a)+\int_{a_t}^{a}\frac{du_\Delta}{da}J(a)da\right] \tag{92}$$

where $J(a)$ is

$$\frac{(a-a_t)^2}{a_t^2 a^2}\frac{1}{m_t-a}\left[\sqrt{\frac{a(1+a)}{m_t(1+m_t)}}E_0-\frac{a}{m_t}\frac{\Lambda_0(\psi,k)}{\sin\psi}\right]$$

An integration by parts reduces equation (92) to

$$(\Delta L)_{tip}=-2\rho V m_t^2 \beta s^2\int_{a_t}^{m}u_\Delta(a)J'(a)da \tag{93}$$

with

$$J'(a)=\frac{a-a_t}{a_t^2 a^2}\frac{1}{mt-a}\left\{\left[\left(\frac{a_t}{a}+\frac{m_t-a_t}{m_t-a}\right)-\frac{a-a_t}{2(1+a)}\left(\frac{1}{a}-\frac{1+m_t}{m_t-a}\right)\right]\sqrt{\frac{a(1+a)}{m_t(1+m_t)}}\,E_0(k)-\frac{a-a_t}{1-a^2}\sqrt{\frac{a(1+a)}{m_t(1+m_t)}}K_0(k)-\frac{a}{m_t}\left[\left(\frac{a_t}{a}+\frac{m_t-a_t}{m_t-a}\right)+\frac{(1-m_t)(a-a_t)}{2(1-a)(m_t-a)}\right]\frac{\Lambda_0(\psi,k)}{\sin\psi}\right\} \tag{94}$$

If the wing is untapered, $J'(a)$ becomes indeterminate when $a=m$. The limiting value is

$$J'(m)=\frac{m-a_t}{m^3 a_t^2(1-m^2)}\left\{\left[\frac{1-3m}{3}\left(\frac{a_t}{m}+\frac{1-a_t}{1-m}\right)-\frac{m-a_t}{10m}\left(3-\frac{8m^2}{1-m^2}\right)\right]E_0(k)+2m\left[\frac{1}{3}\left(\frac{a_t}{m}+\frac{1-a_t}{1-m}\right)-\frac{m-a_t}{10m}\left(\frac{1+3m}{1-m^2}\right)\right]K_0(k)\right\}$$

Further integration must be performed numerically. In order to avoid infinite values in the integrand, note again that

$$u_\Delta(a)=m u_0\frac{d}{da}\sin^{-1}\frac{a}{m} \tag{95}$$

so that equation (93) may be rewritten

$$\left(\frac{\Delta L}{q\alpha}\right)_{tip}=-4m\,m_t^2 s^2\frac{\beta u_0}{V\alpha}\int_{\sin^{-1}\frac{a_t}{m}}^{\pi/2}J'(a)\,d\left(\sin^{-1}\frac{a}{m}\right) \tag{96}$$

**Trailing-edge corrections.**—In deriving the trailing-edge corrections to the total lift, primary and secondary effects will again be combined. Further corrections will be omitted.

For the symmetrical wake correction, the element of area is obtained from equation (80) by setting $y_a$ equal to zero, and substituting $t_0$ for $t_a$. Then the decrement in lift induced by the application of the symmetrical canceling element at the trailing edge is, from equation (20),

$$(\Delta_1 L)_0=-2\rho V\beta s^2\frac{u_0}{K'(m_t)}\int_{m_t}^{1}F\left(\phi,\sqrt{1-m_t^2}\right)\frac{dt_0}{t_0^2} \tag{97}$$

or

$$\frac{(\Delta_1 L)_0}{q\alpha}=\frac{-4s^2}{m_t}\frac{\beta u_0}{V\alpha}\left[1-\frac{1}{K_0'(m_t)}\right] \tag{98}$$

where

$$K_0'(m_t)\equiv\frac{2}{\pi}K\left(\sqrt{1-m_t^2}\right)$$

The effect of canceling the pressure field induced by the symmetrical wake correction at the wing tips is obtained with the aid of the previously derived formula (equation (78)) for the lift associated with a single tip element. The parameter defining the boundary of the canceling tip element is now $t_0$ instead of $a$, and the velocity on the canceling sector is

$$\frac{d(\Delta u)_0}{dt_0}dt_0=\frac{u_0\,dt_0}{K'(m_t)\sqrt{(1-t_0^2)(t_0^2-m_t^2)}} \tag{99}$$

The distance from the apex of the canceling sector to the trailing edge may be expressed as

$$\beta s\left(\frac{1}{m_t}-\frac{1}{t_0}\right) \tag{100}$$

so that the secondary effect of the symmetrical trailing-edge correction becomes

$$(\Delta_2 L)_0 = 2\rho V m_t^2 \beta s^2 \frac{u_0}{K'(m_t)} \int_{m_t}^{1} \left(\frac{1}{m_t} - \frac{1}{t_0}\right)^2 \frac{g(t_0)\,dt_0}{\sqrt{(1-t_0^2)(t_0^2-m_t^2)}} \tag{101}$$

or

$$\frac{(\Delta_2 L)_0}{q\alpha} = \frac{4s^2}{m_t} \frac{\beta u_0}{V\alpha} \left[1 - \frac{1}{K_0'(m_t)} - \frac{2^{3/2}}{\sqrt{1+m_t}} \frac{K_0(k)-E_0(k)}{K_0'(m_t)}\right] \tag{102}$$

with $k = \sqrt{\frac{1-m_t}{2}}$.

Addition of this secondary correction to the primary effect given in equation (98) results in the single correction

$$\left(\frac{\Delta L}{q\alpha}\right)_0 = \frac{-8s^2}{m_t} \frac{\beta u_0}{V\alpha} \sqrt{\frac{2}{1+m_t}} \frac{K_0(k)-E_0(k)}{K_0'(m_t)} \tag{103}$$

By a similar procedure, the effect of canceling one of the oblique trailing-edge fields at the tip is readily obtained and added to the primary effect given by equation (82) to yield

$$(\Delta L)_a = \rho V \beta (s-y_a)^2 \frac{u_a}{a} \frac{1}{\sqrt{m_t}} \left[E_0(k) \sqrt{(m_t-a)(1-a)} - \frac{m_t-a}{\sqrt{1+m_t}} \sqrt{\frac{1+a}{a}} \Lambda_0(\psi, k)\right] \tag{104}$$

with $k = \sqrt{\frac{1-m_t}{1+m_t}}$ and $\psi = \sin^{-1}\sqrt{\frac{(1+m_t)a}{m_t(1+a)}}$ as the combined primary and secondary correction to the lift due to a single oblique trailing-edge cancellation.

For the total correction to the lift due to cancellation of the gradient of the triangular-wing loading in the wake, equation (104) is integrated graphically or numerically across the span as follows:

$$\frac{\Delta L}{q\alpha} = \frac{-4m}{\sqrt{m_t}} \frac{\beta u_0}{V\alpha} \int_0^{at} \frac{(s-y_a)^2}{(m^2-a^2)^{3/2}} \left[E_0(k) \sqrt{(m_t-a)(1-a)} - \frac{m_t-a}{\sqrt{1+m_t}} \sqrt{\frac{1+a}{a}} \Lambda_0(\psi, k)\right] da \tag{105}$$

Numerical examples to be presented will show this component of the lift to be very small, in general.

## WING WITH INTERACTING LEADING AND TRAILING EDGES

In computing the load distribution it was found that, when interaction takes place between the flow fields of the leading and trailing edges, the wing plan form appears to comprise two principal regions separated (see fig. 16) by the Mach line arising at the point of intersection $x_1,y_1$ of the trailing-edge Mach line and the leading edge. Ahead of this line (region I) the flow is most readily described in terms of conical fields. Behind this line the flow is more nearly two-dimensional. On this basis, the total lift will be found in two parts, using for region I the conical-flow expressions for the loading, and for the remainder of the wing the quasi-two-dimensional approximation.

### LIFT ON INBOARD PORTION OF WING

The uncorrected triangular-wing loading will first be integrated over region I, shown shaded in figure 28. For

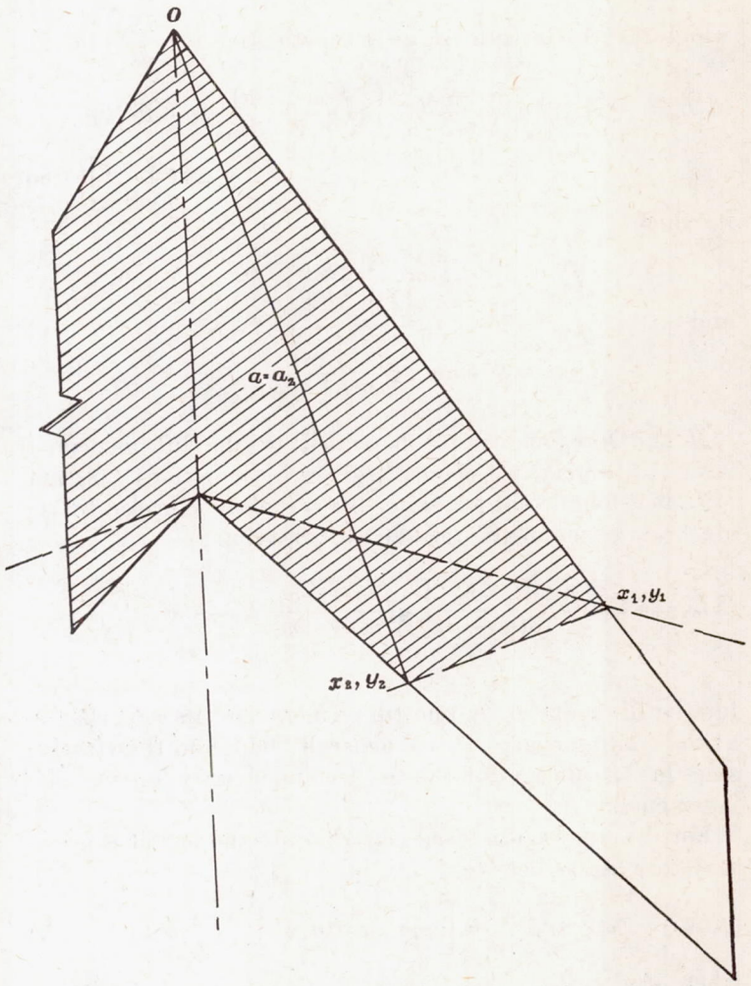


FIGURE 28.—Inboard portion (region I) of high-aspect-ratio wing.

this purpose the region is considered in two parts, separated by the ray $a_2$ from the wing apex to the point $x_2,y_2$. When $a$ is less than $a_2$, the element of area is as before

$$\frac{m_t^2 c_0^2}{2\beta(m_t-a)^2}\,da$$

When $a > a_2$, the element of area is

$$\frac{(1+m)^2 c_0^2}{2\beta(1-m)^2(1+a)^2}\,da$$

Thus, the uncorrected lift in the entire shaded region is

$$L_0 = \frac{2\rho V c_0^2}{\beta} \left[\int_0^{a_2} \frac{m_t^2}{(m_t-a)^2} u_\Delta\,da + \int_{a_2}^{m} \frac{(1+m)^2}{(1-m)^2(1+a)^2} u_\Delta\,da\right] \tag{106}$$

or

$$\frac{L_0}{q\alpha}=\frac{4m}{\beta}\frac{u_0}{V\alpha}c_0^2\left\{\frac{1+m}{(1-m)^3}\left[\frac{1}{\sqrt{1-m^2}}\cos^{-1}\frac{m^2+a_2}{m(1+a_2)}-\frac{\sqrt{m^2-a_2^2}}{1+a_2}\right]+\right.$$
$$\frac{m_t^2}{m_t^2-m^2}\left(\frac{m}{m_t}-\frac{\sqrt{m^2-a_2^2}}{m_t-a_2}\right)+$$
$$\left.\left(\frac{m_t}{\sqrt{m_t^2-m^2}}\right)^3\left[\cos^{-1}\frac{m^2-m_ta_2}{m(m_t-a_2)}-\cos^{-1}\frac{m}{m_t}\right]\right\} \quad (107)$$

with

$$a_2=\frac{2m\,m_t}{1+m+m_t-m\,m_t} \quad (108)$$

When $m_t=m$ (untapered wing), the second part of equation (107) becomes indeterminate. In this case,

$$\frac{L_0}{q\alpha}=\frac{4m}{\beta}\frac{u_0}{V\alpha}c_0^2\left\{\frac{1+m}{(1-m)^3}\left[\frac{1}{\sqrt{1-m^2}}\cos^{-1}\frac{m^2+a_2}{m(1+a_2)}-\frac{\sqrt{m^2-a_2^2}}{1+a_2}\right]+\right.$$
$$\left.\frac{1}{3}\left[\left(1+\frac{m}{m-a_2}\right)\sqrt{\frac{m+a_2}{m-a_2}}-2\right]\right\} \quad (109)$$

The trailing-edge corrections to the loading are to be integrated over the part of the shaded region behind the trailing-edge Mach lines. Integration of the symmetrical wake correction (equation (20)) yields

$$\frac{(\Delta L)_0}{q\alpha}=\frac{-16m^2c_0^2}{\beta(1+m_t)(1-m)^2}\frac{u_0}{V\alpha}\left\{1-\frac{2}{1-m_t}\left[1-\frac{E_0'(m_t)}{K_0'(m_t)}\right]\right\} \quad (110)$$

For each oblique element, the reduction in lift is given by

$$\frac{1}{q\alpha}\frac{d\Delta L}{da}\,da=$$
$$-\frac{2u_a}{\beta V\alpha}\frac{1+m_t}{1+a}(m_t-a)(x_2-x_a)^2\left[\sqrt{\frac{(1+m_t)(1-a)}{2(m_t-a)}}-1\right] \quad (111)$$

with $u_a=\frac{du_\Delta}{da}da$, $x_a=\frac{m_tc_0}{m_t-a}$ and

$$x_2=\left(\frac{1+m}{1-m}+m_t\right)\frac{c_0}{1+m_t} \quad (112)$$

The total lift in region I is then given by

$$\left(\frac{L}{q\alpha}\right)_{\text{I}}=\frac{L_0}{q\alpha}+\frac{(\Delta L)_0}{q\alpha}+\frac{2}{q\alpha}\int_0^{a_2}\frac{d\Delta L}{da}\,da \quad (113)$$

The quantity $\frac{\beta^2}{m^2c_0^2}\left(\frac{L}{q\alpha}\right)_{\text{I}}$ is plotted against $m_t$ in figure 29 for several values of the ratio $m/m_t$.

### LIFT ON OUTER PORTIONS OF WING

In order to find the total lift (except for tip losses) on the remainder of the wing (fig. 30), a double integration with respect to $x$ and $y$ is performed on equation (60). A first integration, with respect to $y$, yields for the indefinite integral

$$\int\frac{u}{V\alpha}dy=\frac{\sigma(x)}{\beta}\sqrt{c_0}\left[\sqrt{\frac{(mx-\beta y)(m_tc_0-m_tx+\beta y)}{m_tc_0-(m_t-m)x}}+\right.$$
$$\left.\sqrt{m_tc_0-(m_t-m)x}\,\tan^{-1}\sqrt{\frac{mx-\beta y}{m_tc_0-m_tx+\beta y}}\right] \quad (114)$$

The values of $\beta y$ to be substituted as limits in equation (114) are indicated in figure 30. Along the leading edge, the right-hand member of equation (114) reduces to zero; along the trailing edge it becomes

$$\frac{\pi}{2}\frac{\sigma(x)}{\beta}\sqrt{c_0}\sqrt{m_tc_0-(m_t-m)x}$$

Then the total lift on the outboard region (both wing halves), except for tip losses, is

$$\left(\frac{L}{q\alpha}\right)_{\text{II}}=\frac{8\sqrt{c_0}}{\beta}\left[\int_{x_1}^{x_2}\sigma(x)\left(f_1\tan^{-1}\frac{f_2}{f_3}+\frac{f_2f_3}{f_1}\right)dx+\right.$$
$$\left.\frac{\pi}{2}\int_{x_2}^{x_t}\sigma(x)f_1\,dx-\int_{\frac{\beta s}{m}}^{x_t}\sigma(x)\left(f_1\tan^{-1}\frac{f_4}{f_5}+\frac{f_4f_5}{f_1}\right)dx\right] \quad (115)$$

where

$$f_1=\sqrt{m_tc_0-(m_t-m)x}$$
$$f_2=\sqrt{(1+m)(x-x_1)} \qquad f_4=\sqrt{m(x-\beta s/m)}$$
$$f_3=\sqrt{(1+m_t)(x_2-x)} \qquad f_5=\sqrt{m_t(x_t-x)}$$

The indicated integrations may be performed numerically or graphically, using values of $\sigma(x)$ taken from the charts of figure 23.

### TIP-INDUCED CORRECTION TO THE LIFT

In deriving a tip correction to the lift, the same simplifying assumption of completely cylindrical flow will be adopted concerning the pressure field to be canceled as was used in obtaining a tip correction to the loading. As in the preceding section, a combined primary and secondary tip correction will be derived. All further corrections will be omitted.

If the notation of equation (63) is used the distance from the apex $x_c,s$ of a canceling element to the trailing-edge tip is $c_t(1-\xi_c)$, and the lift induced by the element and its cancellation at the trailing edge is, from equation (91),

$$(\Delta L)_c=\rho V{m_t}^2u_c\frac{c_t^2(1-\xi_c)^2}{\beta(m_t-m)}\left[\sqrt{\frac{m(1+m)}{m_t(1+m_t)}}E_0(k)-\frac{m}{m_t}\frac{\Lambda_0(\psi,k)}{\sin\psi}\right] \quad (116)$$

where

$$k=\sqrt{\frac{1-m_t}{1+m_t}}$$

as before, and

$$\psi=\sin^{-1}\sqrt{\frac{m_t-m}{m_t(1-m)}}$$

since the outer boundary of each element now has the slope $\frac{m}{\beta}$.

It is seen that only $u_c$ and $(1-\xi_c)^2$ in the coefficient of equation (116) vary with the element. For the first element ($\xi_c=0$), the velocity $u_c$ is the initial value of the uncorrected velocity along the tip section given in equation (65), and, for the other elements, the differential of that velocity. Then

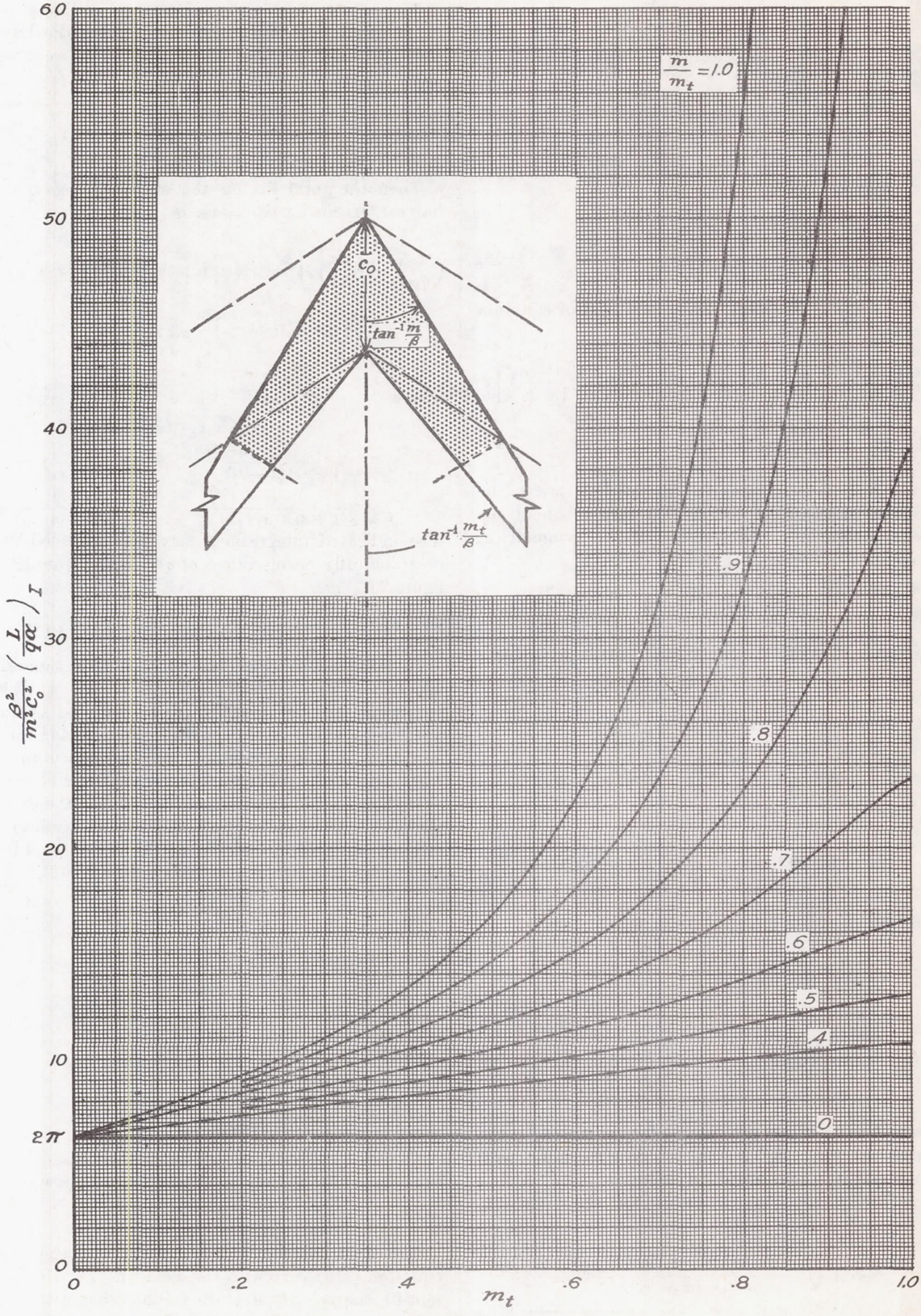


FIGURE 29.—Chart for the computation of lift in region I.

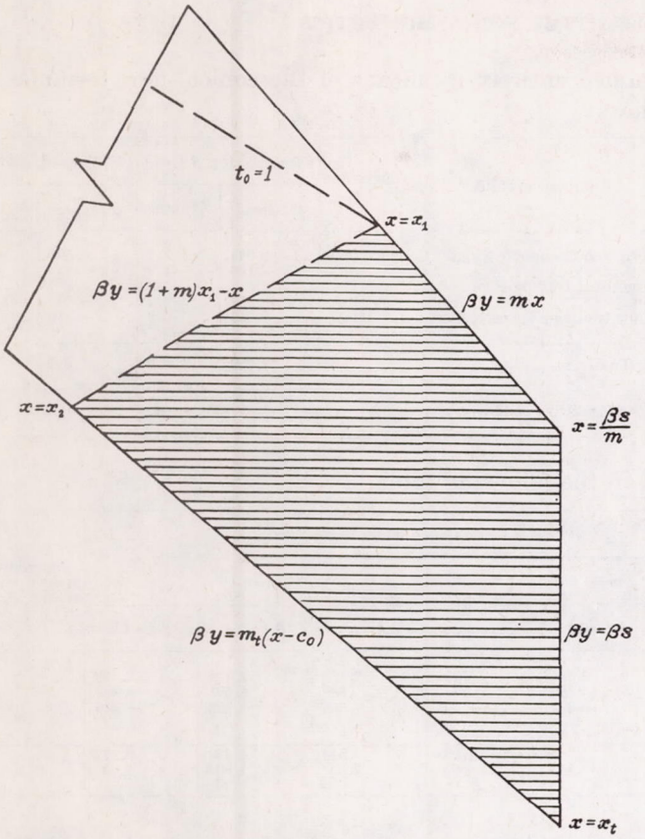


FIGURE 30.—Boundaries of outboard region of high-aspect-ratio wing, for use as limits of integration in equation (114).

the combined primary and secondary tip correction on both wing halves is

$$\frac{\Delta L}{q\alpha}=-\frac{4m_t^2c_t^2\sigma_s}{\beta(m_t-m)\sqrt{m\lambda}}\left[\sqrt{\frac{m(1+m)}{m_t(1+m_t)}}E_0(k)-\frac{m}{m_t}\frac{\Lambda_0(\psi,k)}{\sin\psi}\right]\lim_{\xi_c\to 0}\left[(1-\xi_c)^2\sqrt{\frac{1-\xi_c}{\xi_c(1-\mu\xi_c)}}+\int_{\xi_c}^{1}(1-\xi_c)^2\frac{d}{d\xi_c}\sqrt{\frac{1-\xi_c}{\xi_c(1-\mu\xi_c)}}\,d\xi_c\right] \tag{117}$$

Integration by parts gives, finally,

$$\frac{\Delta L}{q\alpha}=-\frac{8\pi m_t^2c_t^2\sqrt{m}}{3\beta(m_t-m)^3\sqrt{\lambda}}\sigma_s\left[\sqrt{\frac{m(1+m)}{m_t(1+m_t)}}E_0(k)-\frac{m}{m_t}\frac{\Lambda_0(\psi,k)}{\sin\psi}\right]\left[(3m-m_t)K_0(\sqrt{\mu})-2m_t\left(2-\frac{m_t}{m}\right)E_0(\sqrt{\mu})\right] \tag{118a}$$

If the wing is untapered, equation (118a) takes on the value

$$\frac{\Delta L}{q\alpha}=-\frac{\pi c_0^2\sqrt{m}}{\beta(1-m^2)}\sigma_s\left[2mK_0(k)+(1-3m)E_0(k)\right] \tag{118b}$$

Except for the occurrence of $\sigma_s$, $c_t$ and $\lambda$ in the coefficients, the tip correction obtained in the foregoing way is a function of $m$ and $m_t$ only, independent of the tip location. Values of $\frac{\beta\sqrt{\lambda}}{\sigma_s c_t^2}\left(\frac{\Delta L}{q\alpha}\right)_{tip}$ have been plotted in figure 31 in a form similar to the chart of $\left(\frac{L}{q\alpha}\right)_I$ (fig. 29).

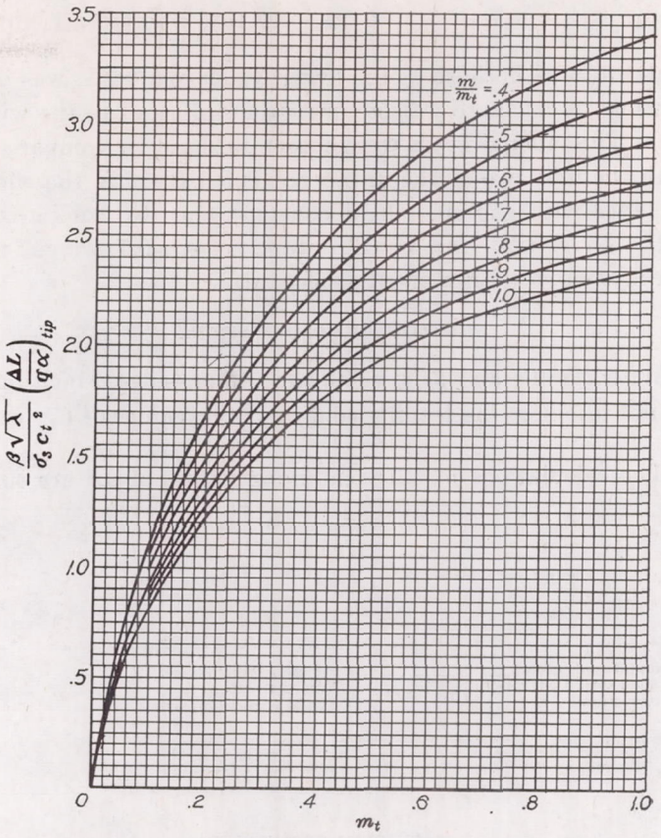


FIGURE 31.—Chart for the correction of the lift for tip effect, using two-dimensional formulas.

## APPLICATION OF LIFT FORMULAS

### CASES COMPUTED

The lift-curve slope $C_{L_\alpha}$ has been calculated for two families of untapered wings with varying aspect ratios as follows:

| $m=0.2$ | | $m=0.4$ | |
|---|---|---|---|
| $\beta\frac{s}{c_0}$ | $\beta A$ | $\beta\frac{s}{c_0}$ | $\beta A$ |
| 0.3 | 0.6 | 0.6 | 1.2 |
| .4 | .8 | .8 | 1.6 |
| .6 | 1.2 | 1.2 | 2.4 |
| | | 1.6 | 3.2 |

and for two tapered wings:

| $m=0.4$, $m_t=0.6$ | | |
|---|---|---|
| $\beta\frac{s}{c_0}$ | $\beta A$ | $\lambda$ |
| 0.6 | 1.6 | ½ |
| .8 | 2.4 | ⅓ |

It should be noted that the untapered-wing cases (except for the last one under $m=0.4$) represent three wings of fixed geometry at two different Mach numbers such that $\beta$ is doubled in going from the first to the second. No calculation was made for $m=0.2$ to correspond to the last case

under $m=0.4$ because at the lower Mach number it was not possible to calculate satisfactory values of $\sigma$ out to the wing tip. The tapered wings were chosen to show, by comparison with the first two of the untapered $m=0.4$ wings, the effect of taper with the span held constant and, by comparison with the second and third untapered $m=0.4$ wings, the effect of taper with a given aspect ratio.

### SUMMARY OF COMPUTATIONS

With $m=0.4$ and $\beta s/c_0=0.6$, the trailing-edge Mach lines do not intersect the leading edge, and the values of $C_{L_\alpha}$ were obtained entirely by means of the conical-flow formulas, as follows:

| Component of lift | Equation No. | Tapered wing, $\beta A=1.6$ | | Untapered, $\beta A=1.2$ | |
|---|---|---|---|---|---|
| | | $\beta^2 L/q\alpha c_0^2$ | % total | $\beta^2 L/q\alpha c_0^2$ | % total |
| Uncorrected triangular wing | (85) | 2.093 | 121.1 | 2.595 | 143.0 |
| Tip effect | (96) | −.190 | −11.0 | −.422 | −23.3 |
| Symmetrical trailing-edge correction | (103) | −.159 | −9.2 | −.340 | −18.7 |
| Oblique trailing-edge correction | (105) | −.015 | −0.9 | −.019 | −1.0 |
| Totals | | 1.729 | 100.0 | 1.814 | 100.0 |
| $\beta C_{L_\alpha}=\beta L/q\alpha S$, per radian | | 1.920 | | 1.512 | |

The calculations for the remaining values of $\beta A$ are summarized in the following table:

| Component of lift | Obtained from | Untapered wings | | | | | | Tapered wing $m=0.4$; $m_t=0.6$; $\beta s=0.8$; $\beta A=2.4$ |
|---|---|---|---|---|---|---|---|---|
| | | $m=0.2$ | | | $m=0.4$ | | | |
| | | $\beta A=0.6$ | $\beta A=0.8$ | $\beta A=1.2$ | $\beta A=1.6$ | $\beta A=2.4$ | $\beta A=3.2$ | |
| Lift on inboard portion | Fig. 29 or equation (113) | 0.366 | 0.366 | 0.366 | 2.128 | 2.128 | 2.128 | 1.981 |
| Lift on outboard portion | Equation (115) | .180 | .386 | .830 | .849 | 2.593 | 4.459 | .462 |
| Tip correction | Fig. 31 or equation (118) | −.085 | −.090 | −.098 | −.363 | −.392 | −.415 | −.092 |
| Totals, $\beta^2 L/q\alpha c_0^2$ | | .461 | .662 | 1.098 | 2.614 | 4.329 | 6.172 | 2.351 |
| $\beta C_{L_\alpha}=\beta L/q\alpha S$, per radian | | .77 | .83 | .92 | 1.63 | 1.80 | 1.93 | 2.20 |

### DISCUSSION OF RESULTS

The results of the calculations are plotted against the reduced aspect ratio $\beta A$ in figure 32. The curves for the untapered wings may be seen to be approaching, at the upper end, the value $2\pi m/\sqrt{1-m^2}$ given by simple sweep theory.

At the lower end, the curves should approach the origin along the line $C_{L_\alpha}=\frac{\pi}{2}A$ given by low-aspect-ratio theory (reference 13). The two points on the $m=0.2$ curve for $\beta A<1$ are not entirely accurate because no account was taken of the interference between the flow fields from the tips. The points are included, however, because, with so much sweep, the wing areas affected are small and the interference effects should be negligible. The resulting curve appears consistent with the corresponding curve calculated by the slender-wing theory of reference 3, although a disparity in plan form lessens the significance of the comparison.

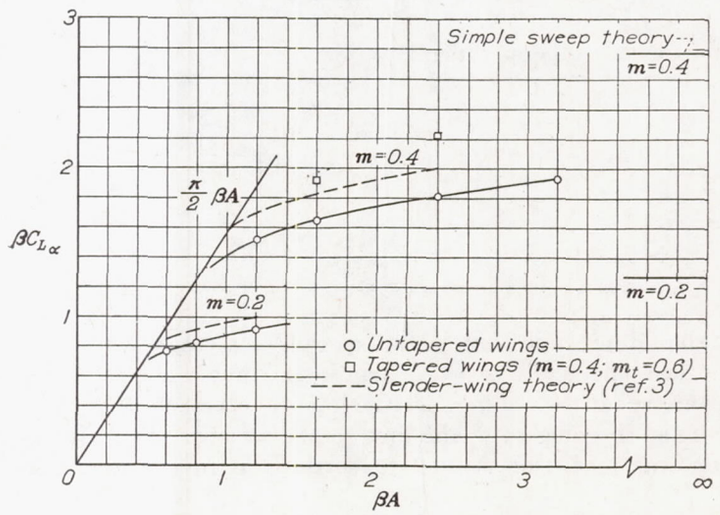


FIGURE 32.—Variation of lift-curve slope with aspect ratio.

The slender-wing-theory values are also plotted for $m=0.4$. In that case, however, the assumption of extreme slenderness is no longer justified and introduces an appreciable error. (It should be mentioned that the asympotote for the slender-wing-theory curves is *below* the value given by simple sweep theory by the factor $\sqrt{1-m^2}$.)

An estimate of the accuracy of the lift formulas of the present report, compared with results which would take into account all the successive reflections at the tips and trailing edge, may be made from the following observations:

The values obtained (in the first table) from equations (96) and (103), which combine primary and secondary corrections, differ from values obtainable for the primary corrections alone by only 1 percent of the total lift in the case of the tapered wing, and 4 percent of the total lift for the untapered wing. Third-order corrections would be only a fraction of those small corrections and would, in turn, be partly canceled out by a fourth-order correction.

The results in the second table, incorporating the two-dimensional approximations, agree within 2 or 3 percent with values calculated entirely by the conical-flow method.

## IV—DRAG DUE TO LIFT

The drag due to lift of a wing with supersonic leading edge is simply the lift times the angle of attack. When the leading edge is subsonic, the drag is reduced by a suction force due to the upwash around the leading edge. In the linearized theory this force appears as the limit of the product of an infinite velocity across an infinitesimal frontal area.

The formula for the suction force on a subsonic leading edge has been derived (see, e. g., Hayes, reference 18) by

assuming the flow near the leading edge to be essentially two-dimensional and applying the results of two-dimensional potential theory. The simple result obtained in that manner has been verified for the swept-back wing of finite span by application of the somewhat different approach of reference 19.

By the two-dimensional approach, the suction force is found to be proportional to the square of the strength of the leading-edge singularity in the perturbation velocity $u$. The latter is the quantity discussed earlier in connection with the adjustment of the two-dimensional loading to the loading on the swept-back wing. With the use of the previous terminology it is possible to write for the longitudinal component of the suction force per unit streamwise length of leading edge,

$$\frac{dT}{dx}=\frac{\rho\pi}{m}\sqrt{1-m^2}\,C_\Delta{}^2 \tag{119}$$

where $C_\Delta$ (equation (53)) is the value, at the leading edge, of the coefficient of $(mx-\beta y)^{-1/2}$ in $u_\Delta$.

Then, if the trailing-edge Mach line does not intersect the leading edge, the thrust is merely

$$\left.\begin{aligned}T&=\rho\pi u_0{}^2\sqrt{1-m^2}\int_0^{\frac{\beta s}{m}}x\,dx\\&=\frac{\rho\pi u_0{}^2\beta^2 s^2}{2m^2}\sqrt{1-m^2}\end{aligned}\right\} \tag{120}$$

The total drag due to lift is obtained by subtracting the thrust from the product of the lift and the angle of attack, or, in coefficient form,

$$C_D=\alpha C_L-C_T \tag{121}$$

where $C_T$ is the thrust coefficient $T/qS$. Thus, in the foregoing case,

$$C_D=\frac{\alpha^2}{S}\left[\frac{L}{q\alpha}-\pi\left(\frac{\beta s}{m}\right)^2\left(\frac{u_0}{V\alpha}\right)^2\sqrt{1-m^2}\right] \tag{122}$$

When a portion of the leading edge is influenced by the trailing edge, the leading-edge singularity takes on, for that portion, the value given by expression (56), which then replaces $C_\Delta$ in equation (119) for the thrust. The total thrust is

$$2\int_0^{\frac{\beta s}{m}}\frac{dT}{dx}\,dx=2\,\frac{\rho\pi}{m}\sqrt{1-m^2}\left\{\int_0^{x_1}C_\Delta{}^2\,dx+\int_{x_1}^{\frac{\beta s}{m}}\left[C_\Delta+(\Delta C)_0+\int_0^{a_0}\frac{d\Delta C}{da}\,da\right]^2 dx\right\} \tag{123}$$

where

$$x_1=\frac{c_0}{1-m}$$

locates the intersection of the trailing-edge Mach line with the leading edge. Integrating the first term and reducing so coefficient form gives

$$C_T=\frac{\pi\alpha^2\sqrt{1-m^2}}{S}\left[\left(\frac{u_0}{V\alpha}\right)^2 x_1{}^2+\frac{4c_0}{m}\int_{x_1}^{\frac{\beta s}{m}}\sigma^2\,dx\right] \tag{124}$$

so that

$$C_D=\frac{\alpha^2}{S}\left\{\frac{L}{q\alpha}-\pi\sqrt{1-m^2}\left[\left(\frac{u_0}{V\alpha}\right)^2 x_1{}^2+\frac{4c_0}{m}\int_{x_1}^{\frac{\beta s}{m}}\sigma^2\,dx\right]\right\} \tag{125}$$

In figure 33, $\frac{1}{\beta}$ times the drag-rise factor $\frac{C_D}{C_L{}^2}$ is plotted against the reduced aspect ratio $\beta A$ for two combinations of sweep and Mach number, $m=0.2$ and $m=0.4$, for untapered wings. Comparison is made with a theoretical minimum for slender wings in supersonic flight obtained by R. T. Jones in an unpublished analysis. Using a method similar to Hayes (reference 18) and assuming the wing to be narrow compared with the Mach cone, Jones has derived a minimum wave-drag coefficient

$$C_{D_w}=\frac{\beta^2}{2\pi A_x}C_L{}^2 \tag{126}$$

where $A_x$ is the aspect ratio defined in the streamwise, instead of the spanwise, direction; that is, if $l$ (numerically equal to $x_t$) is the over-all length of the wing in the stream direction,

$$A_x=l^2/S \tag{127}$$

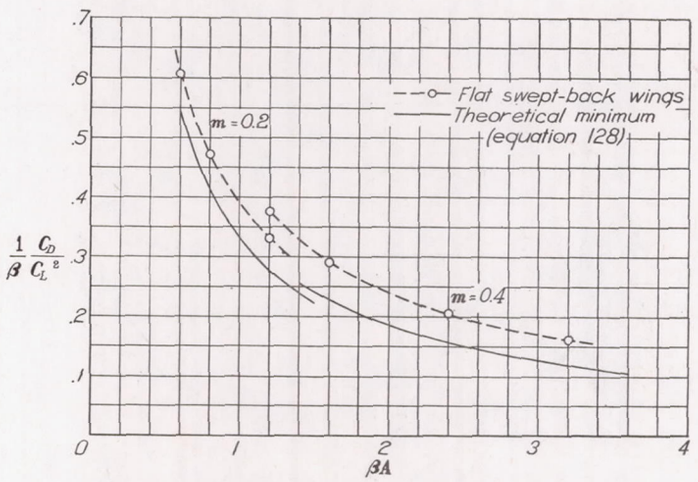


FIGURE 33.—Variation of drag-rise factor with aspect ratio for untapered wings.

The wave drag is to be added to the vortex drag, which is the induced drag of subsonic flow, calculated from the spanwise loading. Using the minimum induced drag obtained from lifting-line theory gives as the minimum supersonic drag-rise factor [8]

$$\frac{C_D}{C_L{}^2}=\frac{1}{\pi A}+\frac{\beta^2}{2\pi A_x} \tag{128}$$

It may be seen that the drag rise of the constant-chord swept-back wings is fairly close to this minimum, especially at the lower values of $m$ for which equation (128) was derived.

## V—SUMMARY OF FORMULAS

The formulas for the loading, lift, and drag coefficients are summarized in the following table, in which the equations are identified by number.

[8] This result has since been published in The Journal of the Aeronautical Sciences, vol. 18, no. 2, Feb. 1951, pp. 75–81.

| Case | $\frac{\Delta p}{q\alpha}=\frac{4u}{V\alpha}$ | | $C_{L_\alpha}=\frac{1}{S}\cdot\frac{L}{q\alpha}$ | $C_D$ |
|---|---|---|---|---|
| —— —— Mach lines | Region | Equations for $u$ | Equa. for $\frac{L}{q\alpha}$ | Equa. No. |
| 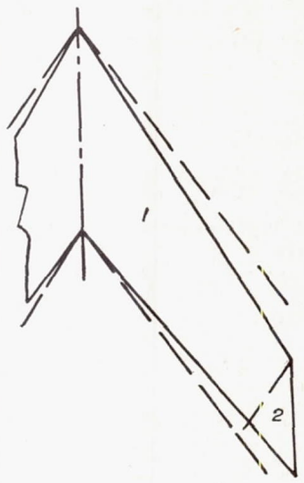 | 1<br>2 | (6)<br>(6)+(15)[a] | (85)+(88) | (122) |
| 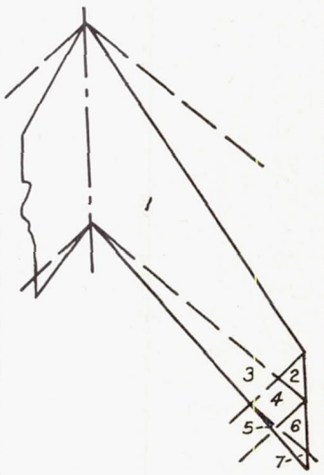 | 1<br>2<br>3<br>4<br>5<br>6<br>7 | (6)<br>(6)+(15)[a]<br>(6)+(26b)<br>(6)+(15)[a]+(26b)<br>(6)+(15)[a]+(26b)+(31)<br>(6)+(15)[a]+(26b)+(32)<br>(6)+(15)[a]+(26b)+(31)+(32) | (85)+(96)+(103)+(105)[a] | (122) |
| 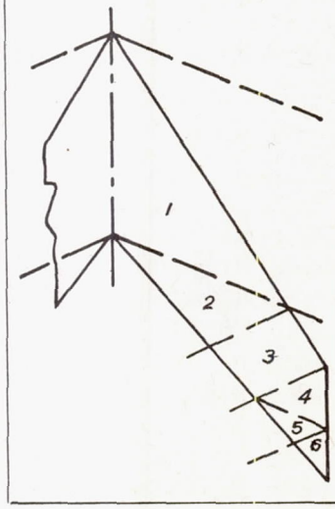 | 1<br>2<br>3<br>4<br>5<br>6 | (6)<br>(6)+(26b)<br>(60)[b]<br>(60)[b]+(73)[a,b,c]<br>(60)[b]+(73)[a,b,c]+(31)<br>Not evaluated | (113)[d]+(115)[b]+(118)[b,e] | (125)[b] |

[a] In evaluating, use fig. 6.
[b] In evaluating, use fig. 23.
[c] In evaluating, use fig. 14.
[d] or see fig. 29.
[e] or see fig. 31.

AMES AERONAUTICAL LABORATORY,
NATIONAL ADVISORY COMMITTEE FOR AERONAUTICS,
MOFFETT FIELD, CALIF., *Mar. 15, 1950.*

# APPENDIX A

## SYMBOLS

### GENERAL

$V$ free-stream velocity

$M$ free-stream Mach number

$\beta$ $\sqrt{M^2-1}$

$u, v, w$ perturbation velocities in streamwise, cross-stream, and vertical directions, respectively

$\rho$ density of air

$q$ dynamic pressure $\left(\frac{1}{2}\rho V^2\right)$

$\Delta p$ pressure difference between upper and lower surfaces, or local lift

$\alpha$ angle of attack, radians

$L$ lift

$T$ leading-edge thrust, or component of leading-edge suction force in flight direction

$C_L$ lift coefficient $\left(\frac{L}{qS}\right)$

$C_{L_\alpha}$ lift-curve slope $\left(\frac{dC_L}{d\alpha}\right)$

$C_D$ drag coefficient $\left(\frac{D}{qS}\right)$

$C_T$ thrust coefficient $\left(\frac{T}{qS}\right)$

### WING DIMENSIONS

$c_0$ root chord

$c_t$ tip chord

$s$ semispan

$S$ wing area

$l$ over-all length in the steamwise direction

$\Lambda$ angle of sweep of the leading edge

$\lambda$ taper ratio $(c_t/c_0)$

$A$ aspect ratio $(4s^2/S)$

$A_x$ streamwise aspect ratio $(l^2/S)$

### RECTANGULAR COORDINATES

$x, y$ Cartesian coordinates in the stream direction and across the stream, in the plane of the wing

$x_a, y_a$ coordinates of apex of conical field used to cancel triangular-wing loading (Equation (8) at tip, equations (21) and (22) at trailing edge)

$x_b, y_b$ coordinates of apex of conical field used in secondary cancellations

$x_c, s$ coordinates of point on tip; apex of conical field used to cancel assumed cylindrical load

$x_0, y_0$ coordinates of intersection of Mach forecone from $x,y$ with edge at which correction is being made

$x_1, y_1$ coordinates of intersection of trailing-edge Mach cone with leading edge ($x_1$ given by equation (61))

$x_2, y_2$ coordinates of intersection of Mach line from $x_1, y_1$ with trailing edge ($x_2$ given by equation (112))

$x^*, y^*$ coordinates of intersection of tip Mach line with trailing edge

$x_t, s$ coordinates of intersection of tip and trailing edge

$\xi$ streamwise distance of $x,y$ back from leading edge, as a fraction of the tip chord (equation (69))

$\xi_0$ distance of $x_0,s$ behind leading-edge tip, as a fraction of the tip chord (equation (70))

$\xi_c$ distance of $x_c, s$ behind leading-edge tip, as a fraction of the tip chord (equation (64))

### CONICAL COORDINATES

In the following, all slopes are measured counterclockwise from a line extending downstream from the apex of the wing or of the pertinent canceling sector:

$m$ $\dfrac{\text{slope of leading edge}}{\text{slope of Mach lines}}=\beta\cot\Lambda$

$m_t$ $\dfrac{\text{slope of trailing edge}}{\text{slope of Mach lines}}$

$a$ $\dfrac{\text{slope of ray from the origin}}{\text{slope of Mach lines}}=\beta\dfrac{y}{x}$

$a_0$ the value of $a$ corresponding to a primary canceling element of which the apex lies on the Mach forecone of the point at which the load is being calculated (equation (13) for tip corrections, equation (25) for trailing-edge corrections)

$a_0'$ limiting value of $a$ for leading-edge correction (equation (47))

$a_2$ $a(x_2, y_2)$ (equation (108))

$a_t$ $a(x_t, s)$

$t_a$ $\dfrac{\text{slope of ray from apex of element } a}{\text{slope of Mach lines}}=\beta\dfrac{y-y_a}{x-x_a}$

$t_b$ $\dfrac{\text{slope of ray from } x_b, y_b}{\text{slope of Mach lines}}=\beta\dfrac{y-y_b}{x-x_b}$

$t_c$ $\dfrac{\text{slope of ray from } x_c, s}{\text{slope of Mach lines}}=\beta\dfrac{y-s}{x-x_c}$

$t_m$ $\dfrac{\text{slope of ray from leading-edge tip}}{\text{slope of Mach lines}}=\beta\dfrac{y-s}{x-(\beta s/m)}$

$t^*$ $\dfrac{\text{slope of ray from } x^*, y^*}{\text{slope of Mach lines}}=\beta\dfrac{y-y^*}{x-x^*}$

$\tau_0$ limiting value of $t_0$ for leading-edge correction (equation (39))

$\tau_a$ limiting value of $t_a$ for leading-edge correction (equation (44))

### COMPONENTS OF STREAMWISE PERTURBATION VELOCITY

$u_\Delta$ basic (uncorrected) perturbation velocity as given by solution for triangular wing (equation (6) for subsonic leading edge)

$u_0$ value of $u_\Delta$ at $a=0$ (equation (7))

$\Delta u$ correction to $u_\Delta$ induced by cancellation of pressure differences outside the wing plan form

$u_a$ constant perturbation velocity on sector used in canceling triangular-wing loading

$u_b$ constant perturbation velocity on sector used in secondary cancellation

$u_c$ constant perturbation velocity on sector used outboard of tip in canceling assumed cylindrical field

$(\Delta u)_0$ symmetrical trailing-edge correction to $u_\Delta$ (equation (20))

$(\Delta_2 u)_0$ correction induced by canceling $(\Delta u)_0$ at leading edge (equation (38))

$(\Delta u)_a$ correction to $u_\Delta$ due to single oblique trailing-edge element (equation (24))

$\Delta u^*$ value of tip correction to $u_\Delta$ at the point $x^*, y^*$

### ARBITRARY MATHEMATICAL SYMBOLS

$C_\Delta$ value of coefficient of $\frac{1}{\sqrt{mx-\beta y}}$ in $u_\Delta$ at the leading edge (equation (53))

$(\Delta C)_0$ decrement in $C_\Delta$ due to reflection of $(\Delta u)_0$ at leading edge (equation (54))

$\frac{d\Delta C}{da}da$ decrement in $C_\Delta$ due to reflection of $(\Delta u)_a$ at leading edge (equation (55))

$\sigma$ Non-dimensional expression for strength of the leading-edge singularity (equation (59))

$\sigma_s$ value of $\sigma$ at leading-edge tip $\left[\sigma\left(\frac{\beta s}{m}\right)\right]$

$\mu$ taper parameter $\left(\frac{m_t-m}{m_t}\right)$

$g$ function defined by equation (79)

$C$ inverse-cosine term of leading-edge correction function (equation (35))

$R$ radical term of leading-edge correction function (equation (36))

$r.\ p.$ real part

### ELLIPTIC INTEGRALS AND FUNCTIONS

$k$ modulus of elliptic integral, defined where used (also with subscripts)

$k'$ complimentary modulus $(\sqrt{1-k^2})$

$\phi$ or $\psi$ argument of elliptic integrals, defined where used (also with subscripts)

$F(\phi, k)$ incomplete elliptic integral of the first kind of modulus $k$ and argument $\phi$

$K, K(k)$ complete elliptic integral of the first kind; that is, $K=F\left(\frac{\pi}{2}, k\right)$

$E(\phi, k)$ incomplete elliptic integral of the second kind of modulus $k$ and argument $\phi$

$E, E(k)$ complete elliptic integral of the second kind; that is, $E=E\left(\frac{\pi}{2}, k\right)$

$K_0$ $\frac{2}{\pi}K$

$E_0$ $\frac{2}{\pi}E$

$K'$ $K(k')$

$E'$ $E(k')$

$Z$ zeta function (equation (41))

$\Lambda_0$ function used in evaluation of elliptic integral of the third kind, circular case (equation (16))

$\Omega$ function used in evaluation of elliptic integral of the third kind, circular case (equation (B11))

## APPENDIX B

## EVALUATION OF THE INTEGRAL IN EQUATION (26)

It is first necessary to recall that $t_a$ is a function (equation (23)) of $x$, $y$, and $a$. After substitution for $t_a$ in equation (26), we may integrate by parts to obtain

$$\int_0^{a_0} \cos^{-1}\frac{(1-a)(t_a-m_t)-(m_t-a)(1-t_a)}{(1-m_t)(t_a-a)}\frac{du_\Delta(a)}{da}da=$$

$$-u_0\left[\cos^{-1}\frac{(1+m_t)\beta y-2m_t(x-c_0)}{(1-m_t)\beta y}-\right.$$

$$(x-\beta y)\sqrt{\frac{\beta y-m_t(x-c_0)}{x-\beta y-m_t c_0}}\times$$

$$\left.\int_0^{a_0}\frac{da}{(\beta y-ax)\sqrt{(1-a)(a_0-a)(m-a)(m+a)}}\right] \quad \text{(B1)}$$

The integral term on the right-hand side of equation (B1) is an elliptic integral of the third kind which may be evaluated through the substitution of

$$\omega=sn^{-1}\sqrt{\frac{2m(a_0-a)}{(m+a_0)(m-a)}} \qquad k=\sqrt{\frac{(1-m)(m+a_0)}{2m(1-a_0)}}$$

If the value of $\omega$ at the lower limit is designated by $\omega_0$, this substitution gives

$$\int_0^{a_0}\frac{da}{(\beta y-ax)\sqrt{(1-a)(a_0-a)(m-a)(m+a)}}=$$

$$\frac{1}{\beta y-a_0x}\sqrt{\frac{2}{m(1-a_0)}}\int_0^{\omega_0}\frac{1-\frac{m+a_0}{2m}sn^2\omega}{1+n\,sn^2\omega}d\omega \quad \text{(B2)}$$

where

$$n=\frac{(m+a_0)(mx-\beta y)}{2m(\beta y-a_0x)} \quad \text{(B3)}$$

or

$$\int_0^{a_0}\frac{da}{(\beta y-ax)\sqrt{(1-a)(a_0-a)(m-a)(m+a)}}=$$

$$\frac{-1}{mx-\beta y}\sqrt{\frac{2}{m(1-a_0)}}\left[\omega_0-\left(1+\frac{mx-\beta y}{\beta y-a_0x}\right)\Pi_3(\omega_0,k,n)\right] \quad \text{(B4)}$$

where

$$\Pi_3(\omega_0,k,n)=\int_0^{\omega_0}\frac{d\omega}{1+n\,sn^2\omega}$$

is the normal form of the elliptic integral of the third kind.

It is first noted that $n>0$. For this case it can be shown that the substitution

$$\nu=tn^{-1}\left(\sqrt{\frac{n}{k^2}},\ k'\right) \tag{B5}$$

gives

$$\Pi_3(\omega_0,k,n)=\omega_0 cn^2(\nu,k')+\frac{sn(\nu,k')\,cn(\nu,k')}{dn(\nu,k')}\left[\frac{\omega_0}{K_0}\Lambda_0(k,\phi)+\Omega\right] \tag{B6}$$

where

$$\phi=\tan^{-1}\sqrt{\frac{n}{k^2}} \tag{B7}$$

is the amplitude of the elliptic function $\nu$, $\Lambda_0$ is the function defined in equation (16), and $\Omega$ is an angular function of $k,\nu$ and $\omega_0$ which will be discussed later.

If

$$\psi=\sin^{-1}\sqrt{\frac{2a_0}{m+a_0}} \tag{B8}$$

then

$$\omega_0=F(\psi,k) \tag{B9}$$

From equation (B5), $sn(\nu,k')=\sqrt{\frac{n}{n+k^2}}$, $cn(\nu,k')=\sqrt{\frac{k^2}{n+k^2}}$ and $dn(\nu,k')=\sqrt{\frac{k^2(1+n)}{n+k^2}}$ may be found, so that equation (B6) may be rewritten without recourse to the Jacobian elliptic functions as

$$\Pi_3(\omega_0,k,n)=\frac{k^2}{n+k^2}F(\psi,k)+\sqrt{\frac{n}{(1+n)(n+k^2)}}\left[\frac{F(\psi,k)}{K_0}\Lambda_0(k,\phi)+\Omega\right] \tag{B10}$$

This expression is to be substituted in equation (B4) and the result used in equation (B1). As previously mentioned, the functions $K_0$ and $\Lambda_0$ are tabulated in reference 11 and $\Lambda_0$ is plotted in figure 6. The function $\Omega$ is given by [9]

$$\Omega=\tan^{-1}\frac{2\sum_{j=1}^{\infty}(-1)^{j+1}q^{(j^2)}\sin 2j\frac{\omega_0}{K_0}\sinh 2j\frac{\nu}{K_0}}{1-2\sum_{j=1}^{\infty}(-1)^{j+1}q^{(j^2)}\cos 2j\frac{\omega_0}{K_0}\cosh 2j\frac{\nu}{K_0}} \tag{B11}$$

with

$$q=e^{-\frac{\pi K'}{K}}$$

(tabulated in reference 15).

[9] The symbol $q$ in equation (B11) is standard notation for the nome of the Jacobian theta function, and is not related to the dynamic pressure $q$ of the text.

## APPENDIX C

### INTEGRATION FOR LOSS OF LIFT AT THE TIP OF WING WITH SUBSONIC LEADING EDGE

From equations (88a) and (6)

$$\left(\frac{\Delta L}{q\alpha}\right)_{tip}=-\frac{4m_t^2ms^2\beta u_0}{V\alpha}\int_{a_t}^{m}\frac{G'(a)}{\sqrt{m^2-a^2}}da \tag{C1}$$

where

$$G'(a)=\frac{a-a_t}{a_t^2a^2(m_t-a)}\left[\left(\frac{a_t}{a}+\frac{m_t-a_t}{m_t-a}\right)\left(\sqrt{\frac{a+a^2}{m_t+m_t^2}}-\frac{a}{m_t}\right)-\frac{a-a_t}{2\sqrt{m_t+m_t^2}\sqrt{a+a^2}}\right] \tag{C2}$$

The terms in $G'(a)$ are of two types; namely, those that contain $\sqrt{a+a^2}$ and those that do not. The former combine with the radical $\sqrt{m^2-a^2}$ in equation (C1) to form elliptic integrals of the first, second, and third kinds. The latter give rise to terms in equation (C1) which are integrable by elementary means. It is convenient, therefore, to consider the integral in two parts, writing

$$-\int_{a_t}^{m}\frac{G'(a)}{\sqrt{m^2-a^2}}da=I_1+I_2$$

where $I_1$ is that part of the integral not requiring elliptic integrals.

Then

$$I_1=\int_{a_t}^{m}\frac{a-a_t}{a_t^2m_ta(m_t-a)}\left(\frac{a_t}{a}+\frac{m_t-a_t}{m_t-a}\right)\frac{da}{\sqrt{m^2-a^2}}$$

$$=\frac{1}{a_t^2m_t(m_t^2-m^2)}\left[\frac{(m_t-a_t)^2}{\sqrt{m_t^2-m^2}}\cos^{-1}\frac{m_ta_t-m^2}{m(m_t-a_t)}-\frac{m_ta_t-m^2}{m^2}\sqrt{m^2-a_t^2}\right] \tag{C3}$$

The remaining terms, involving $\sqrt{a+a^2}$ and $\sqrt{m^2-a^2}$, are integrated by means of the substitution

$$sn\omega=\sqrt{\frac{m-a}{m(1+a)}}\qquad k=\sqrt{\frac{1-m}{2}} \tag{C4}$$

The result is

$$I_2=\frac{1}{a_t^2m_t\sqrt{2mm_t(1+m_t)}}\left\{\left[\frac{m_t-a_t}{m_t}\left(\frac{m_t-a_t}{1+m_t}-\frac{a_t}{m}\right)-\frac{a_t(m-a_t)}{m^2}\right]F(\psi,k)+\frac{2a_t}{m}\left[\left(1+\frac{m_t-a_t}{m_t}\right)E(\psi,k)+\left(a_t-\frac{m_t-a_t}{m_t}\right)\sqrt{\frac{m+a_t}{2a_t}}\sin\psi\right]-\frac{(1+m)(m_t-a_t)^2}{(m_t-m)^2}\left[\left(1+\frac{m}{m_t}+\frac{m_t-m}{1+m_t}\right)\Pi_3(\omega_t,k,n)+\frac{2m(1+m)}{m_t-m}\frac{\partial\Pi_3(\omega_t,k,n)}{\partial n}\right]\right\} \tag{C5}$$

where $\omega_t=\omega(a_t)$, $\psi$ is its amplitude, and

$$n=\frac{m(1+m_t)}{m_t-m} \tag{C6}$$

From equation C(4),

$$\psi=\sin^{-1}\sqrt{\frac{m-a_t}{m(1+a_t)}} \tag{C7}$$

The elliptic integral

$$\Pi_3(\omega_t, k, n)=\int_0^{\omega_t}\frac{d\omega}{1+n\,sn^2\omega}$$

is evaluated in equation (B10). Its derivative with respect to the parameter $n$ may be obtained for this case ($n>0$) in the form

$$\frac{\partial\Pi_3}{\partial n}=\frac{1}{2n}\sqrt{\frac{n}{(n+k^2)(1+n)}}\left\{\left(\frac{1}{1+n}-\frac{n}{n+k^2}\right)\left[\frac{\Lambda_0(\phi,k)}{K_0}F(\psi,k)+\Omega(\omega_t,n,k)\right]-\sqrt{\frac{n}{(n+k^2)(1+n)}}\left[k^2\left(\frac{1}{k^2}+\frac{1+n}{n+k^2}\right)F(\psi,k)-\right.\right.$$

where $\phi$ and $\Omega$ are the angles defined in equations (B7) and (B11) and the elliptic functions $cn\omega_t$ and $dn\omega_t$, obtained from equation (C4), have the values

$$cn\omega_t=\sqrt{\frac{a_t(1+m)}{m(1+a_t)}} \qquad dn\omega_t=\sqrt{\frac{(1+m)(m+a_t)}{2m(1+a_t)}} \tag{C9}$$

## REFERENCES


1. Evvard, John C.: Use of Source Distributions for Evaluating Theoretical Aerodynamics of Thin Finite Wings at Supersonic Speeds. NACA Rep. 951, 1950.
2. Harmon, Sidney M., and Jeffreys, Isabella: Theoretical Lift and Damping in Roll of Thin Wings With Arbitrary Sweep and Taper at Supersonic Speeds. NACA TN 2114, 1950.
3. Lomax, Harvard, and Heaslet, Max. A.: Linearized Lifting-Surface Theory for Swept-Back Wings with Slender Plan Forms. NACA TN 1992, 1949.
4. Lagerstrom, P. A.: Linearized Supersonic Theory of Conical Wings. NACA TN 1685, 1948.
5. Mirels, Harold: Lift-Cancellation Technique in Linearized Supersonic Wing Theory. NACA TN 2145, 1950.
6. Busemann, Adolf: Infinitesimal Conical Supersonic Flow. NACA TM 1100, 1947.
7. Cohen, Doris: The Theoretical Lift of Flat Swept-Back Wings at Supersonic Speeds. NACA TN 1555, 1948.
8. Cohen, Doris: Theoretical Loading at Supersonic Speeds of Flat Swept-Back Wings with Interacting Trailing and Leading Edges. NACA TN 1991, 1949.
9. Cohen, Doris: Formulas and Charts for the Supersonic Lift and Drag of Flat Swept-Back Wings With Interacting Leading and Trailing Edges. NACA TN 2093, 1950.
10. Malvestuto, Frank S. Jr., Margolis, Kenneth, and Ribner, Herbert S.: Theoretical Lift and Damping in Roll of Thin Swept-Back Wings of Arbitrary Taper and Sweep at Supersonic Speeds. Subsonic Leading Edges and Supersonic Trailing Edges. NACA Rep. 970, 1949.
11. Heuman, Carl: Tables of Complete Elliptic Integrals. Jour. of Math. and Physics, V. 19–20, 1940–41, pp. 127–206.
12. Legendre, Adrien Marie: Tables of the Complete and Incomplete Elliptic Integrals. Biometrika Office, University College, Cambridge University Press, Cambridge, England, 1934.
13. Jones, R. T.: Properties of Low-Aspect-Ratio Pointed Wings at Speeds Below and Above the Speed of Sound. NACA Rep. 835, 1946.
14. Ribner, Herbert S.: Some Conical and Quasi-Conical Flows in Linearized Supersonic Wing Theory. NACA TN 2147, 1950.
15. Spenceley, G. W., and Spenceley, R. M.: Smithsonian Elliptic Functions Tables. Smithsonian Institution, Washington, D. C., 1947.
16. Adams, Edwin P., and Hippisley, R. L.: Smithsonian Mathematical Formulae and Tables of Elliptic Functions. Smithsonian Institution, Washington, D. C., 1939.
17. Brown, Clinton E.: The Reversibility Theorem for Thin Airfoils in Subsonic and Supersonic Flow. NACA TN 1944, 1949.
18. Hayes, W. D.: Linearized Supersonic Flow. North American Aviation, Inc., Rep. AL–222, June 18, 1947.
19. Jones, R. T.: Leading-Edge Singularities in Thin-Airfoil Theory. Jour. Aero. Sci., vol. 17, no. 5, May, 1950, pp. 307–310.


GPO 918446